Specificity of developmental- and growth factor-dependent phosphorylation of Akt isoforms in neurons

Dissertation

zur Erlangung des akademischen Grades

doctor rerum naturalium

(Dr. rer. nat.)

im Fach Biologie

eingereicht an der

Lebenswissenschaftlichen Fakultät

der Humboldt-Universität zu Berlin

von

M.Sc. Sandra Schrötter

Präsidentin der Humboldt-Universität zu Berlin

Prof. Dr. Sabine Kunst

Dekan der Lebenswissenschaftlichen Fakultät

Prof. Dr. Richard Lucius

Gutachter/innen: 1. Prof. Peter-Michael Kloetzel

2. Prof. Stephan Sigrist

3. Prof. Nils Blüthgen

Tag der mündlichen Prüfung: 22.08.2016

For Bonnie

Table of contents

Summary

A major pathway involved in neuronal development and the maintenance of neuronal circuits in adult brain is the PI3K - PTEN - Akt pathway. PI3K is the major kinase involved in the generation of PIP_3 at the membrane by the phosphorylation of $PI(4,5)P_2$.This action is antagonized by the well-studied tumor suppressor PTEN. The presence of PIP_3 at the membrane leads to activation of downstream targets such as the protein kinase Akt. Akt kinase comprises three isoforms (Akt1-3) which are activated upon phosphorylation of the residues S473 and T308 (numbered according to Akt1). Knock-out animals for the individual isoforms as well as double knock-outs have shown differential as well as redundant functions of the three isoforms. However, their individual role in neuronal signaling pathways has not yet been studied in great detail.

The aim of this study was to obtain further insight into differential Akt isoform signaling in response to changes in the activity of PI3K and PTEN pathway. A new isoelectric focusing method was established in order to overcome limitations of commonly used biochemical methods (e.g. Western blot). The fully automated capillary-based isoelectric focusing method allowed us to separate Akt proteins according to their charge, therefore, providing a refined read-out to study dynamics of Akt phosphorylation in a neuronal background.

In the course of this project we were able to identify previously undescribed features of Akt phosphorylation and activation. First, we could provide evidence for an uncoupling of the two activating phosphorylation events at S473 and T308 in neuroblastoma cells and differential sensitivities of Akt1 forms towards PI3K inhibition. Secondly, we found a transient shift in Akt isoform activation and abundance during postnatal rat brain development. Thirdly, we were able to show that the activation of different Akt isoforms is dependent of the upstream signal as well as the age of the neuron. Immature neurons were found to be highly responsive to BDNF treatment, whereas mature neurons were most responsive to EGF stimulation leading exclusively to activation of Akt2 in an EGFR- and PI3K/p110α-dependent manner. In contrast, stimulation of Akt phosphorylation by the loss of PTEN led to an activation of mainly Akt1 forms, which suggests inherent differences in the Akt pools that are accessible to growth factors dependent PI3Ks as compared to the pools that are controlled by PTEN.

In summary, this thesis demonstrates the presence of complex phosphorylation events of Akt in a developmental- and signal-dependent manner in neurons.

Zusammenfassung

Ein wichtiger Signalweg während der neuronalen Entwicklung und zur Erhaltung der neuronalen Netzwerkstrukturen im adulten Gehirn ist der PI3K - PTEN- Akt Signalweg. PI3K ist eine Kinase welche hauptsächlich $PI(4,5)P_2$ zu PIP_3 phosphoryliert. Dieser Reaktion wird von dem Tumorsuppressor PTEN entgegengewirkt. Die Erhöhung der PIP_3 Konzentration an der Membran löst die Aktivierung weiterer nachgelagerter Proteine, z. B. Akt, aus. Akt ist eine Kinase die drei verschiedene Isoformen (Akt1-3) besitzt, welche durch die Phosphorylierung von S473 und T308 (nummeriert nach Akt1) aktiviert werden. Knock-out Modelle für die einzelnen Isoformen, sowie Knock-outs von mehreren Isoformen zusammen, haben gezeigt, dass obwohl sich die Funktionen der einzelnen Formen zum Teil überlappen, bei Verlust einzelner Isoformen, nicht alle Funktionen von anderen Isoformen kompensiert werden können. Trotz allem ist bis heute die genaue Rolle der einzelnen Isoformen in einem neuronalen Zusammenhang nur wenig untersucht.

Das Ziel dieser Arbeit war, eine detailliertere Analyse der einzelnen Akt Isoformen nach der Aktivierung des vorgeschalteten PI3K - PTEN Signalweges. Dazu wurde im Labor eine neue Methode zu isoelektrischen Fokussierung etabliert um die bisherigen Limitationen der herkömmlichen biochemischen Methoden (z.B. Western blot) zu überwinden. Die vollautomatische, Kapillaren-basierte Methode der isoelektrischen Fokussierung trennt Proteine nach ihrer Ladung auf und erlaubt uns somit eine Analyse der Dynamik von Akt Phosphorylierungen in neuronalen Zellen.

Im Zuge dieser Arbeit konnten wir bisher unerkannte Merkmale der Akt Aktivierung und Phosphorylierung identifizieren. Zuerst konnten wir zeigen, dass die Phosphorylierung von S473 und T308 in Neuroblastomazellen unabhängig voneinander auftreten kann und das verschiedene Akt1 Moleküle unterschiedlich auf die Inhibition von PI3K reagieren. Außerdem konnten wir Verschiebungen in der Aktivierung und in der Expression der unterschiedlichen Isoformen während der postnatalen Gehirnentwicklung der Ratte feststellen. Des Weiteren konnten wir zeigen, dass die Aktivierung von Akt von dem Signal und dem Alter der Neurone abhängig ist. Noch nicht vollständig differenzierte Neurone reagieren vor allem auf BDNF Stimulation, wohingegen adulte, differenzierte Neurone hauptsächlich auf EGF reagieren und dort explizit Akt2 über EGFR und PI3K-p110α Signale aktiviert wird. Im Gegensatz dazu führt der Verlust von PTEN zu einer Aktivierung von hauptsächlich Akt1. Dies führt uns zu der Schlussfolgerung, dass unterschiedliche Akt Populationen auf Wachstumsfaktoren und auf PTEN Verlust reagieren.

Zusammenfassend zeigt diese Arbeit einen komplexen Zusammenhang der Phosphorylierung von Akt auf, welcher Signal- und Entwicklungsabhängig ist.

Abbreviations

Akt	Proteinkinase B
APS	Ammonium persulfate
BDNF	Brain-derived neurothrophic factor
BSA	Bovine serum albumin
cIEF	Capillary-based isoelectric focusing
CNS	Central nervous system
CO_2	Carbon dioxide
CREB	cAMP response element-binding protein
dH_2O	Distilled water
DIV	Days *in vitro*
DMEM	Dulbecco´s modified eagles medium
DMSO	Dimethylsulfoxide
DNA	Deoxyribonucleic acid
DNA-PK	DNA-dependent protein kinase
DTT	Dithiothreitol
E	Embryonic day
EDTA	Ethylene diamine tetraacetic acid
EGF	Epidermal growth factor
EGFR	Epidermal growth factor receptor
EGFRi	EGFR inhibitor (Gefitinib)
ERK1/2	Extracellular signal regulated kinase ½
FCS	Fetal calf serum
GAPDH	Glycerin aldehyde-3-phosphate dehydrogenase
GF	Growth factor
GFAP	Glial fibrillary acidic protein
GPCR	G-protein coupled receptor
GSK3ß	Glycogen synthase kinase-3 beta
h	Hours
HEK	Human embryonic kidney cells
HRP	Horseradish peroxidase
IB	Immunoblot
IC	Immunocytochemistry
IGF-1	Insulin-like growth factor 1
IP	Immunoprecipitation
kDa	Kilodalton

KO	Knock-out
LFQ	Label free quantification
mA	Miliampere
MAP2	Microtubule-associated protein 2
MAPK	Mitogen-activated protein kinase
mass spec	Mass spectrometry
MCM7	Mini-chromosome maintenance protein 7
min	Minutes
mL	Mililiter
mM	Milimolar
mTOR	Mammalian target of rapamycin
mTORC2	mTOR complex 2
ng	Nanogram
nm	Nanometer
nM	Nanomolar
NMDAR	N-Methyl-D-aspartate receptor
NP	NanoPro 100
P	Postnatal day
PBS	Phosphate buffered saline
PDK1	3-Phosphoinositide-dependent kinase-1
PFA	Paraformaldehyde
PH	Pleckstrin-homology
PHLPP	PH domain and leucine rich repeat protein phosphatases
PHTS	PTEN harmatoma tumor syndrome
pI	Isoelectric point
PI3K	Phosphoinositide-3-kinase
PI3Ki	PI3K inhibitor (GDC-0941)
PIP_2	Phosphatidylinositol-4,5-bisphosphate
PIP_3	Phosphatidylinositol-3,4,5-trisphosphate
PKC	Proteinkinase C
PP	Phosphatase
PP2A	Protein phosphatase 2A
PSD-95	Postsynaptic density protein 95
PTEN	Phosphatase and tensin homologue deleted on chromosome ten
PTM	Posttranslational modification
P/S	Penicillin/Streptomycin
RFP	Red fluorescent protein

RGC	Retinal ganglion cell
rpm	Rounds per minute
RT	Room temperature
RTK	Receptor tyrosine kinase
sec	Seconds
SDS	Sodium dodecyl sulfate
SDS-PAGE	SDS- polyacrylamide gelelectrophoresis
TBS-T	Tris buffered saline with Tween20
TFEB	Transcription factor EB
TPA	Tetradecanoyl phorbol acetate
TrkB	Tyrosine receptor kinase B
TrkBi	TrkB inihibitor (GNF5837)
U	Unit
V	Volt
WB	Western blot
WM	Wortmannin
w/o	without
WT	Wild type
µL	Microliter

1. Introduction

The mature brain is composed of more than one billion neurons [Stiles and Jernigan 2010]. From birth to adulthood the brain mass increases up to 6x of its initial weight due to increasing neuron size and addition of glial cells [Bandeira, Lent, and Herculano-Houzel 2009]. Structural changes still occur during childhood until early adolescence [Stiles and Jernigan 2010]. Brain development is characterized as a complex series of adaptive and dynamic processes. Neurons are the information processing cells of the brain and form synapses with each other to build up networks that are responsible for all our feelings, actions, sensations and thoughts. The appropriate connectivity of neurons is ensured on a molecular level by tightly regulated signaling events. Essential for a correct axonal outgrowth and wiring are attractive and repulsive guidance cues and their respective receptors. The four main guidance molecules during axonal outgrowth are semaphorins, netrins, slits and ephrins [O'Donnell, Chance, and Bashaw 2009]. The axonal guidance process during brain development consists of three main segments. First, the expression of a correct complement of receptors and guidance cues of the neurons and surrounding tissue. Second, an appropriate localization of the receptors to specialized structures at the tips of extending axons, termed growth cones, and correct trafficking of the guidance cues to the extracellular environment. Third, signaling mechanisms must be in place to integrate and transmit signals from the surface receptors into changes in the growth cone actin cytoskeleton [O'Donnell, Chance, and Bashaw 2009]. Actin cytoskeleton reorganization, including, for example, the formation of structures like F-actin patches, lamellipodia and filopodia is linked to Rho activity [Kreis et al. 2014]. A master regulator for Rho activity is the presence of the lipid phosphatidylinositol 3,4,5-trisphosphate (PIP_3) in the plasma membrane [Hawkins et al. 2006]. Being the main kinase involved in PIP_3 production, the phosphoinositide 3-kinase (PI3K) pathway and its negative regulator, the tumor suppressor gene phosphatase and tensin homologue deleted on chromosome ten (PTEN) [Eickholt et al. 2007], regulates various cellular processes, including neuronal differentiation, survival, migration, axonal extension and guidance [Eickholt et al. 2007].

1.1. PI3K/PTEN in health and disease

PI3Ks are a protein family comprising eight different isoforms divided in three classes according to their protein structure, function and associated regulatory subunit [Hawkins et al. 2006]. This worked focused on the class I PI3Ks, which can be further subdivided into class IA and IB. Class IA enzymes consist of a catalytic p110 (α, β, δ) subunit which can be associated with any of the five regulatory subunits: p50α, p55α, p85α, p85β or p55γ. The smaller subgroup of class IB enzymes all have the same catalytic subunit, p110γ, associated with the regulatory subunit p87 or p101 [Gross and Bassell 2014]. The main function of class I PI3Ks is their lipid kinase activity at the plasma membrane. They generate PIP_3 by phosphorylation of phosphatidylinositol 4,5-bisphosphate (PIP_2). Thereby PI3Ks are the main enzymatic activity involved in the generation of PIP_3. The dual specific phosphatase PTEN, on the other hand, directly antagonizes PI3Ks, as it dephosphorylates PIP_3 to PIP_2 at the plasma membrane [Cantley 2002]. PI3K can be activated through two upstream receptors, being receptor tyrosine kinases (RTK) and G-protein coupled receptors (GPCR), following activation by extracellular stimuli (e.g. growth factor binding) [Gross and Bassell 2014]. Aberrant PI3K signaling due to mutations in the catalytic subunit has been implied in a variety of pathological changes. For example, activating mutations in the PI3K-p110α subunit

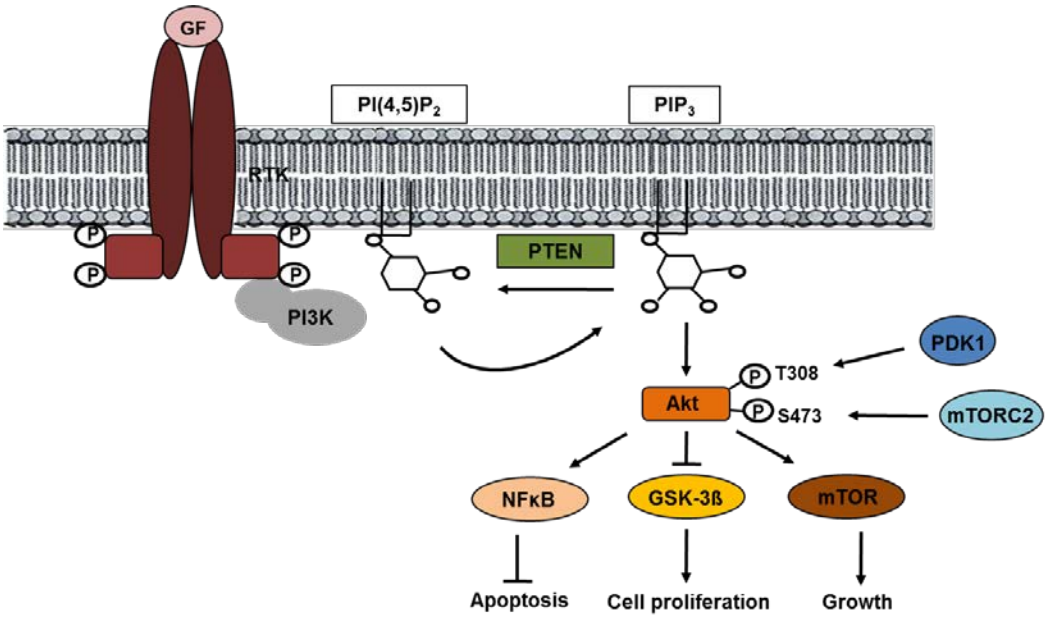

Figure 1: *PI3K-PTEN signaling pathway.* PTEN functions predominately at the plasma membrane, converting phosphatidylinositol 3,4,5-trisphosphate (PIP_3) to phosphatidylinositol 4,5-bisphosphate (PIP_2), thereby directly antagonizing the activity of phosphoinositide 3-kinase (PI3K). PI3K is activated by growth factor (GF) binding to receptor tyrosine kinases (RTK). Upon PIP_3 availability the downstream effector Akt gets phosphorylated at Serine 473 and Threonine 308, by the kinases mTORC2 and PDK1, respectively. Akt has many different effector proteins, some of which are shown in the figure (NFκB, GSK3β, mTOR).

are linked to megalencephaly with developmental delay and epilepsy [Rivière et al. 2012]. A hyperactivation of PI3K due to mutations in the p110α subunit have been grouped with other overlapping clinical diagnoses as 'PIK3CA-related overgrowth spectrum' [Di Donato et al. 2015]. Mutations in the PI3K-p110β subunit have been shown to be connected to fragile X syndrome and autism [Gross and Bassell 2014; Cuscó et al. 2009]. p110γ, the least studied PI3K catalytic subunit in the brain, has been found to be involved in NMDAR signaling. Interestingly, mutations in this specific isoform have been identified in autism spectrum disorder patients [Gross and Bassell 2014]. The PI3K-p110δ subunit is essential for axonal outgrowth and it is activated downstream of the neuregulin-1 receptor ErbB4. Deregulation of p110δ signaling has been found to be involved in schizophrenia, highlighting again, the central function of PI3K signaling during brain development [Eickholt et al. 2007; Law et al. 2012]. Furthermore a role for p110δ has been described in sciatic nerve regeneration [Park et al. 2010]. But independent of the catalytic subunit, activation of PI3K class I enzymes leads to an increase of PIP_3 at the plasma membrane leading to recruitment and subsequent activation of pleckstrin-homology (PH) domain containing proteins (e.g. Akt). This accumulation of PIP_3 can be antagonized by the dephosphorylation of the lipid by PTEN.

PTEN was originally identified as a tumor suppressor gene in 1997 [Li et al. 1997], its mutations leading to a wide variety of cancers and developmental disorders combined under the term 'PTEN hamartoma tumor syndrome (PHTS)', including Cowden syndrome and other proliferative syndromes [Li et al. 1997]. Nowadays it is well established that PTEN mutations also play a major role in brain tumors and neurological disorders such as macrocephaly, autism and mental retardation [Butler et al. 2005; Lugo et al. 2014; Zhou and Parada 2012]. Accordingly, a loss of PTEN in adult mice hippocampal neural stem cells causes an increase in neurogenesis leading to macrocephaly with an enlarged dentate gyrus and a disorganized granule cell layer [Kwon et al. 2006]. Additionally, these mice also show an impaired social behavior and frequent seizures, closely resembling the phenotype found in human patients with PTEN mutations [Amiri et al. 2012]. The PTEN gene is located on chromosome 10q23 [Myers et al. 1997]. While PTEN encompasses protein and lipid phosphatase functions, it is the latter that mediates direct antagonism of PI3Ks. The activity and subcellular localization of PTEN is regulated by posttranslational modifications (PTMs) such as phosphorylation [Kreis et al. 2014]. Phosphorylation of the C-terminus of PTEN also has an influence on the conformational state of the protein. A highly phosphorylated C-terminus leads to a closed protein conformation thereby preventing PTEN membrane binding, whereas an unphosphorylated C-terminus results in an open protein conformation, allowing membrane association of PTEN [Vazquez and Devreotes 2006; Kreis et al. 2014]. In this context the phosphorylation sites S380, T382, T383 and S385 are thought to negatively regulate PTEN phosphatase activity but favor stabilization of the protein [Song, Salmena,

and Pandolfi 2012]. PTEN plays a key role in developing neurons as the antagonist of PI3K signaling. In young neurons PTEN was found to be associated with microtubules, away from the actin rich periphery of growth cones, malfunction or mislocalization at this stage is implied in neurodegeneration and autism [Chadborn et al. 2006; Kreis et al. 2014]. Later in mature neurons, PTEN loss can lead to a severe disarrangement of dendritic spine morphology causing pathologies such as epilepsy or autism [Kreis et al. 2014]. Recently, a longer, membrane-permeable variant of the lipid phosphatase has been identified, termed PTEN-Long [Hopkins et al. 2013; Pulido et al. 2014] This protein can be secreted from cells and antagonize PI3K signaling and cancer progression *in vitro* and *in vivo* [Hopkins et al. 2013]. The balance between PI3K and PTEN signaling is important to maintain a healthy cell. Besides its major function as antagonist in PI3K signaling, PTEN has also been proposed a PI3K-independent function involving its protein phosphatase activity, for example, in cell migration, cell cycle arrest or actin cytoskeleton rearrangement [Song, Salmena, and Pandolfi 2012; Myers et al. 1997; Kreis et al. 2014]. PTEN interacts with the actin filament binding protein Drebrin. PTEN dephosphorylates Drebrin in response to, for example neuronal activity, and can thereby induce dynamic remodeling of the actin cytoskeleton [Kreis et al. 2014].

1.2. Protein kinase B (Akt)

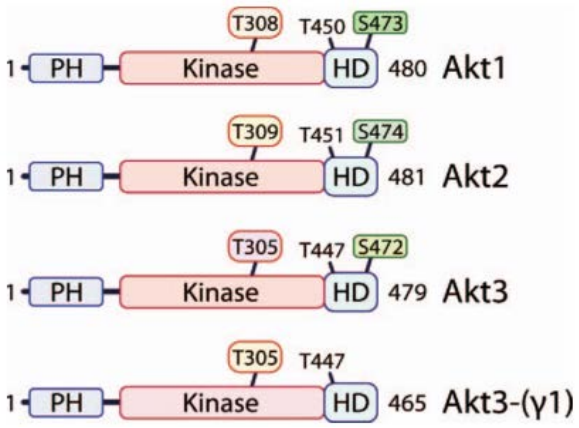

Figure 2: *Schematic view of Akt isoforms* [Matheny and Adamo 2009]. Akt is found in three isoforms, Akt1, Akt1 and Akt3. They possess a N-terminal Pleckstrin homology (PH) domain, a kinase domain and a C-terminal hydrophobic domain (HD). Akt3 is found in an alternative splice variant (Akt3-γ1). Akt isoforms have two activating phosphorylation sites T308 (T309, T305) and S473 (S474, S472) and one constitutive phosphorylation site at T450 (T451, T447).

A major downstream effector of the PI3K/PTEN pathway is Akt. Akt is a Serine/Threonine kinase which was originally discovered as an oncogene in 1977, but has now also been shown to play a role for example during axon outgrowth [Matheny and Adamo 2009; Dajas-Bailador et al. 2014]. There are three Akt isoforms in mammals, encoded by three genes, namely *Akt1*, *Akt2* and *Akt3* [Matheny and Adamo 2009], which encode for the three Akt family members Akt1, Akt2 and Akt3 (also referred to as PKBα, PKBβ and PKBγ) [Testa and Bellacosa 2001]. All three isoforms share approximately ~80% sequence homology and possess an N-terminal PH domain, which enables the proteins to bind PIP_3. Further in the C-terminus lies the kinase domain and a C-terminal hydrophobic domain (see Figure **2**) [Matheny and Adamo 2009].

Over recent years, some work has indicated isoform specific cellular functions in mediating neuronal responses. Distinct functions of the three isoforms in different tissues are regulated by differential activation of the isoforms as well as different expression patterns. Akt1 is the most ubiquitously expressed isoform and $Akt1^{-/-}$ mice are viable but smaller than wild type mice, displaying growth defect in fetal and postnatal stages [WS Chen et al. 2001; Cho, Thorvaldsen, et al. 2001]. However, a significant number of pups died in neonatal stages (P0-P3), suggesting lethal defects during this period. The brain size of $Akt1^{-/-}$ mice is reduced by ~14% but is proportional with the overall reduction in body size [Cho, Thorvaldsen, et al. 2001]. In humans, activating Akt1 mutations have been shown to cause Proteus syndrome, a syndrome characterized by skin, connective tissue and brain overgrowth [Lindhurst et al. 2011]. Downregulation of Akt1 due to aberrant DNA methylation has been linked to patients with schizophrenia [Wockner et al. 2014]. *In vitro*, Akt1 has been found mainly being present in the cytoplasm and its loss may be compensated by Akt2 and/or Akt3 expression, but Akt1 cannot completely compensate loss of Akt2 or Akt3 [Diez, Garrido, and Wandosell 2012; Santi and Lee 2010]. Further, Akt1 has been described as a major contributor to tumor

initiation but does not induce tumor progression [H Guo et al. 2014; Endersby et al. 2011; Turner et al. 2015]. The Akt2 isoform is enriched in Insulin-responsive tissue and seen as the 'metabolic' Akt isoform. Loss of Akt2 leads to a diabetic phenotype in mice, and knock-out animals show no reduction in brain size [Cho, Mu, et al. 2001]. Interestingly, heterozygous $Akt2^{+/-}$ animals were found indistinguishable from wild type animals [Cho, Mu, et al. 2001]. An connection of this isoform with a hypoglycemic phenotype in humans has also been shown [Hussain et al. 2011]. Since mitochondria play a central role in many metabolic cellular processes, together with the observation that Akt2 mainly localizes with these organelles, suggest that out of the three Akt isoforms, Akt2 is the one important for metabolic functions. *In vitro,* the disruption of Akt2 leads to a reduction in neuronal survival and axon length [Diez, Garrido, and Wandosell 2012; Santi and Lee 2010]. Interestingly, loss of Akt1 does not induce a diabetic phenotype or impaired lipid metabolism as found in $Akt2^{-/-}$ mice. Therefore, it has been suggested that Akt2 plays non-redundant functions at least in the control of cellular metabolism [Cho, Thorvaldsen, et al. 2001]. Out of the three isoforms, Akt3 demonstrates the most restricted protein expression pattern, as this isoform is mainly found in brain and testes and the Akt3 protein presents a higher nuclear expression when compared to both other isoforms, at least *in vitro* [Diez, Garrido, and Wandosell 2012; Santi and Lee 2010]. It is also the only isoforms with a reported, alternative, shorter splice variant (Akt3-γ1) [Brodbeck, Hill, and Hemmings 2001]. Diez *et al.* found Akt3 to be the dominant regulator of differentiated neuron growth [Diez, Garrido, and Wandosell 2012]. In agreement, $Akt3^{-/-}$ mice have a ~20% decrease brain size due to smaller and fewer cells. These mice, similar to $Akt1^{-/-}$ mice, also show no impairment of glucose metabolism even though Akt3 is expressed in adipocytes and responsive to Insulin. Homozygous $Akt1^{-/-}$ $Akt3^{-/-}$ double knock-out mice are not viable and die around E11/12 due to major defects in the nervous and cardiovascular development [Z Yang et al. 2005]. In contrast to $Akt1^{-/-}$ mice, $Akt3^{-/-}$ mice show impaired mammalian target of Rapamycin (mTOR) signaling, again suggesting differential signaling and specificity of the three Akt isoforms [Easton and Cho 2005]. The levels of ribosomal protein S6 phosphorylation, a downstream effector of mTOR signaling, was reduced by ~50% in Akt3 knock-out brains [Easton and Cho 2005]. In contrast to the reduced brain size in mice upon Akt3 loss, Akt3 *de novo* missense mutations, as well as mutations in *PIK3CA* (gene encoding the PI3K p110α subunit) leading to increased kinase activity have been found to be associated with megalencephaly syndromes in humans [Rivière et al. 2012]. Further, Akt3 has been identified to be the critical isoform in human glioblastomas being the most frequently amplified isoform. It was found to play a role in DNA repair therefore, promoting progression of these tumors [Turner et al. 2015]. Turner *et al*. also tested tumors derived from dysfunction of the other Akt isoforms. They found a distinct pattern for phosphorylated Akt, Akt1 derived tumors led to increased phosphoAkt most in the

nucleus, Akt2 derived tumors showed membranous phosphoAkt enrichment and Akt3 derived tumors showed high levels of phosphoAkt in the cytoplasm and nucleus [Turner et al. 2015]. In summary, reported redundant and non-redundant roles of the three Akt isoforms and their implication in pathological phenotypes in different cells and tissues emphasize the importance of a more precise analysis of the separate isoforms.

1.2.1. Phosphorylation and activation of Akt isoforms

All Akt isoforms, except Akt3-γ1, possess the two activating phosphorylation sites Threonine 308 and Serine 473, numbered according to Akt1 (see Figure 2). Phosphorylation of the T308 site is sufficient for Akt activation, however full activity is only achieved by phosphorylation of T308 and S473 [Najafov, Shpiro, and Alessi 2012]. Binding of Akt to PIP_3 via its PH domain facilitates a change in protein conformation which allows a second kinase, PDK1, to phosphorylate the T308 site of Akt. PDK1 also contains a PH domain, consequentially is able to associate PIP_3, which generates close proximity of the substrate (Akt) and the kinase (PDK1) at the plasma membrane during growth factor induced activation of PI3Ks [Mora et al. 2004]. PDK1 phosphorylates and directly activates up to 23 proteins of the AGC family, including Akt. PDK1 resides in the cytoplasm in an active conformation (whilst Akt gets activated at the plasma membrane) but substrate access is driven by its recruitment to the plasma membrane. Evidence in support of this was indicated by generating knock-in mice with a catalytic active PDK1 containing a mutant PH domain that prevents PIP_3 binding. These mice show a smaller brain size due to reduced PI3K signaling activity, which was shown by reduced Akt activation after BDNF stimulation [Zurashvili et al. 2013]. The co-recruitment of Akt and PDK1 to the membrane following PIP_3 generation in response to, for example, growth factor stimulation results in close proximity of the two proteins, which leads to phosphorylation of Akt T308 by PDK1. This mechanism represents the primary pathway for Akt activation under normal conditions *in vivo*. The S473 Akt amino acid residue, on the contrary, is phosphorylated by mTORC2, but other kinases (e.g. DNA-PK) have also been proposed [Sarbassov et al. 2005; Ikenoue et al. 2008]. After its phosphorylation S473 can bind PDK1 via its PIF-pocket, which, again, increases the proximity of the substrate (Akt) to the kinase (PDK1), leading to enhanced phosphorylation of the T308 residue [Najafov, Shpiro, and Alessi 2012]. Therefore, it seems that Akt T308 can be phosphorylated by PDK1 in a PIP_3- or in a PDK1 PIF-pocket-dependent manner. At the same time, however, it is evident that the exact order of phosphorylation of the two activating sites is not fully understood yet. Nevertheless, it is now generally accepted, that three components are essential for Akt activation: membrane binding of the protein, phosphorylation of T308 by PDK1 and phosphorylation of S473 by mTORC2.

1.2.2. Beyond S473 and T308: Further regulation of Akt by different modifications and phosphatases

Recently, two further phosphorylation sites at the C-terminus (S477 and T479) have been characterized that promote and even enhance S473 phosphorylation and leading to increases in the activation of Akt [P Liu et al. 2014]. In this way, the phosphorylation of p(S473)Akt causes the hydrophobic motif to bind to an α-helix in the catalytic domain of Akt, which was shown to stabilize the active protein [Hart and Vogt 2011]. Akt hyperactivation can lead to uncontrolled cell proliferation and resistance to apoptosis; therefore, both activating phosphorylation sites not only have different kinases but also different phosphatases controlling the protein activity. Protein phosphatase 2A (PP2A) dephosphorylates the T308 whereas PH domain and leucine rich repeat protein phosphatase (PHLPP) dephosphorylates the S473 site [Hwang et al. 2013; Gao, Furnari, and Newton 2005]. In total 20-22 phosphorylation sites for Akt have been validated [H Guo et al. 2014], resulting in a very complex and tightly regulated signaling component. All three isoforms have a constitutive phosphorylation site at T450 which has been shown to be important for the stability of the protein [Facchinetti et al. 2008]. In general, the stoichiometry or hierarchy of this multitude of phosphorylation events on Akt molecules and their relationship with T308/S473/T450 fully activated Akt species is largely unknown.
Phosphorylation is not the only PTM influencing the activity of Akt. Over the years more and more other PTMs have been the focus of research. It has been shown that ubiquitination of Akt on K63 can lead to signaling activation and protein trafficking [W-L Yang et al. 2009]. Further, sumoylation of Akt at K276 has been shown to increase Akt kinase activity in a phosphorylation-independent manner [Lin, Liu, and Lee 2015]. In contrast, O-GlcNAcylation of Akt has an inhibitory effect on Akt phosphorylation [S Wang et al. 2012].

Generally, Akt is activated by upstream growth factor binding inducing PI3K activity, leading to increased availability of PIP_3 at the plasma membrane, resulting in phosphorylation and therefore, activation of Akt. Downstream, Akt has numerous targets influencing cell proliferation, apoptosis and specifically in neurons it promotes axon specification via glycogen synthase 3ß (GSK3β) and also governs neuronal polarization [Zurashvili et al. 2013]. The regulation of GSK3β by Akt has also been shown to be directly involved in necrosis of neurons [Q Liu et al. 2014]. Akt also directly phosphorylates the 14-3-3 protein and SRPK2 thereby regulating the cell cycle and cell death of rat primary cortical neurons [Jang et al. 2009]. In healthy brains Akt activates the cAMP response element-binding protein (CREB) which functions as a nuclear transcription factor. This interaction has been found to be altered in the hippocampus of diabetic mice, and there leading to cognitive dysfunction [Xiang et al. 2015]. Furthermore, because Akt itself or upstream components

such as PI3K or the epidermal growth factor receptor (EGFR), are mutated in a great variety of cancers leading to Akt hyperactivation, many groups have focused their research on Akt inhibitors as a therapeutic target [Hers, Vincent, and Tavar 2011; Vivanco et al. 2014; She et al. 2008]. Vivanco *et al*. could identify a kinase-independent function of Akt in cancer progression showing the importance of a more detailed understanding of Akt activation, function and isoform specificity [Vivanco et al. 2014].

1.2.3. Influence of growth factors on Akt activity

In mammals, 20 distinct families of RTKs are encoded in the genome, which in response to specific ligand binding regulate a great diversity of cellular processes, including cell survival, proliferation and differentiation, cell metabolism, and cell migration [Schlessinger 2004]. One growth factor known to activate PI3K and therefore Akt, is the epidermal growth factor (EGF) [Laketa et al. 2014]. The RTK binding EGF belongs to the EGFR family consisting of four members, ErbB1-4 or HER1-4, which are ubiquitously expressed in a number of different tissues including epithelial, mesenchymal and neuronal tissue [Roskoski 2014]. Only the 134 kDa protein ErbB1, referred to as EGFR, is able to bind EGF. Following ligand engagement, the receptor dimerizes to be fully functional. ErbB1 can form homo- or heterodimers with all other three members of the EGFR family. Upon activation, heterodimers consisting of ErbB1 and ErbB3 are phosphorylated at potentially six Tyrosine resides, which leads to the recruitment of PI3K by interacting with the regulatory PI3K-p85 subunit [Roskoski 2014]. Therefore, following EGF binding, an increase in PIP_3 at the plasma membrane and downstream phosphorylation of Akt occurs by direct EGFR – PI3K interaction. In contrast, during EGF induced activation of the extracellular-signal-regulated kinase1/2 (ERK1/2) pathway, ErbB1 forms dimers with all other family members and the signal is propagated via the adaptor protein Grb2. In this cascade, Grb2 leads to downstream activation of ERK1/2 via Ras/Raf [Roskoski 2014].

The EGFR has been found overactivated in a wide range of cancers, whilst loss of EGFR protein leads to neurodegeneration with astrocytic proliferation defects and lower survival of postmitotic neurons [Sibilia et al. 1998; Roskoski 2014]. In Drosophila the asymmetric distribution and activation of EGFR was found to be necessary for axonal branching [Zschätzsch et al. 2014]. Severe downregulation of EGFR in neurons is also implied in developmental abnormalities [Bruban et al. 2015]. This emphasizes the importance of a tight regulation of EGFR expression at the plasma membrane during developmental processes.

EGF binding to its receptor induces an internalization of EGFR, which was shown to terminate the signal by, most likely, lysosomal degradation [Laketa et al. 2014]. Interestingly, high PIP_3 levels at the plasma membrane (independent of ligand binding to the receptor) also

leads to internalization of EGFR but results in full recycling of the receptor [Laketa et al. 2014]. The PI3K-dependent activation of Akt by EGF has been shown to differentially influence the Akt isoforms in different esophagal cancer cell lines. In these experiments, EGF treatment led to overlapping and distinctive phosphorylation patterns of the three Akt isoforms and allowed the categorization of cells in three groups. In the first group of cells, all three Akt isoforms were activated by EGF. The second group exhibited activation of Akt1 and Akt2, but not Akt3, whilst the third group responded with Akt1 only following stimulation with EGF [Okano et al. 2000]. Activation of Akt via the EGF-EGFR-PI3K axis has also been shown to initiate medullablastoma migration enhancing metastasis in an EGF concentration dependent manner [Dudu et al. 2012]. An inhibitory role of EGF signaling has been found in neural stem cells, where EGF negatively influences motoneuron differentiation via the PI3K-Akt pathway [Ojeda et al. 2011].

Another growth factor known to induce Akt phosphorylation and therefore, activation is the brain-derived neurotrophic factor (BDNF). BDNF was found to favor neural stem cell proliferation and neuronal growth *in vitro* via activation of Akt [Islam, Loo, and Heese 2009; J Yang et al. 2016]. In order to initiate downstream signaling, BDNF also binds to a RTK, the neurotrophin tyrosine receptor kinase B (TrkB). BDNF binding to TrkB leads to receptor dimerization and subsequent autophosphorylation of different Tyrosine residues leading to activation of downstream effectors including PI3K-Akt and ERK1/2 [Huang and McNamara 2010]. It has been shown that TrkB can also undergo transactivation by non-neurotrophin ligands. For example, in mouse cortical precursor cells TrkB was found to be transactivated by EGF rather than BDNF, thereby regulating migration of early neuronal cells in the cortex [Puehringer et al. 2013]. Malfunction of TrkB has been associated with different neurological diseases such as epilepsy, depression and schizophrenia [Huang and McNamara 2010]. In consonance, a decrease in total BDNF levels also effects brain pathology. Reduced BDNF levels are implicated in diverse neurodegenerative diseases such as Alzheimer disease, Huntington and Parkinson [Bathina and Das 2015].

1.3. Protein separation by capillary-based isoelectric focusing

Classical biochemical methods commonly applied to the analysis of protein phosphorylation often rely on the use of phospho-specific antibodies, for example for Western blot (WB) or ELISA. However, phospho-specific antibodies require a priori knowledge of specific phosphorylation sites and the production of quality antibodies to the phospho-motif can be time-consuming and costly. In recent years, the usage of mass spectrometry (mass spec) for systemic analysis of protein phosphorylation has gained acceptance [St-Denis and Gingras 2012]. For this project, in order to investigate the phosphorylation status of the different Akt

isoforms a new method other than WB was required. The advantage of good working antibodies for the different Akt isoforms and phosphorylation sites in WB harbored the drawback of only analyzing Akt isoforms or Akt phosphorylation. To overcome this limitation we employed an assay that is based on separating proteins according to their isoelectric point (pI). Individual phosphorylation events cause a shift in the pI due to the increase in negative charge on a protein. Here, we used the NanoPro™100 device from Protein Simple Inc. as a capillary-based isoelectric focusing method (cIEF) to investigate the phosphorylation status of Akt in a neuronal background. This method was first described in 2006 for its great advantage of sensitivity as it could assess a protein sample of only 25 cells [O'Neill et al. 2006]. cIEF provides a platform to resolve isoforms and individual phosphorylation events. The assay is highly reproducible as it uses a 5 cm and 400 nL capillary where proteins, following charge separation, are bound covalently to the inner wall by UV-light. The capillaries are then incubated with a specific primary antibody and a horseradish-peroxidase coupled (HRP) secondary antibody which are flowed through the capillary. Visualization of bound antibodies to proteins is carried out by chemiluminescence [O'Neill et al. 2006; Michels et al. 2012]. It was previously demonstrated that due to its high sensitivity, this cIEF assay requires 1000-fold less protein than other isoelectric focusing or WB methods, making it an interesting platform for clinical research where patient samples are sometimes difficult to obtain in large quantities [Michels et al. 2012; JQ Chen et al. 2013]. Using cIEF, analysis of clinical specimen for a variety of oncoproteins unraveled their expression patterns and phosphorylation status presenting a first step for the development of new cancer therapeutics [Fan et al. 2009]. The cIEF method has also been employed in the search for biomarkers by using phosphorylation of ERK1/2 as a read-out [JQ Chen et al. 2013] as well as to assess the efficiency of Tyrosine kinase inhibitors in chronic myeloid leukemia [Aspinall-O'Dea et al. 2015]. Various other studies have used the cIEF method to assess Akt in cancer cells and non-neuronal lines [H Guo et al. 2014; Sabnis et al. 2014; Iacovides et al. 2013]. These studies mainly concentrated on Akt1 and Akt2 expression, as Akt3 could only be found in a subset of breast cancer cells [Iacovides et al. 2013]. The non-phosphorylated forms of Akt1 were found at pI ranging from 5.6 – 5.8 and non-phosphorylated Akt2 was identified between 5.9 – 6.0 [H Guo et al. 2014; Iacovides et al. 2013; Sabnis et al. 2014]. Guo *et al*. detected p(T308)Akt and p(S473)Akt in colon cancer cells, proofing the ability of this method to gain detailed insights into Akt activity and signaling [H Guo et al. 2014]. We used this method to analyze the temporal isoform-specific Akt activation regulated by manipulation of upstream signaling cues such as PI3K activation or PTEN loss. Furthermore we used cIEF to identify a complete Akt profile, with all three isoforms, in neuronal cells and brain tissue.

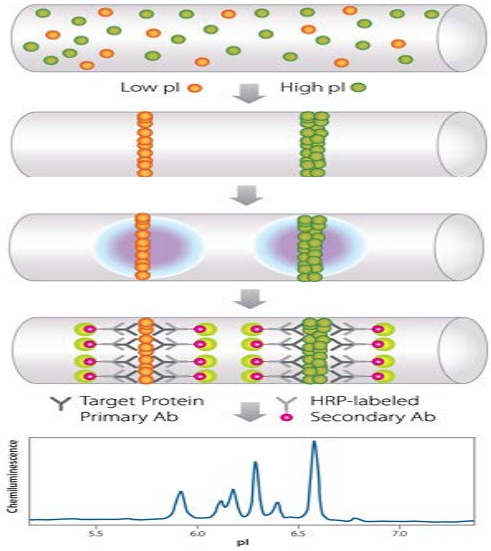

Figure 3: *Schematic view of the capillary isoelectric focusing method.* The lysate is automatically loaded into a glass capillary and proteins are separated according to their charge. After the separation process, the proteins are immobilized by UV light. Target proteins are identified using a specific primary antibody and immuno-probed using a HRP-conjugated secondary antibody and chemi-luminescent substrate. A peak profile corresponding to the amount of protein detected at different pIs is generated as a read-out (figure has been modified after http://www.proteinsimple.com/simple_western_assays.html #charge_based _assays).

1.4. Aim of the project

Motivated by an apparent lack in available information concerning Akt isoform-specific phosphorylation in neurons, this project focused on the change of Akt isoform activity in a set of different experimental paradigms in neuronal cells and brain tissue. Due to the limitations of conventionally used biochemical methods, we established and validated a novel method to analyze the phosphorylation status of the different Akt isoforms. Akt1-3 kinases are specifically activated by two phosphorylation events on residues T308 and S473 upon growth factor signaling. However, we still lack a clear understanding of the complexity and regulation of isoform specificity within the PI3K/PTEN/Akt pathway. We utilized a capillary-based isoelectric focusing method to study dynamics of Akt phosphorylation in neuronal cells and the developing brain and identify previously undescribed features of Akt phosphorylation and activation. For the first time, we were able to show all three Akt isoforms with cIEF in a neuronal background. In this project we could demonstrate the presence of complex phosphorylation events of Akt in a signal-dependent manner in neurons of different developmental stages. We provide evidence for uncoupling of S473 and T308 phosphorylation, as well as differential sensitivities of Akt1 forms upon PI3K inhibition. The analysis of developmental regulated Akt signaling in postnatal rat brain tissue showed a transient shift in Akt isoform phosphorylation and activation pattern during early postnatal brain development, at stages corresponding to synapse development and maturation. This complex relationship between PTMs and activity of Akt and the non-redundant role of the three isoforms built the base for this project for the investigation of Akt phosphorylation of the different isoforms within the PI3K-PTEN-Akt pathway and brain development.

2. Materials and methods

2.1. Materials

2.1.1. Chemicals

Table 1: *List of chemicals*

Name	Company	Catalog number
A66	Selleckchem	No. S2636
Acrylamide	National Diagnostics	No. EC-890
Aqueous Inhibitor Mix	Protein Simple	No. 040-482
Ammoniumpersulfate (APS)	Roth	No. 9592.2
AS252424	Tocris	No. 3671
B27	Life Technologies	No. 17504044
β-Mercaptoethanol	Sigma	No. M7522
BDNF	R&D Systems	No. 248-BD-005
Bicine/CHAPS Lysis Buffer	Protein Simple	No. 040-764
Bovine Serum Albumin (BSA)	Roth	No. 8076.4
DABCO	Roth	No. 0718.1
Dulbecco's Modified Eagle Medium (DMEM)	Invitrogen	No. 31331028
DMSO	Applichem	No. A3672,0100
DMSO Inhibitor Mix	Protein Simple	No. 040-510
Dithiothreitol (DTT)	Applichem	No. A1101,0010
ECL Western Blotting Substrate	Promega	No. W1001
Ethanol	Roth	No. P075.5
Fetal calf serum (FCS)	Biochrom	No. S0115
GDC-0941	Selleckchem	No. S1065
GlutaMax	Invitrogen	No. 25030-024
Glycerine	Sigma	No. G5516
GNF5837	Axon Medchem	No. 2248
Goat Serum	Gibco	No. 16210-072
IC87114	Calbiochem	No. 528118
Insulin	Sigma	No. I9278
Methanol	Roth	No. CP43.4

Milk powder, blotting grade	Roth	No. T145.3
Mowiol	Sigma	No. 81381
NanoPro100 Masterkit	Protein Simple	No. CBS3000
NanoPro Premix G2	Protein Simple	No. 040-972
Neurobasal-A	Invitrogen	No. 21103-049
NP-40	US Biological	No. 3500
PageRuler Protein ladder	Thermo	No. 112289
Paraformaldehyde (PFA)	Merck	No. 1040051000
Penicillin/Streptomycin	Invitrogen	No. 15070-063
Phosphate Buffered Saline (PBS)	Applichem	No. A9191,0012
Phosphatase Inhibitor Cocktail 2	Sigma	No. P5726
Phosphatase Inhibitor Cocktail 3	Sigma	No. P0044
pI Standard ladder 3	Protein Simple	No. 040-646
Ponceau Red	Sigma	No. 09189
Poly-Ornithine	Sigma	No. P8638
Protease Inhibitor Cocktail 3	Calbiochem	No. 539134
Resolving Buffer	National Diagnostics	No. EC-892
RIPA Buffer	Sigma	No. R0278
Roti®-Load	Roth	No. K929.1
Rotiphorese® SDS-PAGE	Roth	No. 3060.2
Sodium Azide (NaN_3)	Sigma	No. S2002
Sodium Chloride (NaCl)	Roth	No. 9265.1
Sodium Deoxycholate	Applichem	No. A1531,0100
Sodium Dodecyl Sulfate (SDS)	Calbiochem	No. 428029
Stripping Buffer	Applichem	No. A7140
Temed	Merck	No. 1107320100
Tetradecanoyl-phorbol-acetate (TPA)	Sigma	No. P8139
TGX-221	Cayman Chemical	No. 10007349
Tris Hydrochloride (Tris-HCl)	Roth	No. 9090.3
Triton-X-100	US Biological	No. T8655
Trypsin EDTA	Life Technologies	No. 25300-062
Tween-20	Calbiochem	No. 655205
Wortmannin	Sigma	No. W1628

2.1.2. Buffers and solutions

Table 2: *List of Buffers*

Name	Chemical composition
Running Gel (8%)	4,8 mL dH_2O 2,5 mL Resolving Buffer 2,7 mL Acrylamide 100 µL APS (10%) 10 µL Temed
Stacking Gel (3,75%)	3,1 mL dH_2O 1,25 mL Stacking Buffer 0,65 mL Acrylamide 25 µL APS (10%) 5 µL Temed
Stacking buffer (pH 6,8)	0,5 M Tris-HCl 0,4% (w/v) SDS 200 mL dH_2O
TBS-T (10x, pH 7,4)	2L dH_2O 50mM Tris-HCl 150 mM NaCl 0,05% Tween-20
DMEM for N1E-115 cells	500 mL DMEM with pyruvate 1% (v/v) mL Penicillin/Streptomycin 10% (v/v) mL FCS 200 mM GlutaMax

Name	Chemical composition
Neurobasal medium for primary neurons	50 mL Neurobasal-A 1% (v/v) mL Penicillin/Streptomycin 2% (v/v) mL B27 200 mM GlutaMax
Blocking solution (in PBS)	2% BSA 1% (v/v) Goat serum 0,1% (w/v) Sodiumazide (0,2% (v/v) Triton-X-100)
Mowiol	5 g Mowiol 20 mL PBS 10 mL Glycerine 2,5% (w/v) DABCO
RIPA lysis buffer (500 mL in H_2O)	50 mM Tris-HCl 150 mM NaCl 0,5% (w/v) Sodiumdeoxycholate 1% (v/v) NP-40 0,1% (w/v) SDS

2.1.3. Cells and animals

Table 3: *Cells and animals*

Name	Company
C57/bl6 mice	FEM
Wistar rats	FEM
N1E-115 cells	stock in the lab

2.1.4. Antibodies

Table 4: *Primary antibodies* (IC: Immunocytochemistry, IB: Immunoblot, cIEF: Capillary isoelectric focusing, m: monoclonal, p: polyclonal)

Name	Company	Source	Concentration
α-Tubulin	Sigma, #T6199	mouse (m)	IB: 1:3000
Akt-pan	Cell Signaling, #9272	rabbit (p)	IB: 1:1000 cIEF: 1:50
Akt1	Millipore, #05-669	rabbit (m)	IB: 1:1000 cIEF: 1:50
Akt2	Cell Signaling, #3063	rabbit (m)	IB: 1:1000 cIEF: 1:50
Akt3	Upstate, #03-383	rabbit (p)	IB: 1:1000 cIEF: 1:50
p(Thr34)Akt	Upstate, #07-789	rabbit (p)	IB: 1:500
p(Thr308)Akt	Cell Signaling, #2965	rabbit (m)	IB: 1:1000 cIEF: 1:25
p(Tyr326)Akt	Santa Cruz, #sc-109904	rabbit (p)	IB: 1:500
p(Thr450)Akt	Cell Signaling, #9267	rabbit (p)	IB: 1:1000 cIEF: 1:25
p(Ser473)Akt	Cell Signaling, #4060	rabbit (m)	IB: 1:1000 cIEF: 1:25
p(Ser474)Akt2	Cell Signaling, #8599	rabbit (m)	IB: 1:1000
Bax	Santa Cruz, #sc-493	rabbit (p)	IB: 1:1000
Cyclin B1	Santa Cruz, #sc-70898	mouse (m)	IB: 1:500
Cyclin E	Santa Cruz, #sc-377100	mouse (m)	IB: 1:1000
EGFR	Millipore, #04-290	mouse (m)	IB: 1:1000
p(Tyr1068)EGFR	Cell Signaling, #2234	rabbit (m)	IB: 1:500
ERK1/2	Cell Signaling, #4695	rabbit (m)	IB: 1:1000
p(Thr202/Tyr204)ERK1/2	Cell Signaling, #4370	rabbit (m)	IB: 1:1000

GAPDH	Calbiochem, #CB1001	mouse (m)	IB: 1:5000
GFAP	SynapticSystems, #173002	rabbit (p)	IB: 1:1000
GSK3ß	Cell Signaling, #9832	mouse (m)	IB: 1:1000
p(Ser9)GSK3ß	Cell Signaling, #9323	rabbit (m)	IB: 1:1000
MAP2	Cell Signaling, #4542	rabbit (p)	IB: 1:1000
MCM7	Santa Cruz, #sc-9966	mouse (m)	IB: 1:500
p(Ser2448)mTOR	Cell Signaling, #5536	rabbit (m)	IB: 1:500
p53	Santa Cruz, #sc-6243	goat (p)	IB: 1:1000
PSD-95	NeuroMab, #K28/43	mouse (m)	IB: 1:5000
PTEN	Cell Signaling, #9559	rabbit (m)	IB: 1:2000
S6 Ribosomal Protein	Cell Signaling, #2217	rabbit (m)	IB: 1:1000
p(Ser235/236)S6	Cell Signaling, #4856	rabbit (m)	IB: 1:1000
Tau1	Millipore, #MAB3420	mouse (m)	IB: 1:1000
TFEB	Bethyl, #A303-673A-T	rabbit (p)	IC: 1:500

Table 5: *Secondary antibodies*

Name	Company	Source	Concentration
Alexa Flour 488 goat-anti-rabbit	Invitrogen, #A11006	rabbit	IC: 1:1000
HOECHST	Sigma, #14530		IC: 1:100.000
HRP-conjugated anti-rabbit-IgG	Vector Labs, #PI1000	rabbit	IB: 1:3000
HRP-conjugated anti-mouse-IgG	Vector Labs, #PI2000	mouse	IB: 1:3000
HRP-conjugated anti-goat-IgG	Santa Cruz, #2020	goat	IB: 1:3000
HRP-conjugated goat-anti-rabbit	Protein Simple, #040-656	rabbit	cIEF: 1:100
HRP-conjugated goat-anti-mouse	Protein Simple, #040-655	mouse	cIEF: 1:100

2.1.5. Kits

Table 6: *Kits*

Name	Company	Catalog number
Coomassie Brilliant Blue R-250 Staining Solutions Kit	BioRad Laboratories	No. 161-0436
Pierce® BCA Protein Assay Kit	Thermo Scientific	No. 23225

2.1.6. Equipment and software

Table 7: *Machines*

Name	Company
Centrifuge 5430R	Eppendorf, Germany
Table centrifuge MiniStar	VWR, USA
NanoPro™100	Protein Simple Inc., USA
Fusion SL Camera	Vilber Lourmat, Germany
HERAcell CO_2 Incubator	Heraeus, Germany
Confocal microscope TCS SP5	Leica, Germany
Mini Protean Tetra System	BioRad Laboratories, USA

Table 8: *Software*

Name	Company
Compass™	Protein Simple, USA
ImageJ	National Institutes of Health, USA
Prism 5	GraphPad Software, USA

2.2. Methods

2.2.1. Cell culture

Culture and treatment of N1E-115 cells

N1E-115 were routinely maintained at 37 °C and 5% CO_2 in DMEM supplemented with 10% heat inactivated FCS, 200 mM GlutaMax and 100 U/mL Penicillin/Streptomycin (P/S). For treatments, N1E-115 cells were seeded in a 12-well plate at a density of 26.000 cells/cm^2. They were kept in DMEM without serum for 48 hours prior to growth factor treatment. 100 nM Insulin was added directly to the medium for indicated time periods. Following treatments, the cells were washed twice with ice-cold PBS and lysed. For Western blot (WB) analysis cells were lysed in 100 µL RIPA buffer, for analysis by capillary isoelectric focusing (cIEF) cells were lysed in 100 µL Bicine/CHAPS buffer per well.

For PI3K inhibition experiments, cells were routinely kept in DMEM containing 10% FCS. Two days after plating the cells, 5nM – 1µM Wortmannin (WM) was applied for up to 30 minutes. Again, right after treatment the cells were washed twice with ice-cold PBS and lysed according to use.

Culture and treatment of mouse primary neurons

Primary cortical neuronal cultures were prepared from wild type or $PTEN^{floxed/floxed}$ C57/bl6 mouse embryos at E16 and kept at 37 °C and 5% CO_2 in Neurobasal-A supplemented with 2% B27, 200 mM GlutaMax and 100 U/mL P/S. Half of the medium was refreshed once a week and cells were kept either for 7 days (7 DIV) or 3 weeks (21 DIV). For biochemical analysis, cortical neurons were seeded in 12-well plates on poly-L-ornithine coated coverslips at a density of 79.000 cells/cm^2. To stimulate the cells, different growth factors (100 nM Insulin, 50 ng/mL BDNF, 40 ng/mL EGF) were applied directly to the medium, gently mixed, and incubated for 15 min.

Prior to EGFR inhibition treatments, cortical neurons were starved in Neurobasal-A medium without B27 for 5 hours. For the last hour of starvation, the EGFR inhibitor (10 nM or 1 µM Gefitinib) was added either in the presence or absence of the receptor agonist.

To test the role of the different catalytic PI3K subunits (p110α,β,γ,δ), unstarved cortical neurons were treated with specific subunit inhibitors (GDC-0941, AS252424, IC87114, A66, TGX-221) for 30 min. Directly after treatment the cells were washed twice with ice-cold PBS and lysed according to use. For WB, cells were lysed in 100 µL RIPA buffer, for subsequent analysis by cIEF cells were lysed in 100 µL Bicine/CHAPS buffer per well.

The time course samples of cortical development *in vitro* (2 DIV – 21 DIV) were kindly provided by Annika Brosig.

Viral infection of primary cortical neurons

Viruses used in this work were kindly provided by Dr. Till Mack. To briefly summarize the generation, a modified lentiviral vector was used, in which a human Synapsin-1 promoter drives the expression of the RFP-Cre transgene. Lentiviruses were produced by co-transfecting HEK293T cells with the lentiviral vector and two helper vectors, pVSVg and pCMV-delta R8.9 [Xue et al. 2009; Lois et al. 2002]. Viral supernatants were collected 48 hours after transfection. The supernatant was aliquoted and stored at -80 °C. For *in vitro* experiments, 150 µL virus particles were added to one well of a 12-well plate with cultured floxed PTEN neurons 12 days after plating (12 DIV). 9 days post-transduction neurons (21 DIV) were harvested in either 100 µL RIPA or Bicine/CHAPS buffer with freshly added inhibitors and lysates were prepared for WB or cIEF.

Culture and treatment of rat primary hippocampal neurons

Primary hippocampal neurons were prepared from P1 Wistar rats and kept at 37 °C and 5% CO_2 in Neurobasal-A supplemented with 2% B27, 200 mM GlutaMax and 100 U/ml P/S. Half of the medium was refreshed once a week and cells were kept for 3 weeks (21 DIV). For immunochemical analysis, the cells were seeded in 24-well plates on poly-L-ornithine coated coverslips at a density of 21.000 cells/cm^2. Treatments were carried out in the same way as described for cortical neurons.

Whole rat brain lysates

For whole brain lysates, kindly provided by Beate Diemar, Wistar rats were sacrificed at different ages (P0 – 30 weeks) and the entire forebrain was collected. The brains were lysed in RIPA buffer, aliquoted and stored at -80 °C until further use.

Astrocyte culture

Astrocytes for this work were kindly provided by Dr. Kai Murk. To briefly summarize the culture, prior to seeding cortical astrocytes, culture dishes were coated with a solution consisting of 0,025% collagen and 15 µg/mL poly-L-ornithine for 30 min at 37 °C and 5% CO_2. After removing the solution from the dishes, astrocytes were seeded immediately. Astrocytes were obtained from E16.5 C57/bl6 mice and plated onto T75-flasks with 15 ml DMEM containing 10% FCS and 1% P/S. They were grown at 37 °C with 5% CO_2 in a cell incubator until they reached 80-90% confluence.

2.2.2. Biochemical methods

Protein isolation

For whole protein extraction the cells were lysed and scraped using RIPA lysis buffer. Following incubation on ice for 20 min, lysates were centrifuged for 20 min at 14.000 rpm at 4 °C. The supernatants were harvested and stored at -80 °C for analysis.

Immunoprecipitation (IP)

21 DIV cortical neurons from a T75 flask were lysed in 900 µL RIPA containing protease and phosphatase inhibitors. The cells were scraped off the flask, transferred into Eppendorf tubes, vortexed and rotated at 4 °C for 25 minutes. After again vortexing the samples they were centrifuged at full speed for 25 minutes. The supernatant was replaced and 1/10 kept to probe in WB later as total cell lysate. To preclear the lysate 60 µL G-protein agarose beads per sample were prepared. The beads were spun down at 4500 rpm for 4 minutes. Followed by two washes with 1x PBS by spinning them down at 6000 rpm for 3 minutes. PBS was aspirated with a syringe between washing steps. All centrifugation steps were performed at 4 °C. Finally beads were washed once with RIPA and then resuspended in 60 µL (original volume) RIPA. The cleared supernatant from above was added to the beads and rotated at 4 °C for 1 hour. Afterwards the lysate - bead mixture was spun down at 6000 rpm for 3 minutes. The precleared supernatant was transferred to new tubes with 10 µL p(T308)Akt antibody and rotated over night at 4 °C. On the next day fresh beads were prepared as described above. The lysate - antibody mixture was added to the newly prepared beads and rotated for 2 hours at 4 °C. The tubes were spun down at 6000 rpm for 3 minutes. The supernatant was harvested and kept to probe later for p(T308)Akt analysis by WB. The pellet was washed 5x in RIPA. Following the last centrifugation the pellet was resuspended in 2x Roti®-load (20 µL/sample) and boiled at 95 °C for 5 minutes. After centrifugation the supernatant was replaced into a new tube using a syringe. 20 µL 1x Roti-load was added to the remaining pellet and again boiled at 95 °C for 5 minutes and centrifuged. The supernatant was added to the previous supernatant, together providing the IP sample to test in WB.

N1E-115 and primary cortical lysates for NanoPro100

N1E-115 cells or primary cortical neurons were washed twice with ice-cold PBS and afterwards lysed with 100 µL Bicine/CHAPS containing 1x aqueous inhibitor and 1x DMSO inhibitor. After incubation on ice for 20 minutes, the lysate was centrifuged for 20 minutes at 14.000 rpm at 4 °C and the supernatant was transferred into a new tube and aliquoted. Aliquots were stored at -80 °C. For λ-phosphatase treatments N1E-115 protein samples were

incubated with or without phosphatase for 30 minutes at room temperature (RT) directly before performing WB analysis or cIEF.

Quantification of protein concentration

The protein concentration of a sample was quantified using the Pierce®BCA Protein Assay kit. The method was carried out following the instructions of the supplier (http://www.piercenet.com/instructions/2161296.pdf). Protein samples were diluted 1:5 and the assay was performed in 96-well plates, which were incubated at 37 °C for 30 minutes. The concentration was then measured photometrical at 562 nm.

SDS-PAGE

Protein samples for immunoblot analysis were obtained from N1E-115 cells or primary cortical neurons (see section 2.2.1). 4x Roti®-load was added to the protein extracts, which were boiled at 95 °C for 5 min. The separation was carried out on a 3,75% stacking gel and a 8% running SDS gel. Until the samples reached the running gel a voltage of 60 V was used, before the voltage was increased to 120 V.

Western blot (WB) analysis

Blotting was carried out with nitrocellulose membrane using a tank transfer system from Bio-Rad. The membrane was blotted for 2 hours at 400 mA. In order to check the blot the membrane was placed in a petri dish with Ponceau red to visualize proteins. The color was washed off with 1x TBS-T before the detection reaction.

Immunodetection

After complete removal of Ponceau red, membranes were blocked in 5% skim milk for at least 30 minutes at RT. The membranes were first incubated with a primary antibody (see Table 4) in 5% skim milk overnight at 4°C. The next day after washing three times with 1x TBS-T, nitrocellulose membranes were incubated with secondary horseradish peroxidase (HRP) conjugated antibody (see Table 5) in 5% skim milk for at least 1 hour at RT. After washing, the immunoreaction was visualized using ECL Western Blotting substrate and expose using Vilber Lourmat System®. After exposure the procedure of immunodetection was repeated for the loading control. Anti-GAPDH (1:5.000) or anti-αTubulin (1:5.000) was incubated overnight at 4 °C in 5% skim milk and HRP-conjugated anti-mouse IgG (1:3.000) was used as secondary antibody.

Membrane λ-phosphatase treatment

The SDS gel and blotting of the proteins to a nitrocellulose membrane were done as described above. After the transfer the membrane was washed twice in 1x TBS-T, followed by one wash in 0,1 M Tris (pH 8,5) and one wash in 0,1 M Tris (pH 8,5) with 5 mM $MgCl_2$ for 10 minutes each, to remove the TBS-T. The membrane was transferred to 0,1 M Tris (pH 8,5) containing 5 mM $MgCl_2$ with or without (control) λ-phosphatase at a final concentration of 10 U/mL and incubate for 5 hours at RT. After the treatment the membrane was washed twice in 1x TBS-T for 10 minutes each. After washing the membrane, immunodetection was carried out as described above.

2.2.3. Immunocytochemistry

Staining of primary hippocampal neurons

Primary hippocampal cultures were kept until 21 DIV (see 2.2.1). In order to fix the cells, half of the medium was replaced by warm 4% PFA for 5 minutes. Afterwards the medium/PFA mixture was removed and replaced solely by 4% PFA for another 15 minutes. The fixed neurons were washed twice with PBS. At this point the neurons can be kept in PBS + sodiumazide at 4 °C.

For staining of the neurons, they were first permeabilized in blocking buffer containing 0,1% Triton-X-100 for 1 hour. After the permeabilization process the cells were incubated with the primary antibody in blocking buffer. After an hour the coverslips were washed three times with PBS, 5 minutes each. The secondary antibody was also prepared in blocking solution and left on the cells for 30 minutes. For antibody dilutions please refer to Table 4 and Table 5. The coverslips were again washed three times with PBS, 10 minutes each. During the last washing step HOECHST dye (1:100.000) was added to the PBS, in order to stain the nucleus of the cells. Finally the coverslips were mounted onto glass slides using Mowiol. Slides were left to harden at RT overnight and afterwards stored at 4 °C.

Confocal microscopy

Confocal images of rat primary hippocampal neurons were acquired with an upright laser microscope (Leica TCS SP5) equipped with a 20x, 40x and 63x (oil-immersion) objective using sequential scanning with the 488 nm line of the Argon laser, and the 543 nm and 633 nm from a helium-neon laser (for AlexaFluor 488, AlexaFluor 568 and AlexaFluor647, respectively). The nuclear HOECHST staining was captured with the 405 nm diode laser. Z-stacks were generated using a 0.3 µm step size. Background correction and adjustment of brightness and accordingly contrast was performed using ImageJ software.

2.2.4. NanoPro100 Akt assay

A master mix of (5-8) nested G2 Premix, pI standard ladder 3 and an additional 5.5 pI standard was prepared. According to a final protein concentration of 75 - 125 ng protein/capillary, Bicine/CHAPS as sample diluent, DMSO inhibitor and the protein sample were added to the ampholyte containing master mix. For the DTT treatment, N1E-115 cell lysates were incubated in Bicine/CHAPS + 53 mM DTT for 5 minutes at RT. Afterwards samples were mixed with the inhibitor and G2 Premix as described above. DTT had a final concentration of 40 mM when samples were loaded in the capillary. Samples and antibodies were transferred to the assay plate. Luminol/peroxide, washing buffer, catholyte and anolyte were used according to manufacturer protocol. During the fully automated process of the NanoPro100 assay the proteins were separated by isoelectric focusing for 40 min at 21000 µW, followed by immobilization through UV exposure for 100 sec. Primary antibodies (see Table 4) were incubated in the capillary for 4 hours with two subsequent wash steps of 150 sec each. The secondary antibody was incubated in the capillary for 1 hour with two subsequent wash steps of 150 sec each. Last, luminol/peroxide reagent was passed through the capillaries and chemiluminescence was detected. Bound primary antibodies were detected with HRP goat-anti-rabbit secondary antibody at 1:100 dilutions. Analysis of the optimal linear detection range identified 240 sec exposure as optimal, which was used for all figures and quantification of cIEF experiments unless stated differently. Peak integration and pI marker calibration was performed using Compass™ software as previously described [O'Neill et al. 2006].

3. Results

The aim of the project was to get further, more detailed insight into the PI3K/PTEN – Akt signaling pathway, with emphasis on the differences on activation of the different Akt isoforms depending on upstream cues. In order to do so, we developed a cIEF assay to monitor Akt in neuronal tissues. Important results are discussed throughout this section in order to clarify the findings for the reader.

3.1. Akt cIEF assay development and peak identification

To investigate the different Akt isoforms and their post-translational modifications (PTM) standardized biochemical methods (e.g. Western blot) have certain limitations. For example, with WB it is possible to assess the total phosphorylated protein isoforms with phospho-specific antibodies or the abundance of one isoform, independent of its PTMs, with isoform-specific antibodies. Therefore, we made use of capillary isoelectric focusing (cIEF). We used the NanoPro100™ from Protein Simple (USA) to separate proteins according to their net charge, allowing the separation and detection of phospho-forms as well as isoforms of the same protein by a single antibody. The basic parameters for this assay were optimized using N1E-115 neuroblastoma cells. Initially we used the panAkt antibody to assess the peak profile of N1E-115 cells. These lysates gave a panAkt profile with 10 peaks. The NanoPro assay detects proteins in their native state therefore, leading to the detection of protein complexes and quaternary structures found in cell signaling pathways. In order to try optimizing our Akt cIEF assay we used DTT to slightly denature the proteins, thereby getting a greater resolution, better peak efficiency and reducing the numbers of non-specific interactions. However, the usage of DTT on the N1E-115 cell lysates did not provide a better resolution in comparison to untreated cell lysates (see Figure 4A). Therefore, we did not use DTT for further experiments. We also established the optimal exposure time for our assay. The NanoPro device provides six pre-set exposure times ranging from 30 - 960 sec. We quantified the area under each detected peak in order to test for linearity with increasing exposure times. We found an optimal range from 240 - 480 sec, the maximum exposure of 960 sec did not improve the signals. In fact, at higher exposure times the area proportions were non-linear (see Figure 4B). After setting the basic parameters for the assay we employed it in different cell types. To study Akt in a neuronal context, we used N1E-115 and primary cortical cell lysates, as well as whole brain lysates. Using WB we could show, that all three Akt isoforms are expressed in all of the different lysates (see Figure 5A). When N1E-115 cell lysate were probed with a panAkt antibody, we identified 10 peaks in the cIEF profile, with corresponding isoelectric points (pIs) of 5.06, 5.14, 5.21, 5.31, 5.42, 5.53, 5.61, 5.68, 5.76 and 5.85. Probing cell lysates of primary cortical neurons, the panAkt antibody

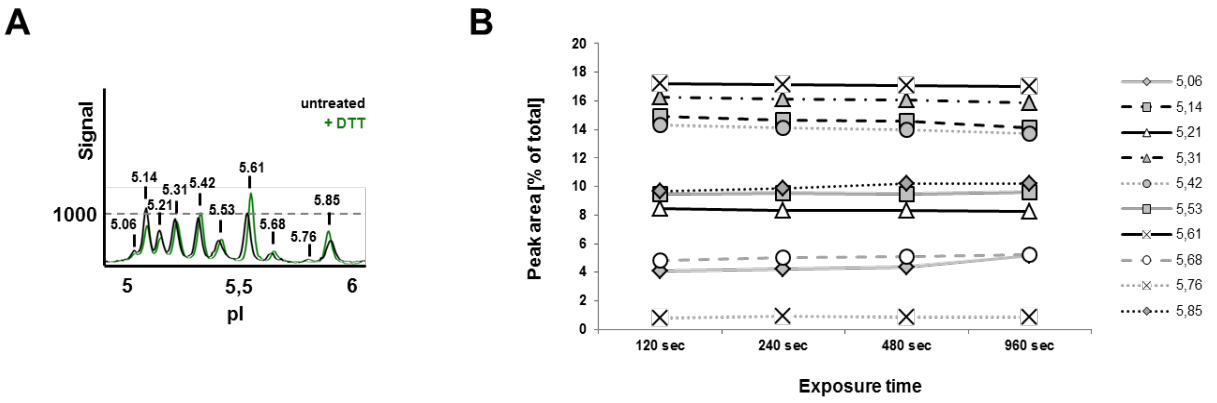

Figure 4: *Optimization of the cIEF Akt assay.* **(A)** Untreated or 40 mM DTT treated N1E-115 cells were analyzed with the panAkt antibody by cIEF in order to compare the resolution of the peaks. **(B)** The area under the peaks (in %) was calculated for different exposure times. A slight change in linearity for some peaks (5.06, 5.14, 5.31) was only observed after 960 sec exposure

resulted in the same peak profile of 10 conspicuous peaks with identical pIs (5.06, 5.14, 5.21, 5.31, 5.42, 5.53, 5.61, 5.68, 5.76 and 5.85), however, one additional, more acidic peak species with a pI of 5.01 was identified. The peak profile detected for brain lysate presented all of the N1E-115 cell specific peaks, with the exception of the 5.85 peak (see Figure 5B). Across the different neuronal samples tested the relative abundance of Akt molecules changed significantly, this is representative of potential context dependent modifications or cell/tissue specific alterations in the isoform expression profiles. To get further, more detailed insight into the neuronal peak profiles, we used the isoform-specific antibodies recognizing Akt1, Akt2 or Akt3 (see Figure 5C). In N1E-115 cells, the most acidic peaks - 5.06, 5.14, 5.21, 5.31, 5.42, 5.53, 5.61, 5.68 - with 5.53 showing the largest signal, were recognized by the Akt1 antibody. The Akt2 antibody gave a more restricted panel with two evident peaks at pIs of 5.68 and 5.85, the latter showing the largest signal. Detection using the Akt3 antibody gave two specific peaks at pIs 5.61 and 5.76, with 5.76 being the dominant signal. In addition, three non-specific peaks with a pI >5.80 were found, which may represent the upper band detected by WB of N1E-115 cell lysate (see Figure 5A). Comparison of the peak profiles of primary cortical neurons with that of brain lysate, showed similar peak patterns, except that the Akt2 antibody recognized an additional peak at 5.61 in whole brain lysate. In accordance with previous publications [WS Chen et al. 2001; Cho, Thorvaldsen, et al. 2001], Akt1 was the most abundant isoform in all three neuronal lysates, however, it exhibited minor changes in the specific pI value across the samples. In neuroblastoma cells, the main Akt1 molecule was found at pI 5.53, in cortical neurons at 5.42, whereas in brain lysate at a pI of 5.61. These results suggest that the extent of PTMs seem to vary between different cell types. In conclusion, these results support the validity of the Akt cIEF assay in in its application to analyze neuronal lysates. cIEF provides highly reproducible results and pIs

detected for the three Akt isoforms are in agreement with previous reports of Akt profiles established in cancer cells [H Guo et al. 2014; Iacovides et al. 2013; Sabnis et al. 2014].

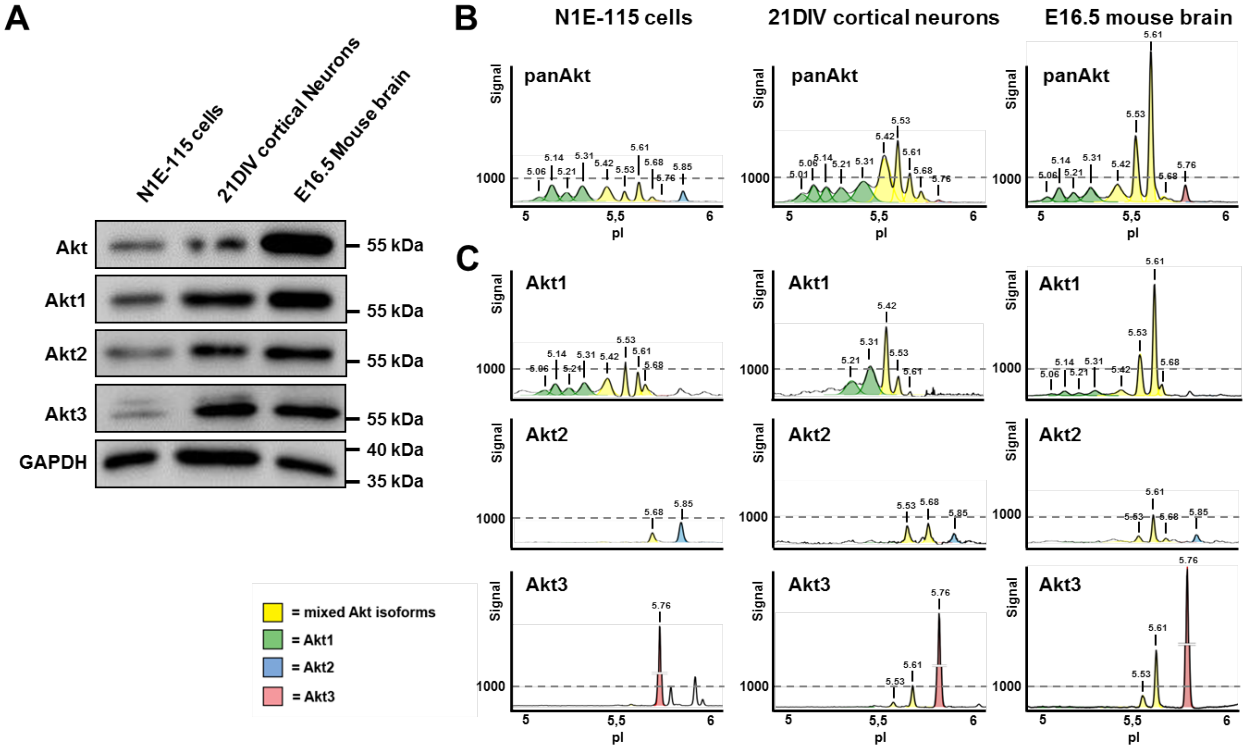

Figure 5: *Akt cIEF assay development and peak identification.* **(A)** Western blot analysis of Akt isoforms (Akt1-3) in cell lysates obtained from N1E-115 neuroblastoma cells, primary cortical neurons (21 DIV) and embryonic mouse brain (E16.5). **(B)** Capillary isoelectric focusing (cIEF) analysis of the cell lysates using a pan-Akt antibody shows a regular Akt profile with 9-10 conspicuous peaks that are separated according to protein charge distribution (isoelectric point, pI). **(C)** cIEF analysis of cell lysates using isoform-specific Akt antibodies. In cIEF profiles, Akt1 peaks are colored in green, Akt2 in blue and Akt3 in red. Peaks with mixed Akt isoforms are colored in yellow.

3.1.1. Identification of phospho-specific Akt peaks in cIEF

In order to determine the phospho-states of the different peaks, phosphate groups in the lysates were removed with λ-phosphatase. The functionality of this treatment was checked by WB analysis using p(S473)-, p(T308)-, and p(T450)Akt antibodies (see Figure 6A). The complete loss of phosphoAkt signal confirms the specificity of the treatment. When the same samples were tested with the panAkt antibody by cIEF, λ-phosphatase treatment resulted in the absence of cIEF peaks between pI 5.06 and 5.42, identifying these as phosphorylated Akt forms (see Figure 6B). At the same time, the 5.53 and 5.76 peaks showed the greatest increase in signal and a new peak at 6.02 emerged. These signals were categorized as the three non-phosphorylated Akt isoforms (see Figure 6B). To confirm unequivocally the loss of phosphorylation by cIEF, we used the phospho-specific antibodies pS473, pT308, or pT450. Phosphorylation on T450 has previously been characterized as a constitutive Akt

phosphorylation event, unresponsive to activation of the protein [Facchinetti et al. 2008] and, indeed, detection using the p(T450)Akt antibody in cIEF produced the exact same peak profile as the panAkt antibody (see Figure 6C). However, the specificity of the p(T450)Akt antibody towards phosphorylated Akt species was confirmed by λ-phosphatase treatment leading to a loss of any signal (see Figure 6D).

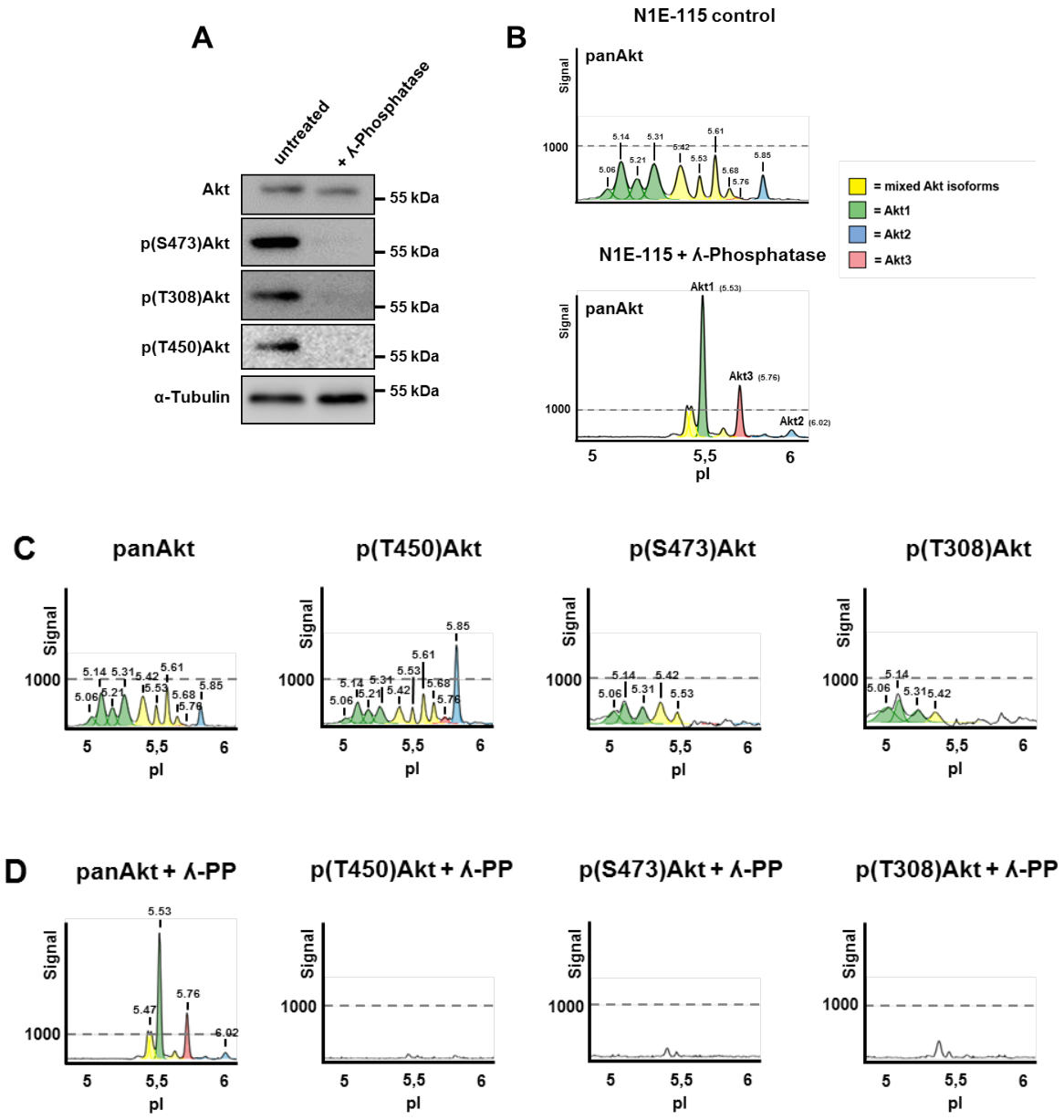

Figure 6: *Identification of phospho-specific Akt peaks and peak distribution after λ-Phosphatase treatment in N1E-115 neuroblastoma cells.* **(A)** N1E-115 cell lysates were treated with λ-Phosphatase before Western blot analysis using indicated antibodies. **(B)** The same cell lysates were analyzed using cIEF; peak profiles demonstrate the loss of peaks with a pI <5.42 after λ-Phosphatase treatment, identifying them as phosphorylation containing peaks. **(C)** N1E-115 cell lysates were analyzed by cIEF using phospho-specific Akt antibodies. **(D)** After λ-Phosphatase treatment of N1E-115 cell lysates, the three phosphorylation-specific Akt antibodies did not detect any peaks, confirming the specificity of cIEF in detecting phosphorylated Akt species.

The new occurring peak with the pI of 6.02 was not detected with the p(T450)Akt antibody. Combing this observation together with the results of the Akt2 isoform-specific antibody, we characterized this peak as non-phosphorylated Akt2. This led us to the hypothesis, that under basal conditions phosphorylated Akt2 is more abundant when compared to the non-phosphorylated form in mouse neuroblastoma cells. The results for the Akt3-specific antibody and the phosphatase treatment indicate that non-phosphorylated Akt3 peaks at 5.76. Because this peak is also recognized by the p(T450)Akt antibody, we assume a degree of heterogeneity within the peak, most likely consisting largely of non-phosphorylated Akt3 with a minor population of phospho-Akt2 molecules. For the first time, we were able to identify the Akt3 protein with cIEF in neuronal cells. Our detected pI of murine Akt3 with 5.76 is slightly higher than the theoretical prediction of 5.71 (http://web.expasy.org/compute_pi/). Antibodies of the two activating phosphorylation sites T308 and S473 recognized, as expected, the most acidic peaks of the cIEF profile. Both antibodies detected four peaks in untreated N1E-115 cells (5.06, 5.14, 5.31 and 5.42), with p(S473)Akt detecting an additional fifth peak at 5.53 (see Figure 6C). These slightly different cIEF profiles of the two activating Akt phosphorylation sites led us to the conclusion that, at least under basal conditions, phosphorylation of the two activating sites can occur independent of each other. Moreover, the T308 and S473 phosphorylation containing peaks most likely also contain other phosphorylation sites and vary in their modifications by other PTMs (i.e. ubiquitination, sumoylation). Up to 22 validated Akt phosphorylation sites have previously been reported [H Guo et al. 2014]. We tested commercially available antibodies for the known phosphorylation sites T34 and Y326 but were not able to obtain specific signals with either WB or cIEF. A summary table with all peaks detected under basal conditions and λ-Phosphatase treated cells can be found in Figure 7.

A

AB / Peak	Akt pan	Akt1	Akt2	Akt3	Akt p(T308)	Akt p(S473)	Akt p(T450)
5.01	x	x			x	x	x
5.06	x	x			x	x	x
5.14	x	x			x	x	x
5.21	x	x					x
5.31	x	x			x	x	x
5.42	x	x	x		x	x	x
5.53	x	x	x	x		x	x
5.61	x	x	x	x			x
5.68	x	x	x	x			x
5.76	x		x	x			x
5.85	x		x				x

B

AB / Peak	Akt pan	Akt1	Akt2	Akt3	Akt p(T308)	Akt p(S473)	Akt p(T450)
5.49	x	x	x	x	x	x	x
5.53	x	x					
5.68	x		x	x			
5.76	x			x			
5.85	x		x				x
6.02	x		x				

= mixed Akt isoforms
= Akt1
= Akt2
= Akt3

Figure 7: *Summary of cIEF identified Akt peaks*. **(A)** Table showing identified cIEF peaks using different Akt antibodies (AB) in cell lysates obtained from neuronal cells. **(B)** Table showing identified cIEF peaks using different Akt antibodies in NIE cell lysates treated with λ-phosphatase. In both tables, Akt1 specific peaks are colored in green, Akt2 in blue and Akt3 in red. Peaks with mixed Akt isoforms are colored in yellow.

3.2. Dynamics of Akt phosphorylation in N1E-115 cells

To get a better understanding of the relationship between the two activating Akt phosphorylation sites (T308 and S473) after growth factor stimulation, we stimulated N1E-115 cells with Insulin for different time periods, before analysis of cell lysates using cIEF and WB. Prior to stimulation, cells were starved for 48 hours in serum-free medium to erase baseline phosphorylation. As shown by WB, no phosphorylation was detectable using this starvation protocol (see Figure 8A, top), which was confirmed by testing cell lysates also with the two phospho-specific antibodies p(T308)- and p(S473)Akt in cIEF (see Figure 8B and C, left panels). To verify proper loading of the capillaries, the lysates of starved N1E-115 cells were probed with the panAkt antibody (see Figure 8A, bottom). A solid Akt phosphorylation was already detectable after 1 min Insulin stimulation with both phospho-specific antibodies in WB and cIEF (see Figure 8A-C). Detection of Akt phosphorylation upon acute Insulin treatment by WB revealed little insight into the phosphorylation dynamics, as it merely revealed a general increase in phosphorylated Akt with no changes in signal strength between 3 and 10 min of Insulin stimulation (see Figure 8A). In comparison, resulting cIEF profiles unraveled unique Akt phosphorylation features, as phosphorylation on S473 and T308 appeared to occur parallel in a cooperative process in time. Peak increases were first observed in the less acidic peaks 5.42 and 5.31. At later time points, there was a gradual appearance and increase of more acidic, and often poorly resolved peaks with pIs of 5.06 - 5.14. This result suggests that Akt undergoes different modifications in response to Insulin signaling in neuroblastoma cells before reaching steady-state levels after 15 min Insulin stimulation. Steady state profiles were characterized by four prominent acidic peaks in both p(S473)- and p(T308)Akt profiles (with pIs of 5.06, 5.14, 5.31 and 5.42), as well as an additional one in case of pS473 (pI of 5.53) (see Figure 8B and C, right panels). The latter peak was only faintly detected by the pT308 antibody and most likely corresponds to the p(S473)Akt form identified in N1E-115 lysates under basal conditions (see Figure 6C). It has to be noted, that the 5.21 peak detected with the panAkt antibody was not detected with neither the p(S473)Akt nor the p(T308)Akt antibody. However, because pT450 detected the 5.21 peak (see Figure 6C) and because it was sensitive to treatment with λ-phosphatase (see Figure 6D), we surmise that this peak may present forms of Akt precursors for S473 or T308 phosphorylation.

We quantified the area under each peaks at each time point to compare p(S473)-and p(T308)Akt levels. We found that the maximal signal for both antibodies was reached after 10 min Insulin treatment, followed by small decreases at 15 min (see Figure 8D and E). The four to five peaks detected with each antibody showed a different behavior over time. The only peak with a steady increase over the entire 15 min was the 5.53 peak with the S473 antibody (see Figure 8D). Comparison of the of S473 and T308 peaks dynamics in time

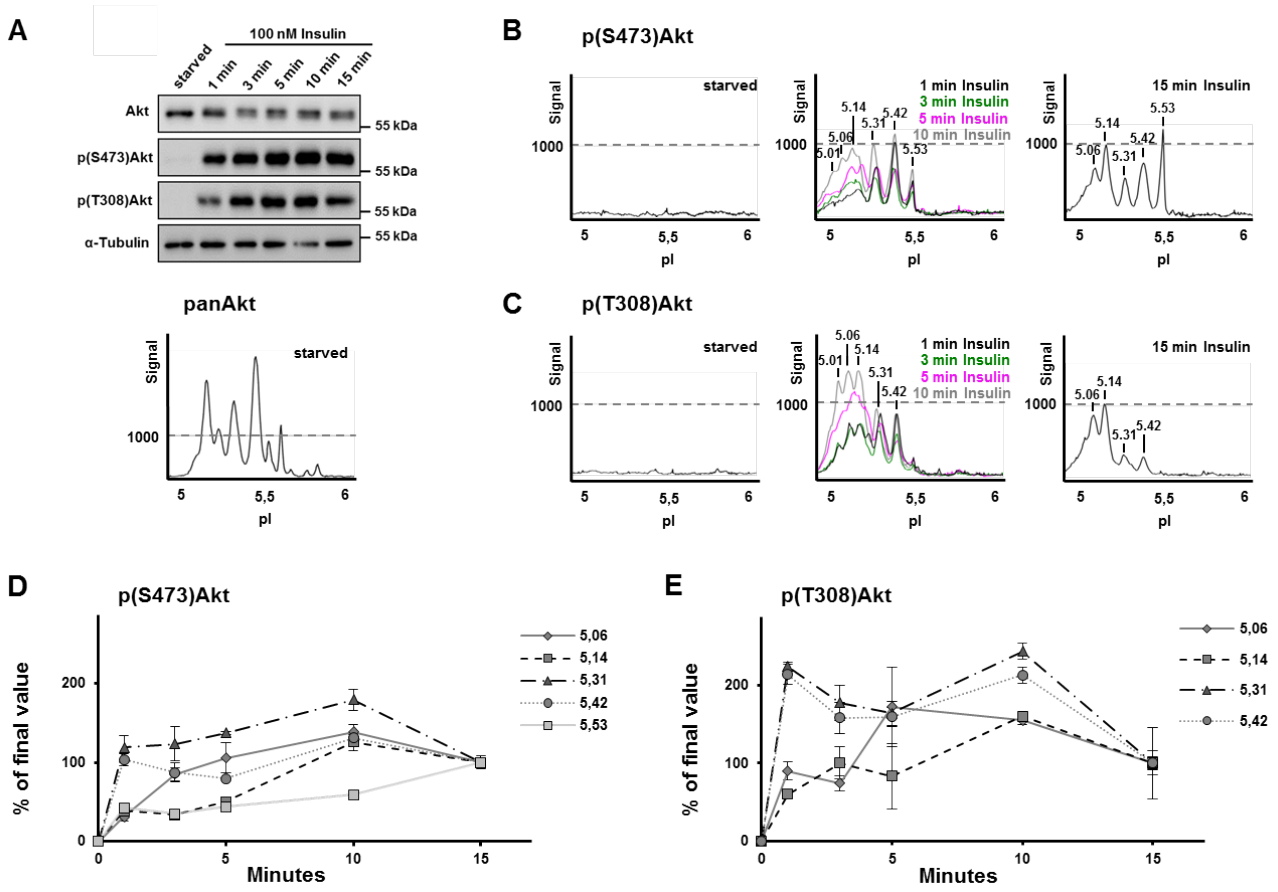

Figure 8: *Dynamics of Akt phosphorylation in response to Insulin in N1E-115 cells.* **(A)** N1E-115 cells were starved for 48 hours before Insulin stimulation for different times (1-15 minutes). Cell lysates were analyzed by Western blotting using indicated antibodies (top). Lysate of starved N1E-115 cells was analyzed by cIEF with the panAkt antibody (bottom). **(B)** N1E-115 cell lysates were analyzed in parallel by cIEF using p(S473)Akt antibody and, **(C)** p(T308)Akt antibody. **(D)** The area under each peak was quantified for p(S473)Akt and, **(E)** the p(T308)Akt antibody, demonstrating the phosphorylation dynamics in time of individual peaks.

identified differences and similarities of specific Akt phosphorylation forms. For example, the peak previously identified as Akt1 (pI 5.06) showed a steady increase during the course of the first 10 min of Insulin treatment followed by a small decrease over the next 5 min of incubation, when monitored with the p(S473)Akt antibody (see Figure 8D). In contrast, when monitored with p(T308)Akt, this peak showed an oscillating pattern with a maximum after 5 min during the 15 minutes Insulin stimulation (see Figure 8E). The peaks previously identified to contain Akt1/Akt2 (pI 5.42) showed overlapping patterns for both phospho-specific antibodies over the time course of stimulation, characterized by a rapid increase to maximal levels at 1 and 10 min of treatment (see Figure 8D and E). It should be noted here that we cannot exclude the possibility that the peaks identified by cIEF are mixed with respect to p(S473)- and p(T308)Akt, as well additional phosphorylation or other modifications. Given the complexity of growth factor-induced Akt phosphorylation cIEF profiles, a certain level of heterogeneity should be expected. Nevertheless, our results

support the assumption that both S473 and T308 phosphorylation events can occur uncoupled of each other during growth factor stimulation.

3.3. Dynamics of Akt dephosphorylation in N1E-115 cells

Experimental conditions for the inhibition of the pathway had to be defined. Using Wortmannin, a steroid metabolite of the fungi *Penicillium funiculosum, Talaromyces wortmannii* [Brian et al. 1957], a well-established, covalent inhibitor of PI3Ks, we first performed concentration- and time course experiments to assess the optimal WM concentration and treatment duration for our experiments. The phosphorylation of Akt, a PI3K downstream effector, was used as a read-out. Shown in Figure 9, we reached a good inhibition of PI3K after 30 minutes treatment with 200 nM WM. These conditions (200 nM, 30 min) were used in all subsequent WM experiments, as it leads to an almost complete loss of Akt phosphorylation at the two activating phosphorylation sites, S473 and T308.

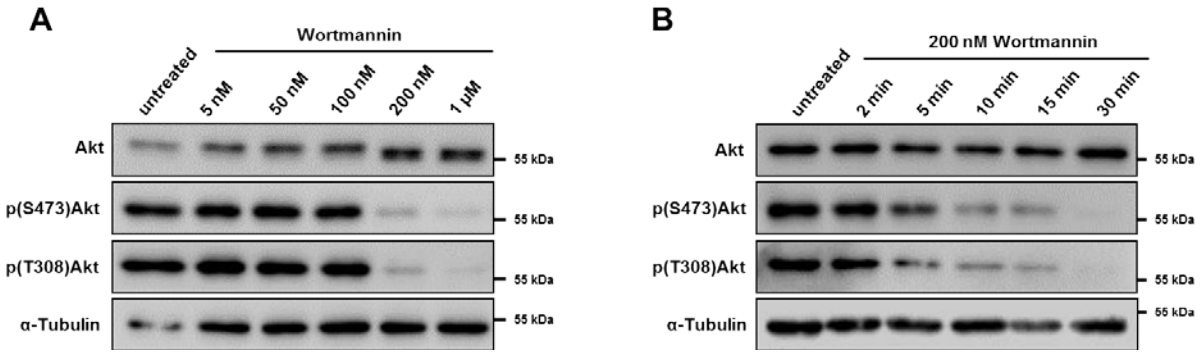

Figure 9: *Wortmannin concentration and time course*. **(A)** N1E-115 cells were treated with 5 nM – 1 µM Wortmannin for 30 minutes, with the two highest concentrations leading to almost complete loss of Akt phosphorylation. **(B)** N1E-115 cells were treated with 200 nM Wortmannin up to 30 minutes. Akt phosphorylation was almost completely lost.

WB analysis confirmed the gradual decrease in p(S473)- and p(T308)Akt over time, with complete removal of Akt phosphorylation after 30 min of WM treatment (see Figure 10A, top). In accordance, no signal in the peak profiles of p(S473)- and p(T308)Akt after 30 min WM treatment was detected by cIEF (see Figure 10B and C, right panel). To verify proper loading of the capillaries, the lysates of 30 min WM treated N1E-115 cells were probed with the panAkt antibody (see Figure 10A, bottom). Analysis of Akt dephosphorylation in response to inhibition of PI3K in time identified differential progression of events. We found, that in comparison to p(S473)-, the p(T308)Akt site seems to be more sensitive to WM treatment in

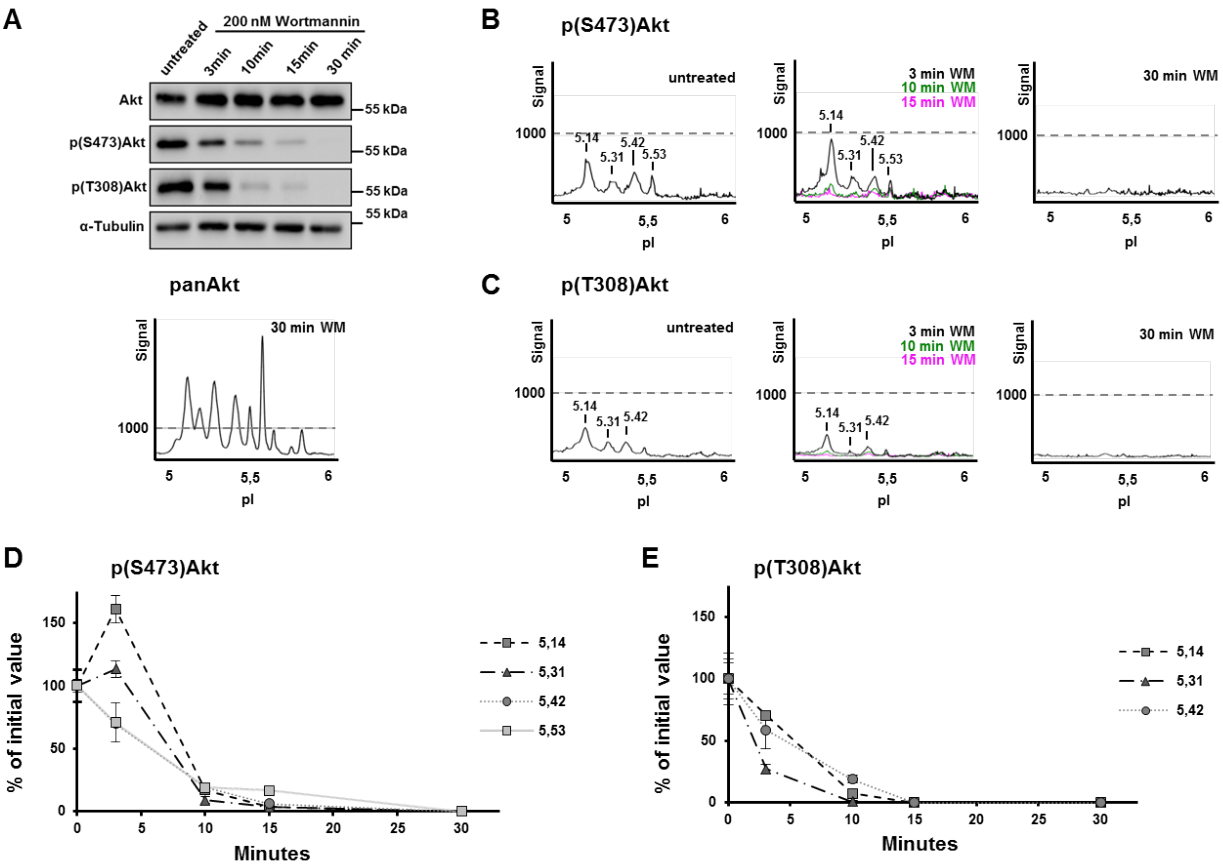

Figure 10: *Dynamics of Wortmannin-induced Akt dephosphorylation in N1E-115 cells.* **(A)** N1E-115 cells were treated with the PI3K inhibitor Wortmannin (WM) at 200 nM for different periods of time (3-30 minutes) before Western blot analysis using indicated antibodies (top). Lysate of 30 min WM treated N1E-115 cells was analyzed by cIEF with the panAkt antibody (bottom). **(B)** Cell lysates were analyzed in parallel using cIEF with p(S473)Akt and, **(C)** p(T308)Akt. **(D)** The area under each peak was quantified for p(S473)Akt and, **(E)** the p(T308)Akt signal.

WB and cIEF analysis (see Figure 10). Upon short WM treatment, cIEF detected an unexpected, specific and transient increase in S473 phosphorylation in the identified Akt1 peak at pI 5.14 (see Figure 10B and D). This effect was specific for the peak with pI 5.14 (and to some extent also for the 5.31 peak), but not for other peaks that showed similar patterns for both S473 and T308 dephosphorylation (see Figure 10B-E). This suggests that at least for some Akt forms, loss of PIP_3 results in transient upregulation of phospho-S473 but not phospho-T308. Importantly, we obtained similar patterns in different neuronal cell system, including primary cortical neurons (not shown here), which suggest this increase to reflect a regulatory component of Akt phosphorylation that occurs upon loss of PI3K signaling inputs.

3.4. Akt dynamics during postnatal brain development

The importance of the PI3K/Akt signaling pathway during brain development is known and recognized in the field. To get more detailed information of the dynamics of Akt phosphorylation and endogenous profile of the different isoforms during normal brain development we used our newly established Akt assay. Therefore, we collected brains from Wistar rats at different postnatal (P0 – P21) and adult stages (10, 30 weeks). Analysis of these brain extracts by WB with antibodies against components of the PI3K and ERK pathway involved in neuronal development showed, that in general, the expression and/or phosphorylation levels of a number of signaling proteins analyzed were downregulated either shortly before (at P15-P21; pERK, pGSK3β, p(T308)-, p(S473)- or p(T450)-Akt) or just after hard wiring was completed (after P21; S6, pS6, GSK3β). A general downregulation during postnatal and adult stages was also found for the panAkt antibody. On the other hand, whereas the amount of Akt1 seemed to remain stable for all the different ages tested, Akt2 and Akt3 protein levels show either steady increases in expression (Akt2) or remain high (Akt3) during postnatal development until P21, before sharply decreasing to lower expression levels (see Figure 11A). Total PTEN expression did not change during the time of development analyzed in this work. It has also to be noted, as the phosphorylation of ERK decreases the total amount of ERK protein seems to increase with age. Further, we analyzed different proteins important for cell division and proliferation as markers for neuronal cell cycle. The G2/mitotic-specific Cyclin B1 is a regulatory protein involved in mitosis and showed decreasing expression levels in postnatal brain. Cyclin E plays a critical role in the G1 phase and in the G1-S phase transition, shows higher expression in P0 and P7 brain lysates than Cyclin B1, but also decreases with age and was only little expressed in the brain of 30 week old mice. Another marker we examined was MCM7, this protein is essential for the initiation of DNA replication, and similar to the expression profile of the Cyclins we see the expected decrease in protein levels proportional to increasing age. In comparison, we analyzed expression levels of PSD-95, a protein which is almost exclusively located in the post synaptic density of neurons and is involved in anchoring synaptic proteins, as a marker for the brain maturation. PSD-95 levels increase with the age of our samples. Accordingly, the expression level of Tau1, a protein functioning in modulating the stability of axonal microtubules, another marker for brain maturation, also increases in older brain samples and shows a high phosphorylation of the protein, as detected by multiple upper bands (see Figure 11A). When the brain samples were analyzed by cIEF, prominent shifts in the peak profile occurred throughout postnatal development for panAkt, Akt1, p(S473)Akt, (see Figure 11B-E), whereas the profiles for Akt2 and Akt3 remained largely unchanged (see Figure 11F, G). The cIEF profile of p(T308)Akt demonstrated dynamic changes similar to that of the p(S473)Akt profile, with a transient increase in highly acidic peaks at P7/P15. We

hypothesize, that the identified cIEF peak shift to more acidic Akt forms that occurred during postnatal development signifies altered phosphorylation during stages corresponding to synapse development and maturation.

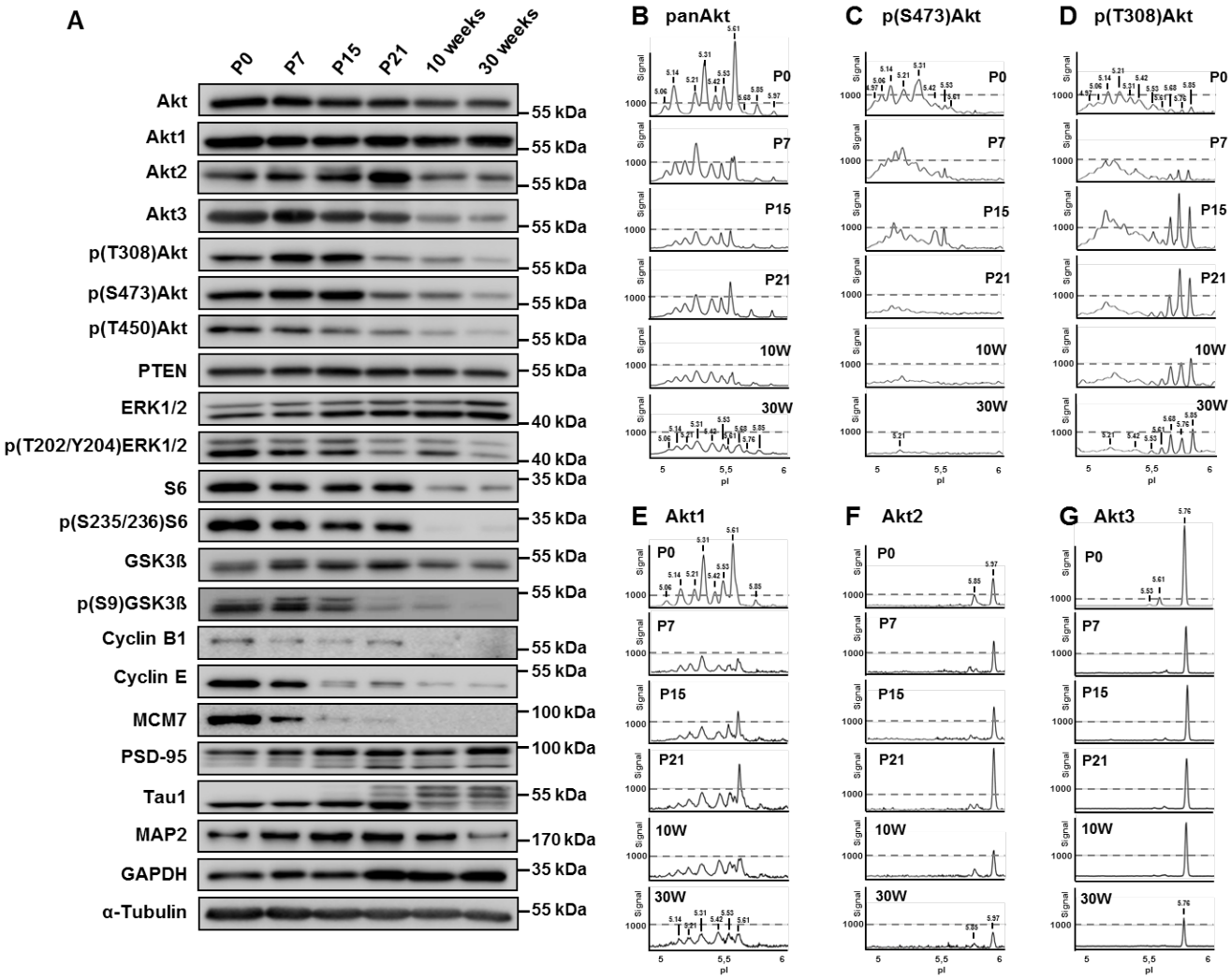

Figure 11: *Analysis of PI3K signaling strength during rat brain development*. **(A)** Western blot analysis of rat brain lysates obtained at different postnatal and adult stages (P0 – 30 weeks) using antibodies against structural and signaling proteins related to neuronal development, including components of the PI3K/PTEN and ERK signaling pathways. The same lysates were analyzed by cIEF using, **(B)** panAkt, **(C)** p(S473)Akt, **(D)** p(T308)Akt, or the isoform specific antibodies recognizing, **(E)** Akt1, **(F)** Akt2 or, **(G)** Akt3. The most prominent changes in Akt peak distribution during brain development and maturation occurs in the Akt1 isoform.

3.5. Non-specific binding of the p(T308)Akt antibody

During our extensive analyses of primary neuronal or whole brain lysates by WB (see section 3.4, 3.6 and 3.7), we consistently noticed an upper band detected by the p(T308)Akt antibody with a size of approximately 70 kDa. This band correlated precisely with the appearance of the basic T308 peaks in cIEF profiles of the same samples. Subsequent analysis identified this band not to be detected in different other cell lines, including N1E-115, HEK293T and COS-7 (data is not shown). During postnatal stages in brain development, the 'upper band' detected with the p(T308)Akt antibody was hardly detected at P0, and increased gradually until P15 to maximum levels (see Figure 12B). Furthermore, its expression and first appearance in very mature neuronal cultures (20 DIV) sparked our interest to identify the exact origin of this signal (see Figure 12A). Initial experiments with λ-phosphatase treatment using Akt isoform-specific antibodies *in vitro* were inconclusive at the level of identifying whether this band corresponded to an additional Akt band. However, λ-phosphatase treatment of transferred proteins on a nitrocellulose membrane revealed the disappearance of the band verifying it to be phospho-specific (see Figure 12C). Probing primary neuronal lysates with the p(T308)Akt antibody in cIEF gave a profile similar to that found for N1E-115 cells, showing 4 distinct, acidic peaks at 5.14, 5.31, 5.42 and 5.53. Additionally, 3-4 very basic peaks with their pI ranging from 5.75 to 5.9 appeared (see Figure 23C). Again, these peaks were only detected in primary neuronal or whole brain lysates. A series of pharmacological treatments (including PI3K inhibitors) to establish the relationship of these T308 bands/peaks to specific T308-Akt bands/peaks showed that they do not share the same pharmacological profile (data not shown).

In order to identify the nature of these additional signals detected by WB and cIEF, we used the p(T308)Akt antibody for immunoprecipitation (IP) of the protein from adult mouse brain. The IP was run on a SDS-Gel, stained with Comassie and the upper band at ~70 kDa excised. Following in-gel digestion, the band was then analyzed by mass spectrometry (mass spec). The mass spec experiments were performed by Erik McShane in the group of Prof. Matthias Selbach at the Max-Delbrück Center for Molecular Medicine in Berlin. The results obtained suggested the additional signals detected by WB and cIEF to be a classic form of protein kinase C (PKC) (see Figure 12D). PKC is phosphorylated by PDK1, the same kinase phosphorylating Akt at T308 [Mora et al. 2004]. Therefore, a cross-reactivity of the p(T308)Akt antibody with PKC is against expectation but not digressive as both proteins show a high sequence homology around the T308 region of Akt (see Figure 12E). To confirm the nature of the upper band and the additional basic peaks in cIEF to be PKC we treated neurons with TPA for 24 hours, as it has been reported to downregulate classic PKCs [Leondaritis, Petrikkos, and Mangoura 2009]. After the 24 hour TPA treatment the upper band in WB as well as the most basic peaks in cIEF detected with the p(T308)Akt were no

longer detected (see Figure 12F). Therefore, we conclude, that the p(T308)Akt antibody from Cell Signaling that we used in our experiments shows a cross-reactivity with phosphorylated PKC proteins.

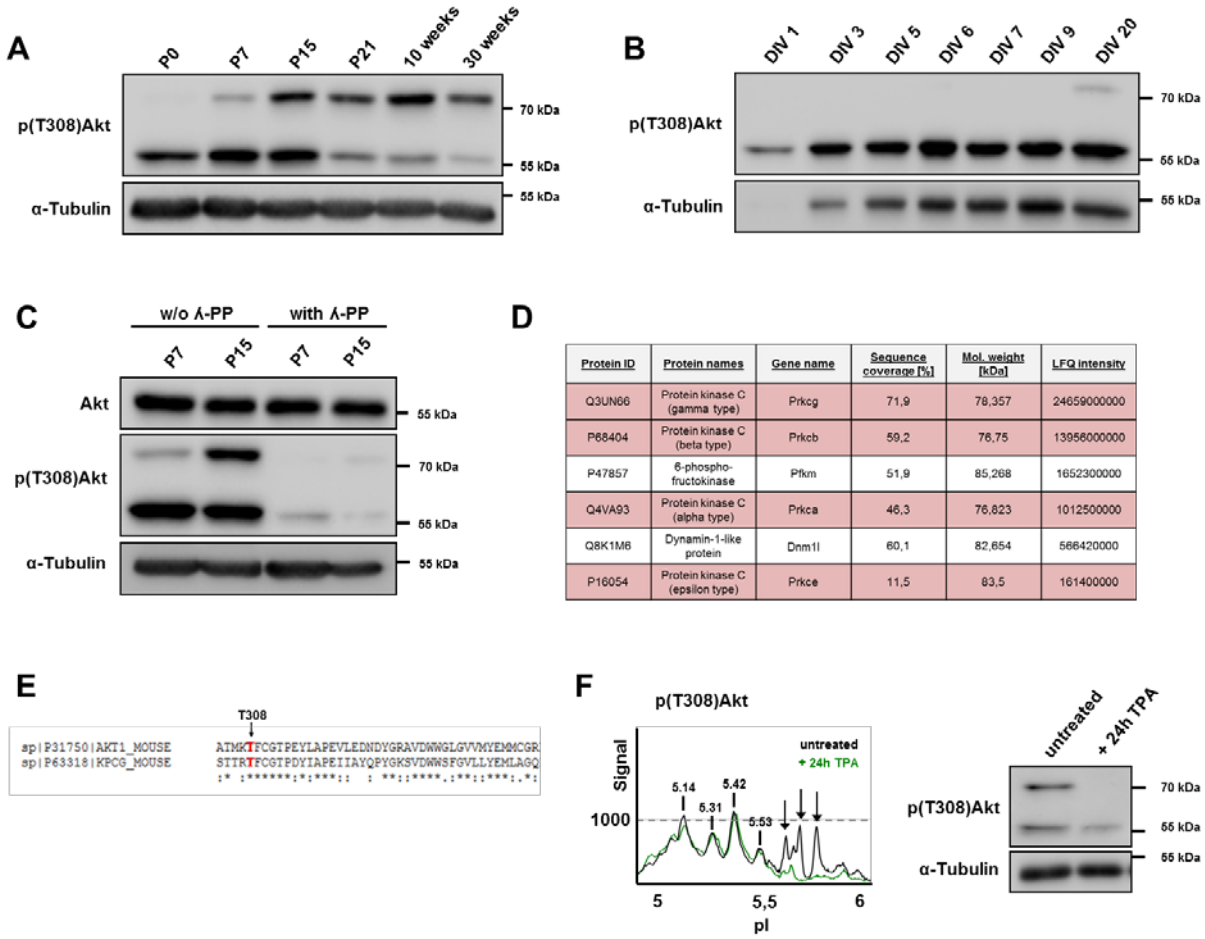

Protein ID	Protein names	Gene name	Sequence coverage [%]	Mol. weight [kDa]	LFQ intensity
Q3UN66	Protein kinase C (gamma type)	Prkcg	71,9	78,357	24659000000
P68404	Protein kinase C (beta type)	Prkcb	59,2	76,75	13956000000
P47857	6-phospho-fructokinase	Pfkm	51,9	85,268	1652300000
Q4VA93	Protein kinase C (alpha type)	Prkca	46,3	76,823	1012500000
Q8K1M6	Dynamin-1-like protein	Dnm1l	60,1	82,654	566420000
P16054	Protein kinase C (epsilon type)	Prkce	11,5	83,5	161400000

Figure 12: *Non-specific p(T308)Akt band.* **(A)** Rat whole brain lysates showed, additionally to the Akt band at ~55 kDa, an upper band at ~70 kDa when probed with p(T308)Akt antibody. **(B)** The same band was detected in mature (20 DIV) primary cortical neurons. **(C)** When the nitrocellulose membrane was treated with λ-phosphatase the band was lost. **(D)** The table shows the top six hits from the mass spec analysis performed on the isolated ~70 kDa band from a SDS gel after IP with the p(T308)Akt antibody from whole mouse brain lysates. The results are ranked for their label free quantification (LFQ) intensity [Cox et al. 2014]. PKC isoforms are highlighted in red. **(E)** A sequence alignment of Akt1 and PKCγ, the top hit from mass spec analysis, shows the similarities in the protein sequence around the T308 site of Akt. **(F)** 21 DIV cortical lysates were treated with TPA for 24 hours. When probed with cIEF (left panel) the three most basic peaks disappeared. Probing the same lysates by WB (right panel), showed no detection of the upper p(T308)Akt band after TPA treatment.

3.6. Differential sensitivity of Akt to growth factor stimulation in immature and mature neurons *in vitro*

Numerous studies have highlighted the importance of the PI3K/PTEN/Akt pathway during almost all major stages of the neuronal maturation program, including neurite outgrowth, neuronal polarization, axonal branching and synapse formation [Waite and Eickholt 2011; Eickholt et al. 2007; Cosker et al. 2008]. Activation of this pathway has been reported to primarily depends on growth factors like BDNF, Insulin and IGF-1 [Sosa et al. 2006; Islam, Loo, and Heese 2009]. To get further insight into growth factor signaling during neuronal maturation, we used the newly established cIEF assay to compare Akt phosphorylation upon growth factor stimulation in immature (7 DIV) and mature (21 DIV) primary cortical neurons *in vitro*. 7 DIV cortical neurons have already polarized and both axons and dendrites extend and adopt complex branched morphologies. Additionally, during this stage, bulk synaptogenesis is beginning. In contrast, in 21 DIV cortical neurons further growth and branching of dendrites is terminated, spines are mature and action potentials can be measured.

7 DIV neurons were treated with EGF, BDNF or Insulin for 15 min. WB analysis revealed the greatest increases in phospho-Akt (S473 and T308) in cultures that had been treated with BDNF, although all three growth factors activated the PI3K pathway and led to enhanced Akt phosphorylation. It could further be noted, that BDNF, out of the growth factors tested, exclusively activated MAPK/ERK1/2 signaling (see Figure 13A). When the same cell lysates were analyzed by cIEF, BDNF led also in this assay to the highest increase in Akt phosphorylation for both activating phosphosites, S473 and T308 (see Figure 13B and C). The majority of peaks that were increased upon BDNF stimulation (pI 5.06 – 5.31) are consistent with phosphorylated Akt1 species (see Figure 5C for comparison). EGF and Insulin treatment only induced minor increases in phospho-Akt species when analyzed by cIEF. Interestingly, it seemed that the T308 phosphorylation site was more sensitive to Insulin treatment than the S473 phosphorylation site (see Figure 13B, C bottom panel). In contrast to 7 DIV cortical neurons, when 21 DIV neurons were treated with EGF, BDNF and Insulin, the increase in Akt phosphorylation was generally less pronounced. BDNF, again, led to a larger increase in Akt and ERK1/2 phosphorylation than EGF when the samples were analyzed by WB (see Figure 14A). Insulin treatment showed no visible effect on Akt phosphorylation when analyzed by WB or cIEF (see Figure 14). Interestingly, EGF led to a very restricted increase in the 5.31 and 5.42 peaks detected with both, the p(S473) and p(T308) antibodies. cIEF analysis revealed the BDNF treatment primarily affected the T308 phosphorylation site of Akt in mature neurons, and only to a smaller extend the S473 phosphorylation site (see Figure 14B and C). Thus the comparison of growth factor treatment

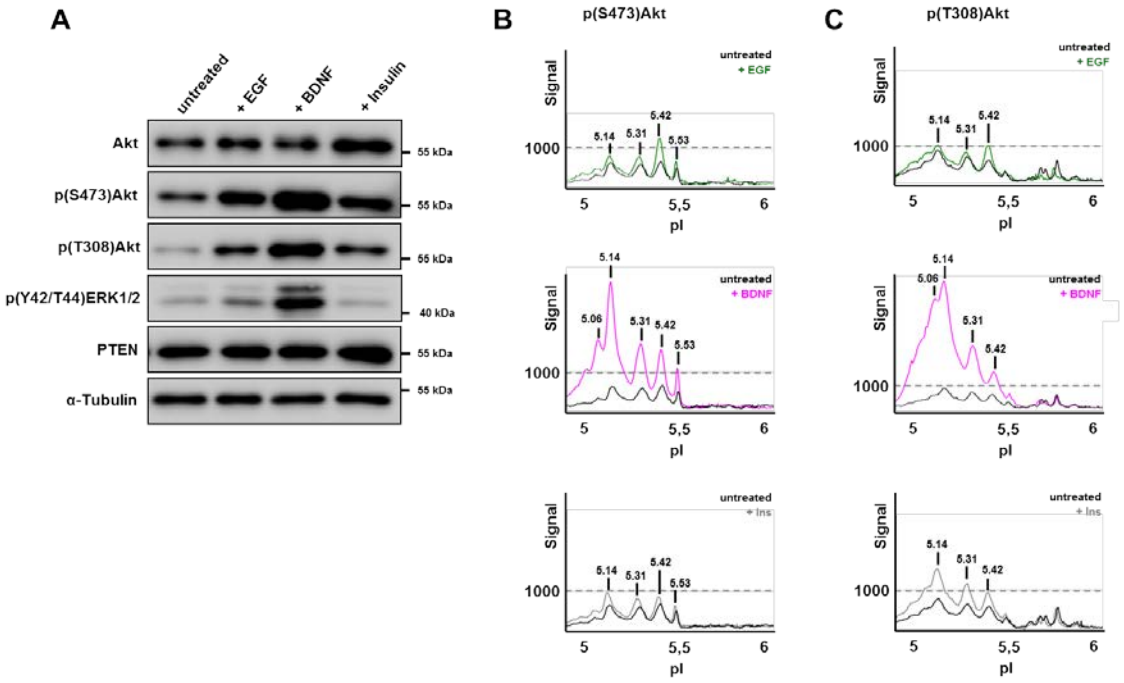

Figure 13: *Analysis of growth factor treatment of 7 DIV primary cortical neurons.* **(A)** Cortical neurons were treated with EGF, BDNF or Insulin for 15 minutes and subsequently analyzed by WB using phospho-specific Akt antibodies. **(B)** The same lysates were analyzed by cIEF using the p(S473)Akt and **(C)** the p(T308)Akt antibody. For both phosphorylation sites BDNF had the strongest effect on Akt phosphorylation.

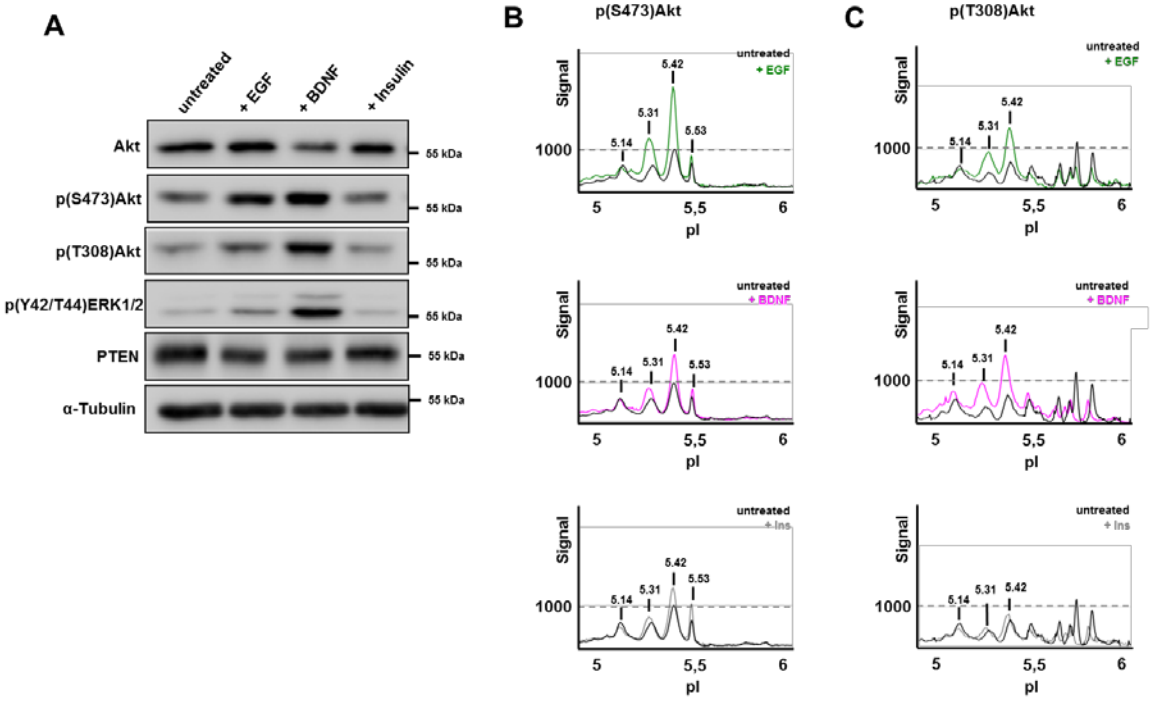

Figure 14: *Analysis of growth factor treatment of 21 DIV primary cortical neurons.* **(A)** Cortical neurons were treated with EGF, BDNF or Insulin for 15 minutes and subsequently analyzed by WB using phospho-specific Akt antibodies. **(B)** The same lysates were analyzed by cIEF using the p(S473)Akt and **(C)** the p(T308)Akt antibody. The largest increase in Akt phosphorylation was found after treatment with EGF.

of immature (7 DIV) and mature (21 DIV) neurons showed a different signaling outcome depending on the developmental stage of the neurons and the growth factor applied. Immature neurons were more susceptible to BDNF stimulation whereas mature neurons mainly responded to EGF stimulation. This difference in signaling was primarily found by employing cIEF for Akt phosphorylation as readout for upstream PI3K activity. Conventional WB showed the up-regulation in Akt phosphorylation upon growth factor stimulation, but could not be used to assess the differences in different Akt isoform signaling. Using the p(T308)Akt antibody in cIEF also showed three basic peaks which were not detected in previously in N1E-115 cells. For further characterization of these peaks please refer to section 3.5.

3.7. Differential regulation of Akt phosphorylation by PTEN and growth factors in primary neurons

We could show a difference in growth factor signaling response of Akt depending on the maturation of neurons *in vitro* (see section 3.6). Generally, the activation of Akt by the presence of PIP_3 is largely dependent on the balance of PI3K and PTEN. The loss of PTEN as a PI3K antagonist leads to an increase in PIP_3 availability at the membrane and subsequent phosphorylation and activation of Akt. We made use of primary cortical cultures from $PTEN^{fl/fl}$ mice and the newly established cIEF Akt assay to assess whether loss of PTEN results in the same Akt species being activated as seen after growth factor stimulation. Cortical $PTEN^{fl/fl}$ neurons (at 12 DIV) were left untreated, were infected with a control RFP lentivirus or with increasing amounts of a Cre lentivirus and lysed at 21 DIV. With this approach we achieved a gradual loss of PTEN proportional to the amount of Cre virus used, corresponding to that phosphoAkt (S473 and T308) was found increased upon PTEN loss (see Figure 15A). cIEF analysis of $PTEN^{fl/fl}$ neuronal lysates with the p(S473)antibody showed a large increase in mainly Akt1 identified peaks after PTEN loss through Cre recombinase (see Figure 15B). This increase in phospho-specific Akt peaks was also found mostly to be linear to the amount of Cre virus used, interestingly, there was no difference in S473 phosphorylation after application of 75 µL or 150 µL virus. Quantification of the area under the peaks for the p(S473)Akt antibody revealed a up to 6-fold increase in S473 phosphorylation for the most acidic Akt1 peak (5.06) at the highest virus concentration (see Figure 15C). To get a better understanding of the regulation of the PI3K/PTEN/Akt pathway we compared cIEF profiles for the two activating Akt phosphorylation sites (S473, T308) after growth factor stimulation and upon PTEN loss. Stimulation of 21 DIV cortical neurons with EGF, BDNF or Insulin led to a general increase in phosphorylated Akt, although Insulin seems to have minimal effect on Akt activation in mature neurons (see Figure 16).

Remarkably, as Akt profiles in response to growth factor stimulation are largely identical, loss of PTEN induces a strong increase in mostly Akt1 identified peaks. In summary it can be said, that more basic phosphorylation forms of Akt (5.42, 5.53) appeared to be more sensitive to growth factor treatment and phosphorylation of the more acidic Akt forms (5.06, 5.14) is upstream regulated by PIP_3 and therefore, more sensitive to PTEN loss. This holds true for the S473 as well as the T308 phosphorylation. Our results suggest inherent differences in the Akt pools (in terms of post translational modification, in particular phosphorylation) that are accessible to growth factors as compared to the pools that are controlled by availability of PIP_3 per se, at least in mature primary neurons.

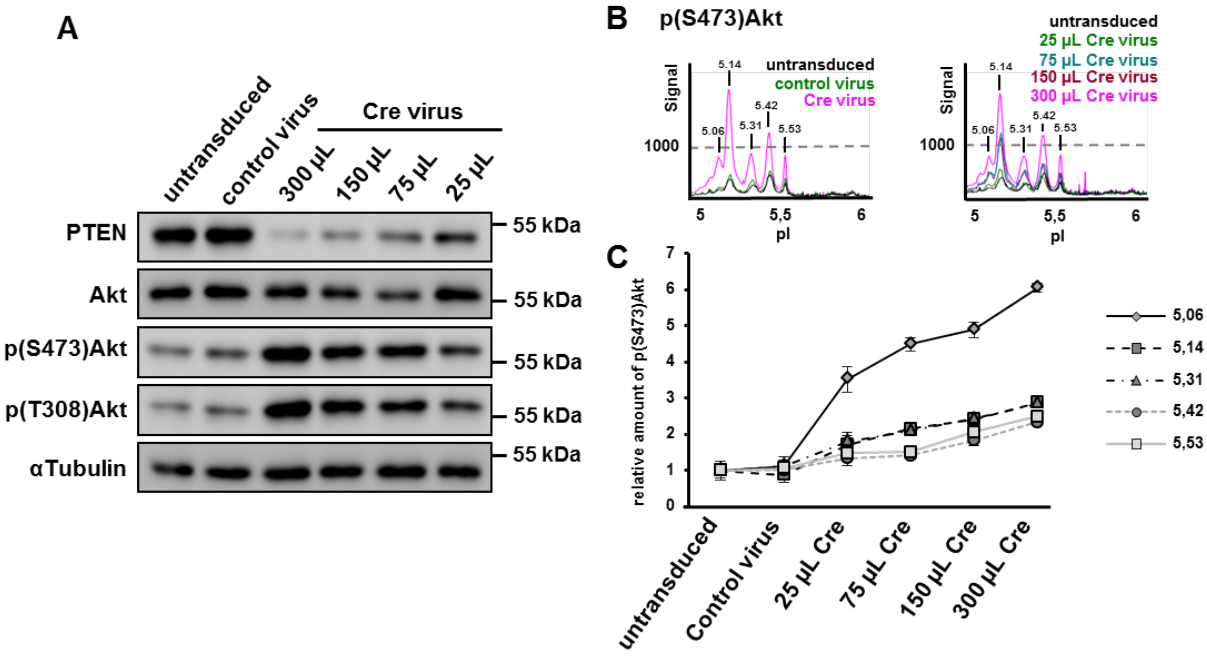

Figure 15: *Effect of gradual PTEN loss on Akt phosphorylation in primary cortical neurons.* **(A)** Cortical neurons obtained from $PTEN^{fl/fl}$ mice were infected at 12 DIV with control virus or Cre virus, before cell lysis and Western blot analysis at 21 DIV. Increasing concentrations of Cre virus leads to a gradual loss of PTEN and a concomitant increase in Akt phosphorylation at S473 and T308. **(B)** Cell lysates were analyzed in parallel by cIEF using p(S473)Akt. The peak profiles demonstrate that PTEN-loss increases mostly the most acidic Akt (Akt1) peaks. **(C)** The area under each peak was quantified for p(S473)Akt. At the highest concentration used, Cre-induced PTEN-loss led to a 6x increase in S473 phosphorylation of Akt1 (pI 5.06).

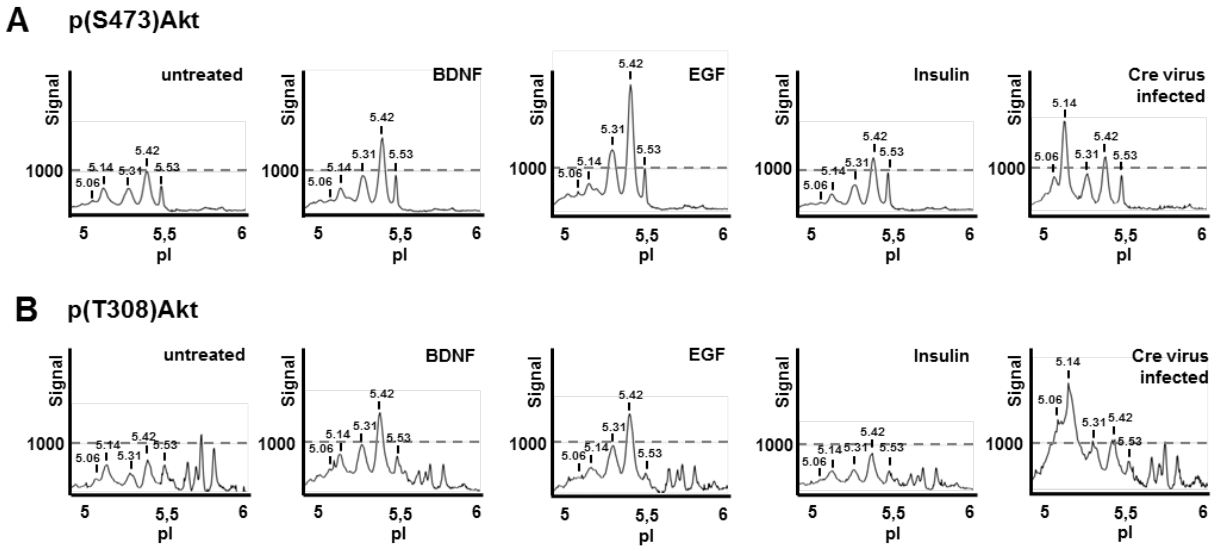

Figure 16: *Context-dependent Akt phosphorylation signatures in cortical neurons*. 21 DIV cortical neurons were stimulated with BDNF, EGF or Insulin for 15 minutes. In parallel, cortical neurons obtained from $PTEN^{fl/fl}$ mice were infected at 12 DIV with Cre virus and cultured until 21 DIV. All cell lysates were analyzed by cIEF with, **(A)** p(S473)Akt antibody and, **(B)** p(T308)Akt antibody. Whilst Akt peak distributions in response to growth factor treatment are largely identical, PTEN-loss induces a strong increase in the most acidic Akt1 phosphorylated peaks.

3.8. EGF leads to Akt2 phosphorylation in mature cortical neurons

3.8.1. EGF signaling leads to a restricted Akt2 activation in mature neurons

The phosphorylation profile of Akt detected by cIEF varied depending on the changes in upstream signaling. The loss of PTEN led to an increase in phosphorylation of Akt1 molecules, whereas growth factor treatment primarily affected the more basic peaks representing mixed Akt1/Akt2 species. We believe that the shown differential regulation of Akt signaling in response to upstream cues might have important implications for downstream signaling that have to date been unappreciated. When analyzing mature cortical neurons (21 DIV) after growth factor treatment we noticed that, in contrast to 7 DIV neurons, suddenly EGF had the largest effect on Akt phosphorylation. The cIEF p(S473)Akt profile after EGF treatment showed a very restricted increase in pI 5.31 and, especially, the pI 5.42 peak. We therefore decided to identify the composition of these peaks further by cIEF analysis of lysates using Akt isoform specific antibodies. Unexpectedly, EGF stimulation of 21 DIV cortical neurons led exclusively to an increase in phosphorylation of the Akt2 isoform, as shown by an acidic shift in the peak distribution (see Figure 17A, middle panel). In sharp contrast, cIEF profiles of control versus EGF stimulated lysates analyzed with the Akt1- or

Akt3-antibodies were indistinguishable between the two groups. These results provide first evidence for a function of a specific Akt isoform, Akt2, in conveying EGF mediated responses in neurons. In comparison, BDNF also induced Akt phosphorylation but this activation was restricted to mainly Akt1 and, possibly, Akt3.

Akt2, being the 'metabolic' Akt isoform, has been implicated to be involved in neuronal morphology and survival [Santi and Lee 2010; Diez, Garrido, and Wandosell 2012]. We decided to investigate this very restricted induction of Akt2 phosphorylation upon EGF treatment. We established in previous experiments that Akt2 specific, EGF induced responses occur only in mature neuronal cultures, and not in immature cortical cultures (see Figure 13 and 14B, C). We next excluded the possibility that the EGF – Akt2 effect might be due to a minor population of astrocytes in our primary cultures. Therefore, we used primary astrocyte cultures, treated them with EGF in the same way as we did for the neuronal cultures, lysed the cells and analyzed them by WB and cIEF. The starved astrocytes showed an increase in p(S473)- and p(T308)Akt after EGF treatment, this was seen by WB as well as cIEF (see Figure 18A, B). The astrocyte phosphoAkt profile differs significantly from the phosphoAkt profile after EGF treatment of mature cortical neurons (compare to Figure 14). In astrocytes, EGF stimulation leads to the appearance of additional acidic peaks (5.01, 5.21) when compared to the cIEF profiles of EGF-treated mature neurons. When EGF treated astrocytes were probed with an Akt2-specific antibody we did not find the very restricted panel observed in neurons, but a broader appearance of different acidic peaks (see Figure 18C). The glial fibrillary acidic protein (GFAP) was used as an astrocytic marker in WB analysis. Normalization of WB densiometry results for GFAP levels to GAPDH levels gave a ratio of 1,5 for our starved astrocyte cultures, whereas in untreated mature neuronal cultures the ratio was 0,09 (see Figure 18D), meaning in our neuronal cultures are 17x less astrocytes than in the total astrocytes cultures. These results suggest a minor astrocyte population in our neuronal cultures. Therefore, we conclude that Akt in astrocytes is responsive to EGF, but if at all they only mark a minor contribution to the EGF - Akt2 specific effect observed in our primary cortical cultures.

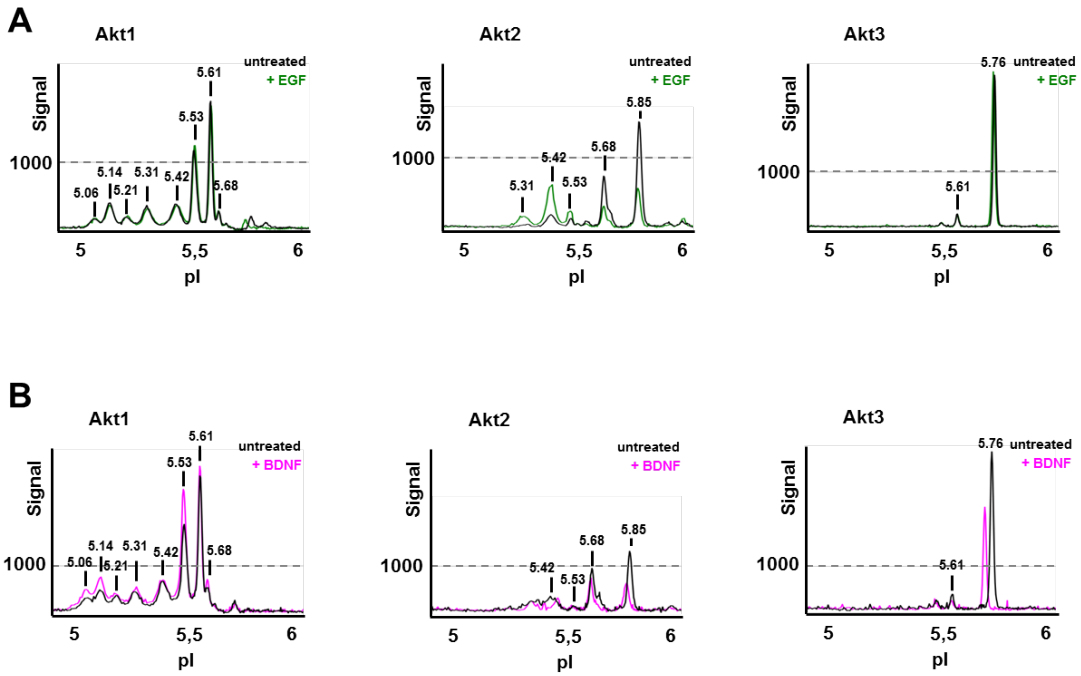

Figure 17: *Analysis of Akt isoforms after growth factor treatment.* **(A)** 21 DIV cortical neurons were treated with EGF, lysed and analyzed by cIEF using Akt isoform specific antibodies (Akt1, Akt2, Akt3). Only Akt2 showed an increase in phosphorylation in response to EGF treatment as seen by the increase in more acidic peaks after the stimulation. **(B)** 21 DIV cortical neurons were treated with BDNF, lysed and analyzed by cIEF using Akt isoform specific antibodies (Akt1, Akt2, Akt3). BDNF treatment induced a small increase in Akt1 phosphorylation.

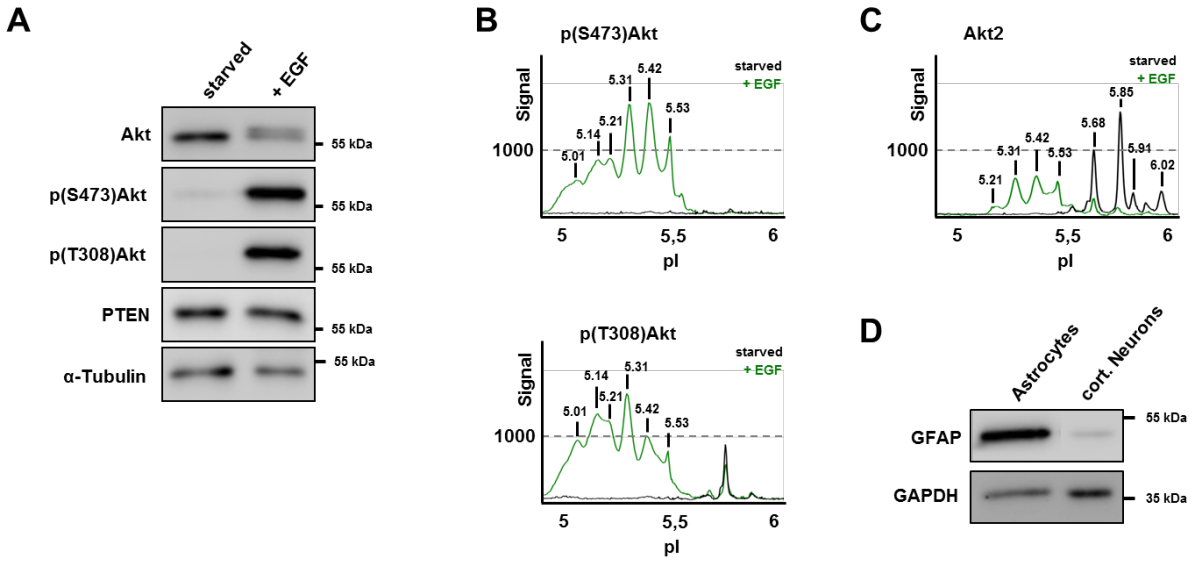

Figure 18: *Akt profiles after EGF treatment of primary astrocytes.* Starved astrocytes were treated with EGF, leading to an increase in p(S473)- and p(T308)Akt. Lysates were analyzed by **(A)** WB and **(B)** cIEF. **(C)** The same lysates were probed in cIEF with the Akt2-specific antibody showing a great shift towards more acidic, higher phosphorylated peaks. **(D)** WB analysis of GFAP in astrocyte and 21 DIV neuronal cultures.

3.8.2. EGF – Akt2 signaling is mediated by the EGFR

It has been previously shown that during migration of newborn cortical neurons, EGF can transactivate the TrkB receptor [Puehringer et al. 2013]. In order to characterize the specific receptor type responsible for EGF signaling transduction in our mature neuronal cultures we employed pharmacological approaches. We used Gefitinib, the first identified, selective inhibitor of the EGFR Tyrosine kinase domain that is approved for clinical use to treat, non-small cell lung cancer, amongst others. To inhibit the BDNF TrkB receptor, we employed GNF5837, a potent inhibitor with selectivity for Trk receptors over a range of other kinases. First we assessed the specificity of Gefitinib (EGFRi) in 7 DIV and 21 DIV cultures. WB analysis showed that addition of the inhibitor alone did not change the activation/phosphorylation state of Akt, neither at S473 nor T308. As previously found, EGF did not lead to an upregulation of phosphorylation of Akt in 7 DIV neurons. In contrast, BDNF stimulation resulted in increased phosphoAkt, which was independent of EGFR (see Figure 19A). In mature neurons (21 DIV) EGF led to an increase in phosphoAkt (S473 and T308), which could be antagonized by application of Gefitinib to the cells. Similarly, stimulation with BDNF resulted in phosphorylation of Akt, but to a lesser extent than seen in 7 DIV neurons. Nevertheless, the activation was independent of EGFR (see Figure 19B). Therefore, these results let us to conclude that EGF signaling, but not BDNF signaling, in mature neurons occurs via the EGFR.

In the general mechanism for the activation of RTKs, activating ligands or growth factors bind to the ectodomains of two receptors and induce the formation of an activated dimerization state. The cytoplasmic kinase domains then catalyze the phosphorylation of Tyrosine residues that lead to protein kinase activation. One specific EGFR Tyrosine residue that is phosphorylated following EGF binding to the receptor is Y1068. We monitored the phosphorylation of Y1068, which showed a robust increase following EGF treatment, but not in the presence of the EGFRi Gefitinib. To rule out a role of TrkB transactivation after EGF treatment we performed the same experiment also for GNF5837, the TrkBi. Again, in 21 DIV neurons we saw a strong increase in phosphoAkt after EGF treatment. This effect was largely independent of TrkB inhibition, as only a minor decrease of phosphorylated Akt was found after EGF treatment in the presence of GNF5837 (see Figure 20). In comparison, the stimulation with BDNF in the presence of GNF5837 did not result in an increase in phosphoAkt therefore confirming the TrkB receptor as a key receptor in BDNF signaling.

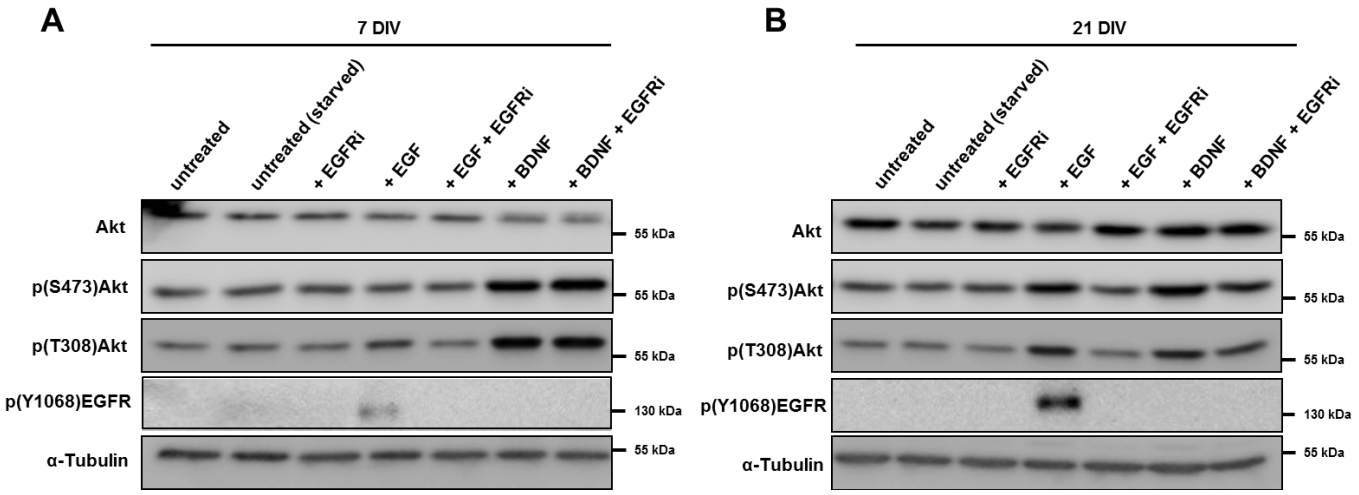

Figure 19: *Specificity test of Gefitinib (EGFRi) in cortical neurons.* **(A)** Immature (7 DIV) or **(B)** mature (21 DIV) cortical neurons were treated with Gefitinib to inhibit EGFR signaling after EGF or BDNF treatment. EGF on led to an increase in phosphoAkt in mature neurons and was prevented by addition of Gefitinib. BDNF led to phosphorylation of Akt in immature as well as mature neurons, being independent of EGFR inhibition. EGF treatment also induced phosphorylation of EGFR.

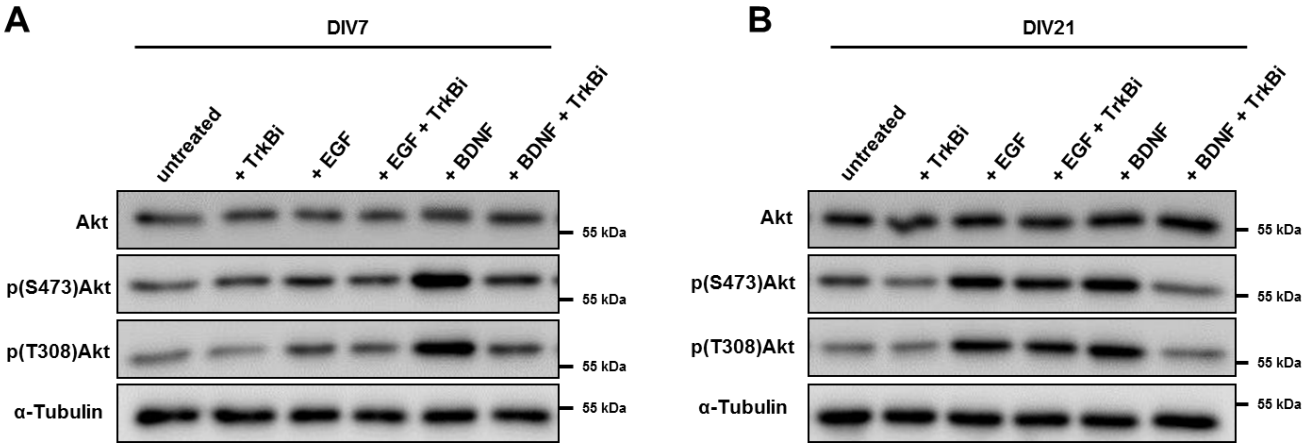

Figure 20: *Specificity test of GNF5837 (TrkBi) in cortical neurons.* **(A)** Immature (7 DIV) or **(B)** mature (21 DIV) cortical neurons were treated with GNF5837 to inhibit TrkB signaling after EGF or BDNF treatment. EGF on led to an increase in phosphoAkt in mature neurons and was not affected by TrkB inhibition. BDNF led to phosphorylation of Akt in immature as well as mature neurons, being dependent on TrkB signaling, as its effect on Akt phosphorylation was lost after GNF5837 treatment.

To further confirm the role of EGFR in the specific EGF – Akt2 signaling, we used cell lysates of Gefitinib treated cortical neurons for cIEF analysis. Probing lysates of EGF stimulated cell gave us the same restricted increase in Akt2 phosphorylation as previously seen, here shown for the p(S473)Akt, p(T308)Akt and Akt2 antibody (see Figure 21). In the presence of Gefitinib (EGFRi) the increase of the phospho-specific Akt peaks at 5.31 and 5.42 was abolished. The only phosphoAkt species affected by TrkB inhibition was the peak at 5.53 (see Figure 21A, right panel). Therefore, we cannot exclude a minor contribution of the TrkB receptor to the EGF – Akt2 signaling, but the main receptor involved in this pathway is specific to EGFR. Having established the receptor involved in our characterized EGF - Akt2 signaling axis, we analyzed EGFR expression *in vitro* and *in vivo*. We used primary cortical neurons from mice, as well as whole brain lysates from Wistar rats. *In vitro*, we were able to detect EGFR expression at mature stages at 16 and 21 DIV (see Figure 22A), which correlates with the EGF signaling difference we observed in immature and mature neurons. *In vivo*, the one embryonic stage tested (E19) did not show any detectable EGFR protein expression. Immediately after birth (P0/1) protein levels of the receptor were increasing. From P7 to P15 WB analysis showed robust expression of a double band specifically detected with anti-EGFR of approximately 170 kDa and 180 kDa. (see Figure 22B). A maximal expression and disappearance of the lower band was found three weeks after birth (P21). EGFR expression levels were high until about 10 weeks of age, and then a slight decrease in the expression was observed. In summary, EGFR is strongly expressed in the rat brain from late postnatal stages onwards.

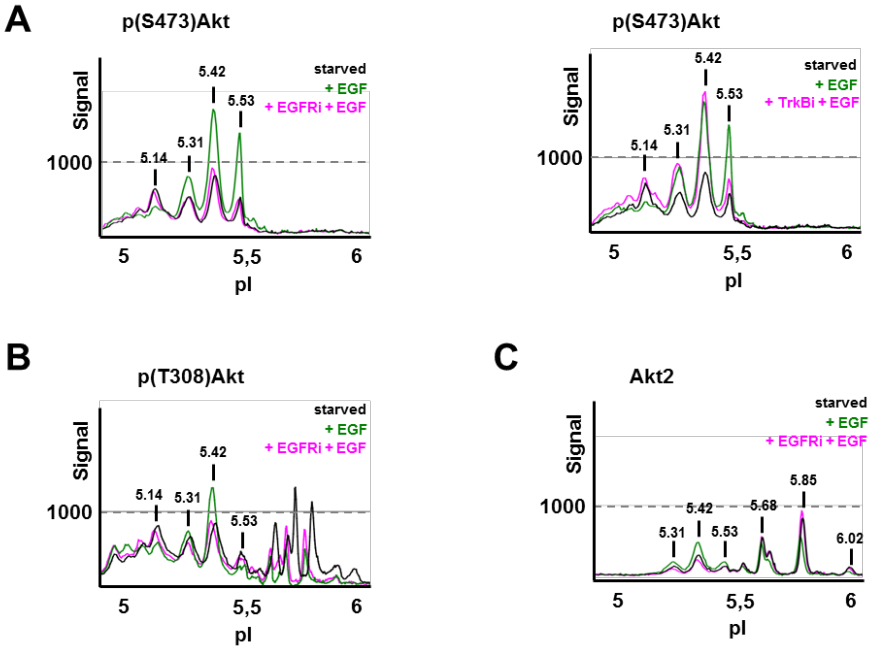

Figure 21: *cIEF analysis of EGF and Gefitinib treated mature cortical neurons*. 21 DIV cortical neurons were treated with EGF with or without Gefitinib (EGFRi) present. The cell lysates were probed with **(A**, left panel) p(S473)Akt, **(B)** p(T308)Akt and **(C)** Akt2 antibodies. **(A**, right panel) To test for a role of TrkB signaling, cells were also treated with EGF and GNF5837 (TrkBi), lysed and probed with p(S473)Akt.

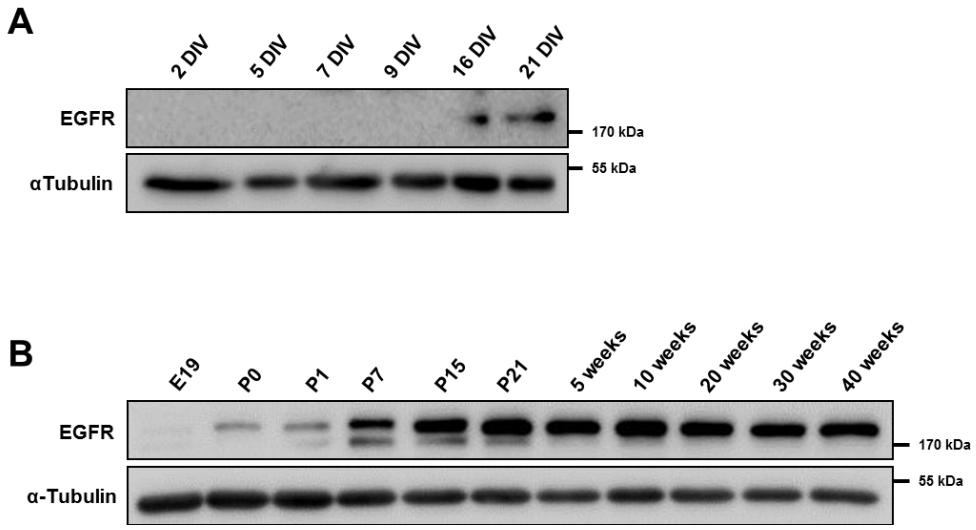

Figure 22: *Expression of EGFR in primary cortical neurons and during postnatal rat brain development*. **(A)** Primary cortical neurons from mice were cultured from indicated time points, lysed and analyzed by WB. Only in later stages (16 and 21 DIV) EGFR expression was detected. **(B)** Whole brain lysates were obtained at indicated time points from Wistar rats. EGFR expression was not detectable in the embryonic stage tested (E19) but increased after birth. Initially two bands were detected which merge to one band at 21 days of age, were also a maximal plateau in expression was reached. Expression decreased slightly in old animals.

3.8.3. EGF – Akt2 signaling in mature neurons proceeds via the catalytic p110α subunit of PI3K

Class I PI3Ks consist of a catalytic p110 (α, β, γ, δ) subunit, which is associated with different regulatory subunits. Dysfunction of the different catalytic subunits has been linked to the development of a variety of pathologies [Denley et al. 2008]. To further characterize the newly identified EGF – Akt2 signaling axis in mature neurons we made use of specific pharmacological inhibitors targeting the catalytic subunit of class I PI3Ks (p110α, β, γ, δ). We tested different inhibitors under basal conditions in the absence of any growth factor stimulation in neurons to determine optimal working concentrations for our cell systems. All inhibitors used in this study function by competing for access of the co-substrate ATP to the enzyme and inhibit the kinase activity of the PI3K catalytic subunit.

To inhibit all subunits, a general PI3K inhibitor (GDC-0941) was used. GDC-0941 shows a higher specificity for PI3K and less toxicity than previously used inhibitors in this study, for example Wortmannin [Folkes et al. 2008]. Further it is orally bioavailable and is being evaluated in clinical trials [Folkes et al. 2008]. A66 is a PI3K-p110α inhibitor, which is highly selective for the alpha subunit. It shows a selectivity of greater than 20-fold the PI3K-p110δ isoform typically being the closest off-target to the PI3K-p110α activity [Fairhurst et al. 2009]. The PI3K-p110β inhibitor that we used, TGX-221, has an IC_{50} of 5 nM against the purified kinase and 1000-fold selectivity over PI3K-p110α [Jackson et al. 2005]. Previously it was

published, that p110β is the dominant subunit responsible for PI3K-Akt signaling in neurons [Gross and Bassell 2014]. The PI3K-p110γ inhibitor AS252424 has been shown to have an IC_{50} of 35 nM and a 10-fold selectivity for the PI3K-p110γ isoform versus the α, β, or δ isoforms *in vitro* [Condliffe et al. 2005]. The PI3K-p110δ inhibitor IC87114 has an IC_{50} of approximately 500 nM and at a concentration of 5 µM it was found to completely abrogated p110δ-induced Akt phosphorylation [Denley et al. 2008]. This inhibitor is 58-fold more selective for PI3Kδ when compared to PI3Kγ, and over 100-fold selective compared to PI3Kα and PI3Kβ. IC87114 selectively antagonizes PI3Kδ over at least a concentration range of 0.3–10 µM [Sadhu et al. 2003]. Pharmacologic approaches are an appealing strategy to validate the role of the PI3K pathway because they are rapid and easily titratable. The used synthetic PI3K inhibitors exhibit a high selectivity towards a specific catalytic subunit and are a valuable tool.

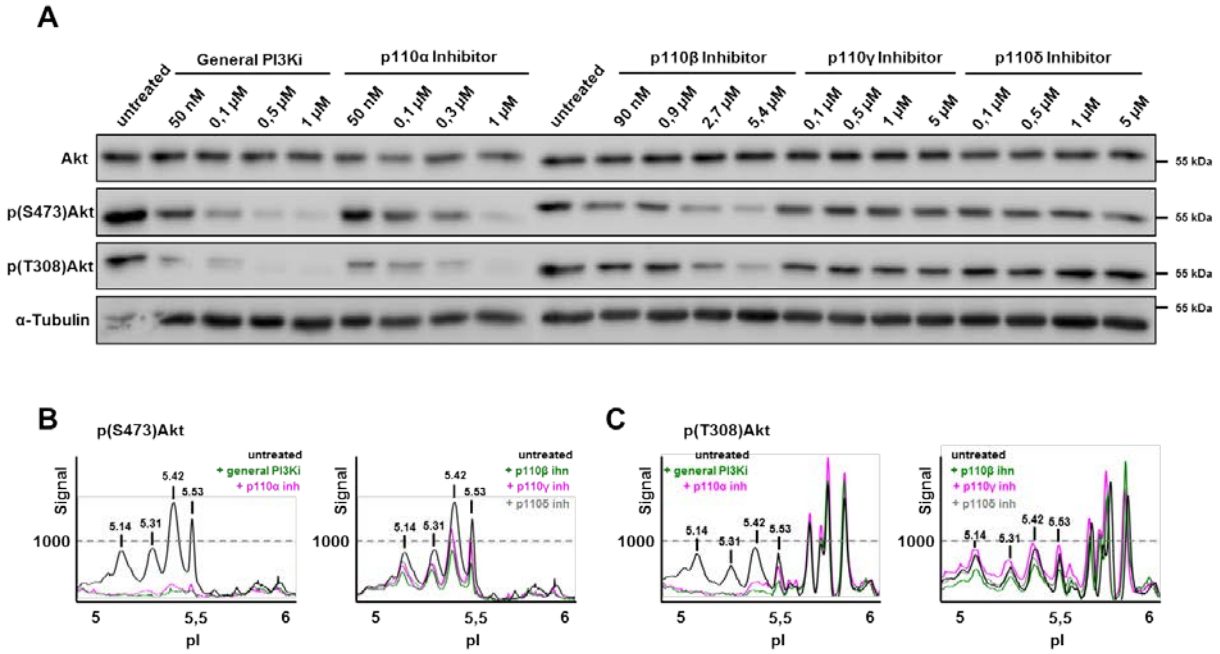

Figure 23: *Assessment of PI3K catalytic subunit inhibitors in mature cortical neurons.* **(A)** Concentration curve for a general PI3K inhibitor (PI3Ki) and four subunit specific inhibitors (p110α,β,γ,δ) tested in 21 DIV cortical neurons and analyzed by WB. **(B**) Cortical neurons treated with 0,5 µM general PI3Ki, 1 µM p110α inhibitor (left), 2,7 µM p110β inhibitor, 1 µM p110γ inhibitor and 1 µM p110δ inhibitor (right) were analyzed by cIEF using the p(S473)Akt and **(C)** p(T308)Akt antibody.

We performed a concentration curve for all five inhibitors in mature neurons (21 DIV). Interestingly, p110α seemed to be the major subunit influencing Akt phosphorylation downstream of PI3K under basal conditions in mature neurons (see Figure 23). As expected, a general inhibition of PI3K led to a reduction of Akt phosphorylation already at small concentrations and a complete loss of Akt phosphorylation when applied at higher concentrations, which we identified by both WB and cIEF (see Figure 23). Inhibition of p110γ and p110δ did not influence PI3K – Akt signaling at least in WB. Similar results were seen for

p110β inhibition for lower concentrations tested. When higher concentrations (2,7 µM and 5,4 µM) were tested a sizeable reduction in Akt phosphorylation was measureable (see Figure 23). This effect, however, may be due to the fact that, at these higher concentrations the p110β inhibitor can affect other PI3K isoforms [Ni et al. 2012].

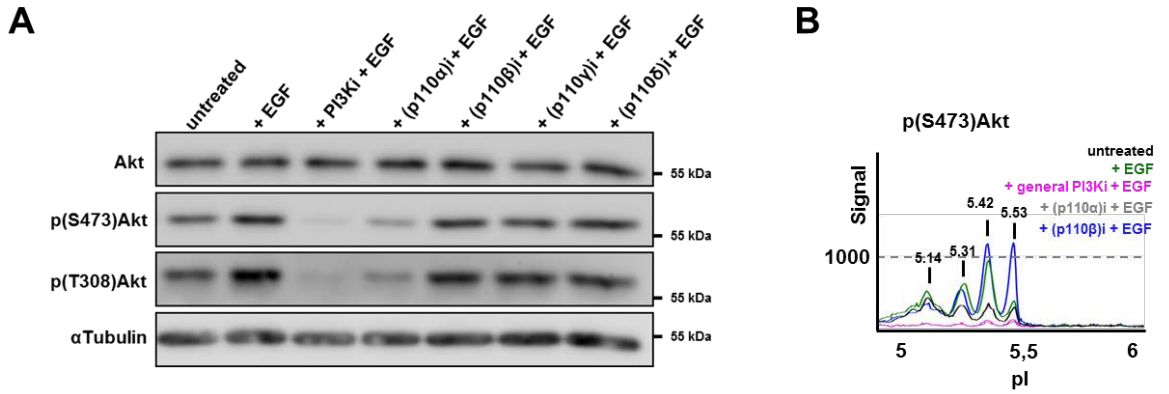

Figure 24: *Inhibition of the PI3K p110 regulatory subunits prior to EGF treatment of mature cortical neurons*. 21 DIV cortical neurons were treated EGF alone, a general PI3K inhibitor (PI3Ki) or specific inhibitors for the different p110 subunits (p110α-δi) prior to EGF treatment. The cell lysates were analyzed by **(A)** WB or **(B)** cIEF. EGF treatment led to an increase in phosphoAkt which was abolished by the addition of a general PI3K inhibitor or inhibition of p110α.

After establishing suitable working concentrations for the specific inhibitors to target the different catalytic p110 subunits of PI3K, we used them to further characterize the EGF - PI3K - Akt2 signaling in neurons. WB blot analysis showed that in EGF stimulated mature neurons, upon PI3K general inhibition, the EGF induced increase in phosphoAkt is lost. We can therefore conclude that PI3K has a role in Akt activation downstream of EGFR. Treating mature neurons with p110 specific-subunit inhibitors prior to EGF treatment resulted in decreased phosphorylation of Akt only after general PI3K or p110α blockage. The inhibition of p110β, γ, δ did not affect EGF mediated increases in p(S473)Akt (see Figure 24A). This result indicates an involvement of the PI3K-p110α subunit in EGF – Akt2 signaling independent of the other three catalytic subunits in mature neurons. The peak at pI 5.53, which was found increased after EGF treatment in the presence of PI3K-p110β inhibitor (see Figure 24B) could indicate that upstream activity of p110β, which deviates from the other PI3K-p110 subunits, plays a role on the phosphorylation of Akt. In this context it is of interest that PI3K-p110β is the only p110 subunit activated by Rac1 GTPase and not by Ras GTPases [Fritsch et al. 2013], suggesting a differential Akt activation by Rac1.

In summary, we were able to characterize a novel EGF dependent signaling pathway in mature cortical neurons involving EGFR, activation of the PI3K p110α subunit, triggering specifically Akt2 and not the other Akt isoforms. Furthermore, this signaling was only found in mature (21 DIV) but not young (7 DIV) primary cortical neurons.

3.9. Time-dependent analysis of EGF stimulation in mature cortical neurons

3.9.1. EGF treatment does not induce translocation of the autophagic marker TFEB

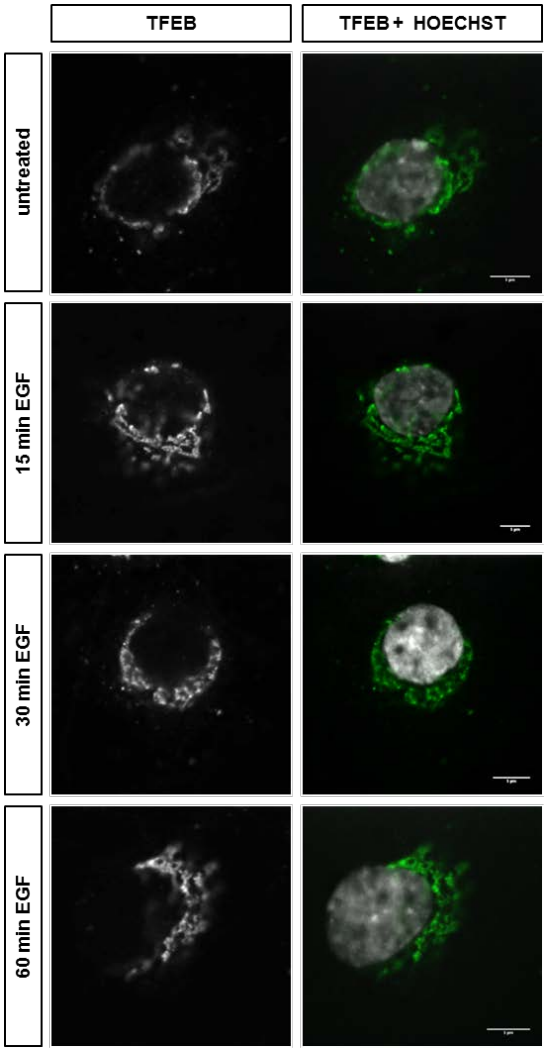

Figure 25: *Analysis of TFEB localization after EGF treatment*. 21 DIV hippocampal rat neurons were treated with EGF for up to 60 minutes. Immunocytochemical staining showed no nuclear translocation of TFEB (green) during EGF stimulation.

After establishing a new EGF-PI3K/p110α-Akt2 signaling axis in mature neurons the next step involved the analysis of possible downstream targets and or/cellular responses. By personal communication with Lawrence Rajendran (University of Zurich, Switzerland), he suggested a role for Akt2 signaling in the process of autophagy via the regulation of the transcription factor EB (TFEB). TFEB is a master regulator of lysosomal biogenesis and positively regulates autophagosomal formation [Settembre et al. 2012]. Phosphorylated TFEB is inactive and stays in the cytoplasm, upon activation it localizes to the nucleus. Assuming the activation of Akt2 by EGF plays a role in autophagy it would result in a nuclear translocation of TFEB. We used immunocytochemistry to stain for TFEB in mature hippocampal neurons. After analysis of different time points after EGF stimulation we could not detect any localization changes of TFEB either to the nucleus or within the cytoplasm (see Figure 25). Therefore, we conclude that the activation of Akt2 by EGF does not play a role in the early steps of autophagy, at least the steps involving recruitment of TFEB to the nucleus.

3.9.2. Analysis of PI3K-dependent downstream effectors after EGF stimulation

During the course of this study, the group of Emilio Hirsch generated a new p(S474)Akt2 specific antibody [Braccini et al. 2015], which was made commercially available by Cell Signaling Technologies. We made use of this new tool, in order to confirm our results described in the previous section (see section 3.8). We performed time course experiments to assess the activation of Akt2 by the phosphorylation of its S474 site. 21 DIV primary cortical neurons were stimulated with BDNF, as well as acute and overnight treatments with EGF. WB analysis showed a general increase in phosphoAkt (panAkt) and phosphoAkt2 forms with time. Statistical analysis of four independent experiments revealed this increase to be significant at the time points 15 and 30 min following growth factor stimulation. We detected no change in total Akt, nor in Bax, a proapoptotic member of the Bcl-2 family negatively regulated by PI3K signaling, or p53, a major tumor suppressor negatively regulated by PI3K signaling, levels. Further we did not detect any changes in the phosphorylation levels of the Akt downstream target mTOR, a Serine/Threonine kinase that regulates various processes including cell growth, cell proliferation, cell survival, protein synthesis, and transcription (see Figure 26A). In densiometry measurements, again of four independent experiments, a significant increase in p(S473)Akt was seen after short-term EGF or short-term BDNF stimulation (see Figure 26B). In contrast, a significant increase in p(S474)Akt2 was only found after short-term EGF treatment (see Figure 26C). This again confirms the every specific EGF - Akt2 signaling axis previously identified in this study. WB results suggest an increase in pS6, a well know downstream target of Akt involved in the regulation of cell size, cell proliferation, and glucose homeostasis, after 15 min BDNF treatment and a decrease in pS6 levels after 15 min EGF treatment, but these results were not found to be significant and their quantification is therefore not shown here. Hence, we can confirm the specificity of EGF signaling on the activation of Akt2 but we could not identify a direct effect on two established downstream targets of the PI3K/Akt pathway, namely mTOR and ribosomal protein S6.

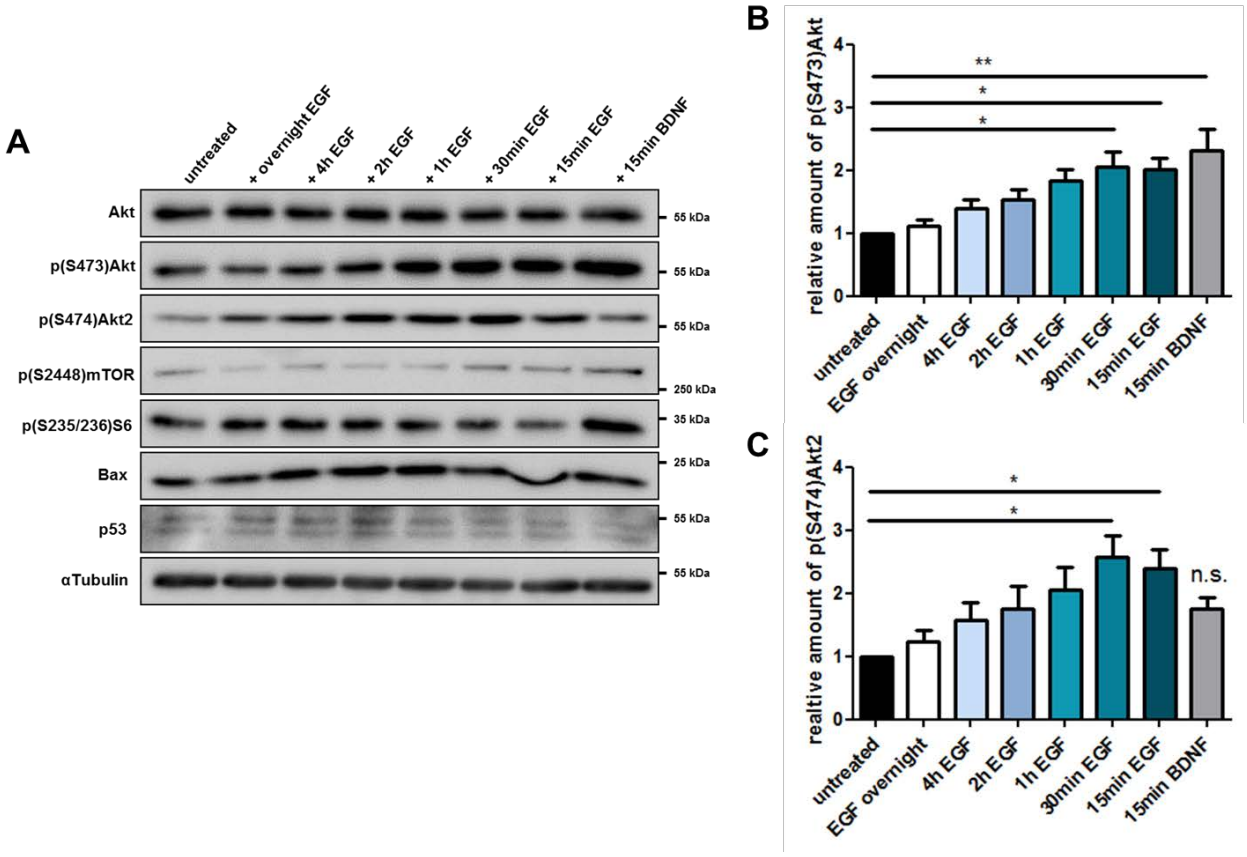

Figure 26: *EGF stimulation time course of primary cortical neurons*. 21 DIV cortical neurons were treated with EGF for 15 min until overnight (~16 h) or for 15 min with BDNF. **(A)** The lysates were analyzed by WB showing a strong increase in phosphoAkt after short-term growth factor treatment. No changes for Bax, p53, p(S2448)mTOR and total Akt were observed. **(B)** Densiometry measurements of 4 independent experiments were quantified for p(S473)Akt showing a significant increase after EGF and BDNF treatment. **(C)** But only short-term EGF treatment led to a significant increase in p(S474)Akt2.

4. Discussion

4.1. Advantages and limitations of using cIEF for Akt analysis

The aim of this project was the generation of a robust system to analyze phosphorylation of the different Akt isoforms using an antibody-based approach. Therefore, we established an assay based on the isoelectric point of proteins, with separation of the proteins according to their charge. cIEF provides short separation times, high resolution, and minimal sample consumption [O'Neill et al. 2006; Righetti, Sebastiano, and Citterio 2013]. It is frequently used in the pharmaceutical industry to check lot-to-lot consistency and control the quality of products [Michels et al. 2012]. We established an assay to monitor the Akt phosphorylation status in neuronal and brain tissue. All three isoforms were identified in neuroblastoma cells, primary cortical neurons and whole brain lysates. Akt1 was found to be the main Akt isoform present in all these tissues, although the main Akt1 molecule varied in between samples. The largest Akt1 peak in neuroblastoma cells was identified at pI 5.53, in cortical neurons at pI 5.42 and in embryonic mouse brain at a pI of 5.61, suggesting variation of PTMs on this isoform depending on the cell type (see Figure 5). It has been published that Akt3 constitutes ~50% of total Akt in the brain [Turner et al. 2015], we could not confirm this result, as Akt3 was found to be equally expressed as Akt2, both isoforms together composing ~40% of total Akt. We were able to show the three Akt isoforms in their non-phosphorylated state (see Figure 6) and identify phosphorylation-specific peaks using the p(S473)-, p(T308)-, and p(T450)Akt antibodies. The advantage of using phospho-specific antibodies is their recognition of a specific phosphorylation site which is conserved in all three Akt isoforms, therefore not favoring binding to one isoform or another. The p(T450)Akt antibody, as well as the panAkt antibody, detected a peak at 5.21 which was not recognized by the other phospho-antibodies. However, this peak together with all other peaks with a pI<5.42 was removed by λ-phosphatase treatment, identifying them to be phospho-specific. We assume the 5.21 peak to a precursor form for other phosphorylation events and PTMs. The phosphatase results in our study showed a new peak at 6.02 representing unphosphorylated Akt2, therefore, suggesting that Akt2 occurs mainly with PTMs in the cells and tissues tested during this project. In accordance, this peak was also found in starved HCT116 cells, wild type as well as after $Akt1^{-/-}$ but not $Akt2^{-/-}$ [H Guo et al. 2014]. All peaks detected with the panAkt antibody are in agreement to previously published results in human cancer cell lines, although Akt seems to have more modifications in our tested neuronal background because more acidic peaks were detected than previously described (5.06, 5.14) [Sabnis et al. 2014; H Guo et al. 2014; Iacovides et al. 2013]. Unfortunately, additional commercially available antibodies (T34 and Y326) did not work in either WB or cIEF, therefore, prohibiting a more

detailed characterization of the phosphorylation containing peaks. As a next step to unravel the constitution of the peaks containing posttranslational modified Akt molecule, one would have to start investigating also other PTMs than phosphorylation, e.g. ubiquitination or sumoylation. Taken together cIEF is not a substitute for conventional WB, but cIEF provides more information regarding the activation status of target proteins than WB, in addition to its higher sensitivity and better assay reproducibility. For example, cIEF can be used to estimate relative levels of phosphorylation of a protein (e.g. Akt). We developed an 'Akt activation index' for PTEN overexpression experiments in 293T cell line. Overexpression of different PTEN plasmids in 293T cells results in small or undetectable decreases in p(S473)Akt and p(T308)Akt phosphorylation by WB. Using the p(T450)Akt antibody in cIEF revealed consistent reduction of Akt activation to different levels. We calculated a ratio of phospho-specific Akt peaks to total Akt peaks in cIEF analysis. Using this method in PTEN dosage experiments in human 293T cells, we have achieved reliable assessment of small changes in Akt activation levels (e.g. a 20-30% reduction), which was not feasible using traditional WB techniques. This raises the question of how much of the total Akt pool is double phosphorylated, hence maximal activated under given conditions. To our knowledge, this question has not been answered yet. cIEF analysis of Akt molecules only provides a relative number, therefore, we think this question can only be addressed by a proteomic approach. In summary, cIEF provides a valuable additional analytical tool for the analysis of signaling pathways. This approach has great potential in the analysis of patient samples as well as in evaluation of the efficiency of kinase inhibitors and related drugs in the future.

4.2. Effect of upstream signaling on Akt activity *in vitro*

4.2.1. Insulin stimulation/ PI3K inhibition of neuroblastoma cells

In order to assess the phosphorylation states of Akt we performed several growth factor stimulation, PI3K inhibition or PTEN deletion experiments. In comparison to previous approaches utilizing a panAkt antibody [Sabnis et al. 2014; H Guo et al. 2014], we focused on working with the phospho-specific S473 and T308 antibodies to determine the correlation and the temporal dynamics and patterns of these activation-specific phosphorylation events. As another confirmation for our cIEF method, we detected the same phospho-specific peaks, independently, in the different neuronal lysates tested (neuroblastoma cells, primary cortical neurons, brain tissue). We were able to unambiguously resolve 4-5 major Akt peaks positive for the activating phosphorylations at T308 and S473, namely 5.06, 5.14, 5.31, 5.42, 5.53 (5.53 was detected only by the p(S473)Akt antibody) (see Figure 6, 8, 10-16, 21, 23, 24). Interestingly, slight variations were found in P0 rat brain were additional peaks at 4.97 and

5.21 were seen (see Figure 11). Also in astrocytes two additional peaks at 5.01 and 5.21 were detected by the both phospho-specific Akt antibodies (see Figure 18). Again, this highlights the variety of PTMs on Akt molecules in different cell types and cellular context. Taken the results from the isoform-specific tests and phosphatase treatment of N1E-115 cells we conclude that the more acidic peaks, with pI ≤5.31, correspond primarily to Akt1, whereas the more basic peaks, 5.42 and 5.53, are more heterogeneous in their composition, consisting mostly of Akt1 and Akt2 forms. These results are again in agreement with previously published results of Akt2 cIEF after Insulin stimulation in HCT-116 cells [H Guo et al. 2014]. The heterogeneity of peaks in modifications of Akt molecules (irrespective of isoform compositions) was seen in acute profile changes after Insulin treatment. Some peaks were poorly resolved or appeared with small shoulder peaks and this was more evident for the most acidic S473/T308-phosphorylated Akt forms (pI 5.06, 5.14, 5.31). This highlights the fact that the S473/T308-phosphorylated Akt forms apparently are further differentiated with respect to additional phosphorylation (and/or other post-translational) modifications. One can only surmise that these distinct S473/T308-phosphorylated Akt molecules may differ in their engagement into substrate recognition and phosphorylation of the numerous Akt substrates *in vivo*. We probed our samples with the panAkt antibody as a loading control for our assay. When comparing the total Akt profile of starved N1E-115 cells with 30 min WM treated N1E-115 cells, we found striking differences (see Figure 8 and 10). In both cases, Akt was deprived of any phosphorylations on its activating phosphorylation sites, as shown by cIEF with the S473 and T308 antibody. As it has previously been shown that other PTMs (e.g. ubiquitination [W-L Yang et al. 2009], acetylation [Sundaresan et al. 2011], sumoylation [Lin, Liu, and Lee 2016] or O-GlcNAcylation [S Wang et al. 2012] can influence the activity of Akt, we hypothesize that co-dependences of PTMs may contribute to the control of Akt regulation in situations of general limitation of nutrients and reduced PIP_3 levels following PI3K inhibition. Guo *et al*., propose that the phosphorylation of the T308 residue is dependent on prior phosphorylation of S473 during Insulin stimulation of HCT-116 cells [H Guo et al. 2014]. We cannot confirm this finding with our results of Insulin stimulation experiments in N1E-115 neuroblastoma cells. In fact, we were able to show an uncoupling of these phosphorylation events during Insulin stimulation and PI3K inhibition experiments. In lysates of Insulin treated cells we found at least one peak (pI 5.53) which was only recognized by the p(S473)- but not the p(T308)Akt antibody (see Figure 8). Furthermore, after PI3K inhibition by WM we observed an acute but transient net increase of a subset of S473 Akt1 forms (pI 5.14) but not in T308 phosphorylation (see Figure 10). For the T308 phosphorylation a mechanism to resist dephosphorylation by PP2A has been shown [Chan et al. 2011], a similar scenario is conceivable in the regulation of the S473 residue. Another possibility would be that the transient increase in the 5.14 peak is independent of Akt phosphorylation, but due to other

PTMs. Nevertheless, these data suggest, that at least for some Akt forms, acute loss of PIP_3 results in transient upregulation of phospho-S473 but not phospho-T308.

4.2.2. Dynamic regulation of Akt phosphorylation by PTEN loss and growth factors in primary cortical neurons

We utilized our assay to monitor the effect of growth factor signaling on Akt phosphorylation in immature (7 DIV) and mature (21 DIV) neurons. In immature neurons the largest increase in Akt phosphorylation, in WB and cIEF, was observed after BDNF treatment, whilst EGF and Insulin treatment only had a minor effect (see Figure 13). These results confirm the important role of BDNF signaling during neuronal differentiation where it was found to signal via PI3K-PDK1-Akt-mTORC1-S6K to function, for example, in axon formation and growth [Zurashvili et al. 2013]. In this study Zurashvili *et al*., also suggest, that Akt3 is the responsible isoform for BDNF-mediated neuronal survival. To our surprise, when mature neurons were treated with the same growth factors the activation profile for Akt had changed completely. By WB analysis, BDNF still led to an increase in Akt phosphorylation but only a minor effect was measured using cIEF. Insulin did not induce any additional phosphorylation of Akt as detected by WB or cIEF. Instead, EGF had the greatest effect on p(S473)- and p(T308)Akt. Probing lysates of EGF treated primary neurons, we found an increase in the 5.31 and 5.42 peaks with the p(S473)- as well as the p(T308)Akt antibody (see Figure 14). Therefore, we conclude that the signaling response to growth factors differs depending on the age of the neuron. As suggested for BDNF or NT-4 binding to TrkB leading to different downstream signals [Islam, Loo, and Heese 2009], we also hypothesize that BDNF and EGF activation of PI3K lead to a different downstream response. Nonetheless, both growth factors seemed to activate the more basic phosphorylation-specific peaks. When Akt phosphorylation was increased in response to PTEN loss we saw a different cIEF profile. PTEN loss led to a high phosphorylation of mainly Akt1 containing peaks (see Figure 15 and 16). Important to know, deletion of PTEN is supposed to impact primarily the pool of PIP_3 on the plasma membrane and only secondarily intracellular pools of $PI(3,4)P_2$ or $PI(3,4)P_2$ pools on the plasma membrane [Posor et al. 2013; Kreis et al. 2014]. Respectively, Braccini *et al*. recently published a study suggesting that Akt2 but not Akt1 can be activated on endosomal membranes by Insulin by a pathway involving a class II PI3K and the localized production of $PI(3,4)P_2$ [Braccini et al. 2015]. This indicates that the lipid composition on the plasma membrane, not just the availability of PIP_3 per se, has an influence on the activated downstream signaling cascade. These results show unequivocally that, although Akt can be regulated by both growth factors and PTEN, these two pathways do not result in the generation of the same S473/T308 Akt species. Indeed, this is, to the best to our knowledge, first molecular evidence that PTEN-deficient neurons demonstrate a distinct molecular

signature compared to growth factor-stimulated cells, at least of the level of downstream Akt phosphorylation. Akt phosphorylation after PTEN loss has also recently found to be necessary for regeneration of retinal ganglion cells (RGC) after optic nerve crush injury. Activation of Akt and subsequent inactivation of GSK3β led to enhanced activity of eIF2Bε allowing increased protein synthesis, which results in improved regenerative potential [X Guo, Snider, and Chen 2016]. Interestingly, this regenerative potential after PTEN loss was found to be largely dependent on Akt3 and not Akt1 [Miao et al. 2016]. This might be due to the difference in cell types. We tested cortical neurons, whilst the two studies focused on regeneration of RGCs axons. In the retina, Akt3 was found to be the most active isoform [Miao et al. 2016].

For glial cells it has been shown, that Akt phosphorylation was significantly higher in PTEN-deficient astrocytes than WT astrocytes. However, the total Akt phosphorylation was not predictive for tumorigenesis. Tumorigenesis was delayed by loss of Akt1 and enhanced by loss of Akt2 [Endersby et al. 2011]. Over the past years, particularly in the cancer field, the importance of upstream PI3K signaling in PTEN-deficient cells has gained attention. In colon cancer cells with heterozygous PTEN loss inactivation of p110β but not p110α inhibited cancer development [Berenjeno et al. 2012]. Nonetheless p110α can level the effect of PTEN loss on tumorigenesis in other tissues, e.g. thyroid cancer, ovarian cancer [Berenjeno et al. 2012; Schmit et al. 2014]. This underlines the importance of tissue-specific analysis of the different Akt isoforms and their signaling cascades. To evaluate the nature of growth factor-induced PI3K signaling in mature neurons in more detail, we made use of the specific PI3K p110 subunit inhibitors. The expected loss of Akt phosphorylation after complete (general) PI3K inhibition was largely recapitulated by specific loss of p110α activity, indicating its dominant role in PI3K signaling in physiological conditions in mature cortical neurons. p110α was also identified as the major subunit involved in PI3K-Akt2 signaling after stimulation with EGF. These findings support the crucial role of p110α in receptor Tyrosine kinase signaling. In the literature the non-redundant roles of the PI3K subunits have already been described. As mentioned above, p110β was found to be the major isoform involved in cancer progression in PTEN-deficient cells and p110α to be responsible for cancer progression in cells with aberrant RTK signaling [Schwartz et al. 2015].

4.2.3. Specific activation of Akt2 after EGF stimulation in mature cortical neurons

In previous publications the importance of TrkB activation by EGF or BDNF has been shown to play a role in neuronal migration, proliferation of neuronal stem cells and vascular neuroprotection [Puehringer et al. 2013; Islam, Loo, and Heese 2009; S Guo et al. 2012]. In this study, we were able to demonstrate an EGF-specific activation of Akt2 in mature cortical neurons. TrkB, in our hands, appears to play only a minor role in this signaling axis, hinting towards its suggested role earlier in neuronal differentiation, in late-phase neurogenesis [Islam, Loo, and Heese 2009]. The main signaling response was generated through EGFR with subsequent activation of the PI3K-p110α subunit. EGFR expression was only detected in mature neuronal cultures (16 and 21 DIV). Supporting our results, the phosphorylation of Akt after EGF stimulation has been shown to be dependent on Presenilin1 in primary cortical neurons. The loss of Presenilin1 led to a decrease in neuronal EGFR protein expression [Bruban et al. 2015]. Another study in mature neurons, proposes *in vitro* EGF treatment to enhance NMDAR-mediated calcium influx and synaptic plasticity [Tang et al. 2015]. In contrast, EGFR plays a role also earlier during neuronal development in branching and pruning in *Drosophila* CNS. EGFR localization was found to be regulating filopodia dynamics, thereby mediating axon branch development [Zschätzsch et al. 2014]. Taken together, EGF signaling via its receptor EGFR plays a relevant role during brain development and is neuroprotective in adult brain and after brain injury. To date little is generally known concerning the precise function of EGF-Akt signaling in mature neurons. In medulloblastoma cells, EGF was found to phosphorylate Akt, leading to enhanced migration [Dudu et al. 2012]. In esophageal cancer cells, redundant and distinct phosphorylation patterns of the three different Akt isoforms have been found after EGF stimulation [Okano et al. 2000]. Therefore, more research focusing on the roles of Akt isoform-specific functions in neurons has to been done. Speed *et al*. could show, that Akt2, not Akt1, is activated by Insulin and involved in dopamine transporter cell surface expression [Speed et al. 2010]. Since we also found a specific activation of Akt2 after EGF stimulation, we started to explore the specific signaling cascade further. We could not detect significant phosphorylation changes any of the most common Akt substrates (S6, mTOR, GSK3β) after acute treatment. In lymphoblasts Akt2 has been shown to play a role in p53 stabilization via its kinase activity on the E3 ubiquitin ligase MDM2 [Boehme, Kulikov, and Blattner 2008]. Therefore, we also investigated p53 as a possible downstream target of EGF-Akt2 signaling. In timecourse experiments we could not detect any expression changes (see Figure 26). Interestingly, in pilot experiments with long-term EGF treatment, stimulating cortical neurons *in vitro* for 7 days, we found an upregulation in Bax and p53 expression, both being pro-apoptotic genes (data not shown). The involvement of Akt2 in this response

has to be further assessed, e.g. by the use of Akt2 shRNA. An effect of Akt2 on protein synthesis has already been shown in the context of its interaction with the elongation factor 2 (EF2) in cardiac myocytes. This Akt2-EF2 complex depends on the phosphorylation status of Akt2, as it falls apart when Akt2 gets activated, allowing EF2 to bind to ribosomes and increase protein synthesis [Bottermann et al. 2013]. Therefore, we hypothesize Akt2 as a new participant in pro-apoptotic signaling in response to cellular stress caused by prolonged growth factor stimulation. The fact that prolonged activation of the PI3K pathway influences the cells homeostasis has been reported previously. In 19 DIV neurons an activation of PI3K for 2 days has led to a 38% increase in both, inhibitory and excitatory synapses, the effect was found to be independent of the developmental state of the culture [Cuesto et al. 2011]. Hence, further investigation in the exact role of PI3K – Akt2 after extensive EGFR signaling and subsequent pro-apoptotic response has to be done.

4.3. Analysis of signaling proteins related to neuronal development in postnatal rat brain

Despite the widely accepted importance of the PI3K/Akt pathway during neuronal development [Waite and Eickholt 2011], there is currently little knowledge concerning the endogenous profile and regulation of Akt phosphorylation during normal brain development. For the total protein levels of Akt, GSK3β and ERK1/2 our results are in accordance with previous studies performed on mouse cortical and hippocampal development [Beurel et al. 2012]. Although the inhibitory S9 phosphorylation of GSK3β seems to reach a later maximum (P7) than reported (P1), nonetheless, levels of this phosphorylated protein decrease when the total abundance increases until its maximum at P21 [Beurel et al. 2012]. Between the different Akt isoforms, Akt3 shows a brain specific expression and was found to play a crucial role in postnatal brain development [Tschopp et al. 2005]. Although the essential isoform for embryonic development and survival is Akt1, both isoforms are required for development, as double knock-out $Akt1^{-/-}Akt3^{-/-}$ mice are not viable [Z Yang et al. 2005]. It has to be noted, that genes associated with the PI3K signaling pathway were found to be poorly conserved between humans and mice, therefore leading to a lack of mouse models where the functionality of main effectors of the PI3K cascade is altered [Monaco et al. 2015]. Nonetheless in accordance with the published Akt knock-out mice models, we detected Akt1 protein expression level almost equal throughout the tested time points, whereas Akt3 declined in older brains. In contrast, Akt2 expression showed a peak at P21 before decreasing. This might suggest a specific role of this isoform in the non-neuronal cell development at this time point. Postnatal brain development is characterized by dramatic changes in the cellular composition of the brain. During the first week, the net number of

neurons increase dramatically followed by an increase in non-neuronal cells in postnatal weeks two and three [Bandeira, Lent, and Herculano-Houzel 2009]. A spatial and temporal shift of Akt activity has also been published for embryonic mouse development where Akt is highly phosphorylated during mitosis [Marques and Thorsteinsdóttir 2013]. The changes in S473 and total Akt profiles were most evident when comparing the P0 and P7 samples in our experiment. This suggests a substantial reprogramming of Akt phosphorylation and activation during these crucial developmental stages, indicating also an important role for Akt activation during postnatal development. In summary we can conclude, that our analysis of structural and signal proteins during postnatal brain is in good agreement with previous studies but also shows, that WB analysis does not provide all the information on protein expression. So far unappreciated peak shifts in Akt isoforms suggest dynamic modifications during the postnatal period we investigated (see Figure 11).

4.4. Conclusion and outlook

This thesis provides first steps to decipher PI3K – Akt signaling in a developmental- and signal-dependent manner in greater detail. The importance of distinguishing between signal input and output became apparent when we compared the outcome of growth factor activated PI3K and PTEN loss on Akt activity. We showed that different Akt pools were phosphorylated by the different upstream stimuli. A summary of the growth factor responses of the different developmental stages of neurons found in this project is shown in Figure 27. Diez *et al*. studied the specific roles of the different isoforms in differentiated neurons, thereby already pointing out that although the three isoforms show substantial compensation for each other in some processes, disruption of individual isoforms can also cause reduced neuron viability [Diez, Garrido, and Wandosell 2012]. Triple, but not single knock-out of the Akt isoforms has been identified to play a role in Tau hyperphosphorylation, therefore suggesting an involvement in Alzheimer disease [L Wang et al. 2015]. Additionally, non-redundant functions of Akt isoforms have also been found in astrocytes and there being involved in gliomagenesis [Endersby et al. 2011]. In cell lines the subcellular localization of the different isoforms has been previously assessed and found to differ enormously. Akt1 was found to be present in the cytoplasm and nucleus, Akt2 was found to co-localize with the mitochondria and Akt3 was mainly localized in the nucleus and at the nuclear membrane [Santi and Lee 2010]. All these studies point out the importance of differentiation between the different Akt isoforms and not just assuming them to be one protein. With the cIEF assay in our lab we were able to establish an important tool for further investigation of Akt signaling responses. In the course of this project we could show a specific EGF-EGFR-PI3K/p110α-Akt2 signaling cascade. It would be of further interest to investigate the downstream

functionality of this signaling pathway. Therefore, we are currently working on producing Akt2-shRNA in order to confirm its role in the induction of apoptosis after longterm EGF treatment. It is also planned to start a mass spec approach to compare interaction partners of EGF in the presence and absence of EGF. Akt2, being the ´metabolic´ isoform, has recently been shown to influence glutathione biosynthesis and activating mutations of Akt2 leading to enhanced tumorigenesis in breast cancer [Lien et al. 2016]. We would like to further exploit the metabolic role of Akt2 after EGF treatment.

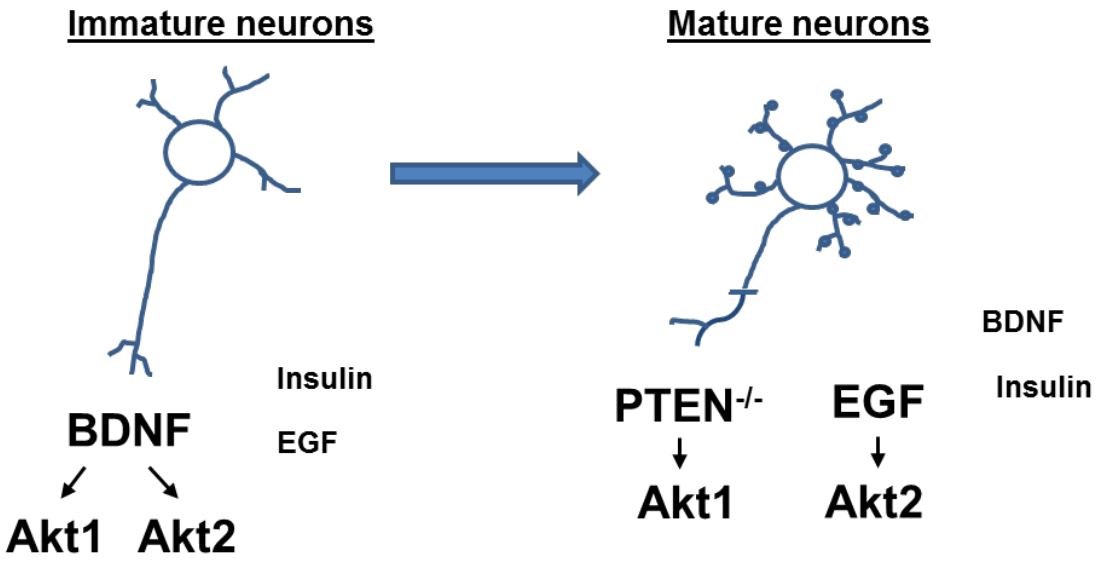

Figure 27: *Schematic view of Akt isoform activation*. In immature primary cortical neurons (7 DIV) BDNF led to an increase in phosphorylation of Akt1 and Akt2. Insulin and EGF stimulation only had a minor effect. In contrast, in mature neurons (21 DIV) EGF led to activation of specifically Akt2 whereas PTEN loss induced phosphorylation of Akt1. Here, BDNF and Insulin showed only a mild effect.

5. References

Amiri, A., W. Cho, J. Zhou, S.G. Birnbaum, C.M. Sinton, R.M. McKay, and L.F. Parada. 2012. “Pten Deletion in Adult Hippocampal Neural Stem/Progenitor Cells Causes Cellular Abnormalities and Alters Neurogenesis.” Journal of Neuroscience. 32(17): 5880–5890.

Aspinall-O’Dea, M., A. Pierce, F. Pellicano, A.J. Williamson, M.T. Scott, M.J. Walker, T.L. Holyoake, and A.D. Whetton. 2015. “Antibody-Based Detection of Protein Phosphorylation Status to Track the Efficacy of Novel Therapies Using Nanogram Protein Quantities from Stem Cells and Cell Lines.” Nat. Protocols. 10(1): 149–168.

Bandeira, F., R. Lent, and S. Herculano-Houzel. 2009. “Changing Numbers of Neuronal and Non-Neuronal Cells Underlie Postnatal Brain Growth in the Rat.” Proceedings of the National Academy of Sciences of the United States of America. 106(33): 14108–14113.

Bathina, S., and U.N. Das. 2015. “State of the Art Paper Brain-Derived Neurotrophic Factor and Its Clinical Implications.” (Icv).

Berenjeno, I.M., J. Guillermet-Guibert, W. Pearce, A. Gray, S. Fleming, and B. Vanhaesebroeck. 2012. “Both p110α and p110β Isoforms of PI3K Can Modulate the Impact of Loss-of-Function of the PTEN Tumour Suppressor.” The Biochemical journal. 442(1): 151–9.

Beurel, E., M.A. Mines, L. Song, and R.S. Jope. 2012. “Glycogen Synthase Kinase-3 Levels and Phosphorylation Undergo Large Fluctuations in Mouse Brain during Development.” Bipolar Disorders. 14(8): 822–830.

Boehme, K. a, R. Kulikov, and C. Blattner. 2008. “p53 Stabilization in Response to DNA Damage Requires Akt/PKB and DNA-PK.” Proceedings of the National Academy of Sciences of the United States of America. 105(22): 7785–7790.

Bottermann, K., M. Reinartz, M. Barsoum, S. Kötter, and A. Gödecke. 2013. “Systematic Analysis Reveals Elongation Factor 2 and α-Enolase as Novel Interaction Partners of AKT2.” PLoS ONE. 8(6).

Braccini, L., E. Ciraolo, C.C. Campa, A. Perino, D.L. Longo, G. Tibolla, M. Pregnolato, Y. Cao, B. Tassone, F. Damilano, M. Laffargue, E. Calautti, M. Falasca, G.D. Norata, J.M. Backer, and E. Hirsch. 2015. “PI3K-C2γ Is a Rab5 Effector Selectively Controlling Endosomal Akt2 Activation Downstream of Insulin Signalling.” Nature Communications. 6(May): 7400.

Brian, P.W., P.J. Curtis, H.G. Hemming, and G.L.F. Norris. 1957. “WORTMANNIN , AN ANTIBIOTIC PRODUCED BY PENICILLIUM WORTMANNI.” Transactions of the British Mycological Society. 40(3): 365–368, IN3.

Brodbeck, D., M.M. Hill, and B.A. Hemmings. 2001. “Two Splice Variants of Protein Kinase B Gamma Have Different Regulatory Capacity Depending on the Presence or Absence of the Regulatory Phosphorylation Site Serine 472 in the Carboxyl-Terminal Hydrophobic Domain.” Journal of Biological Chemistry. 276(31): 29550–29558.

Bruban, J., G. Voloudakis, Q. Huang, Y. Kajiwara, M. Al Rahim, Y. Yoon, J. Shioi, M.A. Gama Sosa, Z. Shao, A. Georgakopoulos, and N.K. Robakis. 2015. “Presenilin 1 Is Necessary for Neuronal, but Not Glial, EGFR Expression and Neuroprotection via G-Secretase-Independent Transcriptional Mechanisms.” FASEB Journal. 29(9): 3702–3712.

Butler, M.G., M.J. Dasouki, X. Zhou, Z. Talebizadeh, M. Brown, T.N. Takahashi, J.H. Miles,

C.H. Wang, R. Stratton, R. Pilarski, and C. Eng. 2005. “Subset of Individuals with Autism Spectrum Disorders and Extreme Macrocephaly Associated with Germline PTEN Tumour Suppressor Gene Mutations.” Journal of Medical Genetics . 42 (4): 318–321.

Cantley, L.C. 2002. “The Phosphoinositide 3-Kinase Pathway.” Science. 296(5573): 1655–1657.

Chadborn, N.H., A.I. Ahmed, M.R. Holt, R. Prinjha, G.A. Dunn, G.E. Jones, and B.J. Eickholt. 2006. “PTEN Couples Sema3A Signalling to Growth Cone Collapse.” Journal of cell science. 119(Pt 5): 951–957.

Chan, T.O., J. Zhang, U. Rodeck, J.M. Pascal, R.S. Armen, M. Spring, C.D. Dumitru, V. Myers, X. Li, J.Y. Cheung, and a. M. Feldman. 2011. “Resistance of Akt Kinases to Dephosphorylation through ATP-Dependent Conformational Plasticity.” Proceedings of the National Academy of Sciences. 108(46): E1120–E1127.

Chen, J.Q., J.H. Lee, M.A. Herrmann, K.S. Park, M.R. Heldman, P.K. Goldsmith, Y. Wang, and G. Giaccone. 2013. “Capillary Isoelectric-Focusing Immunoassays to Study Dynamic Oncoprotein Phosphorylation and Drug Response to Targeted Therapies in Non-Small Cell Lung Cancer.” Molecular Cancer Therapeutics. 12(11): 2601–2613.

Chen, W.S., P.Z. Xu, K. Gottlob, M.L. Chen, K. Sokol, T. Shiyanova, I. Roninson, W. Weng, R. Suzuki, K. Tobe, T. Kadowaki, and N. Hay. 2001. “Growth Retardation and Increased Apoptosis in Mice with Homozygous Disruption of the akt1 Gene.” Genes and Development. 15(17): 2203–2208.

Cho, H., J. Mu, J. Kim, and J. Thorvaldsen. 2001. “Insulin Resistance and a Diabetes Mellitus – Like Syndrome in Mice Lacking the Protein Kinase Akt2 (PKB ␢).” Science. 292(June): 1728–1732.

Cho, H., J.L. Thorvaldsen, Q. Chu, F. Feng, and M.J. Birnbaum. 2001. “Akt1/PKBa Is Required for Normal Growth but Dispensable for Maintenance of Glucose Homeostasis in Mice.” Journal of Biological Chemistry. 276(42): 38349–38352.

Condliffe, A.M., K. Davidson, K.E. Anderson, C.D. Ellson, T. Crabbe, K. Okkenhaug, B. Vanhaesebroeck, M. Turner, L. Webb, M.P. Wymann, E. Hirsch, T. Ruckle, C. Rommel, S.P. Jackson, E.R. Chilvers, L.R. Stephens, and P.T. Hawkins. 2005. “Sequential Activation of Class IB and Class IA PI3K Is Important for the Primed Respiratory Burst of Human but Not Murine Neutrophils.” Blood. 106(4): 1432–1441.

Cosker, K.E., S. Shadan, M. van Diepen, C. Morgan, M. Li, V. Allen-Baume, C. Hobbs, P. Doherty, S. Cockcroft, B.J. Eickholt, M. Van Diepen, C. Morgan, M. Li, V. Allen-Baume, C. Hobbs, P. Doherty, S. Cockcroft, and B.J. Eickholt. 2008. “Regulation of PI3K Signalling by the Phosphatidylinositol Transfer Protein PITPα during Axonal Extension in Hippocampal Neurons.” Journal of Cell Science. 121(6): 796–803.

Cox, J., M.Y. Hein, C.A. Luber, I. Paron, N. Nagaraj, and M. Mann. 2014. “Accurate Proteome-Wide Label-Free Quantification by Delayed Normalization and Maximal Peptide Ratio Extraction, Termed MaxLFQ.” Molecular & Cellular Proteomics . 13 (9): 2513–2526.

Cuesto, G., L. Enriquez-Barreto, C. Carames, M. Cantarero, X. Gasull, C. Sandi, A. Ferrus, A. Acebes, and M. Morales. 2011. “Phosphoinositide-3-Kinase Activation Controls Synaptogenesis and Spinogenesis in Hippocampal Neurons.” Journal of Neuroscience. 31(8): 2721–2733.

Cuscó, I., A. Medrano, B. Gener, M. Vilardell, F. Gallastegui, O. Villa, E. González, B.

Rodríguez-Santiago, E. Vilella, M. Del Campo, and L.A. Pérez-Jurado. 2009. “Autism-Specific Copy Number Variants Further Implicate the Phosphatidylinositol Signaling Pathway and the Glutamatergic Synapse in the Etiology of the Disorder.” Human Molecular Genetics . 18 (10): 1795–1804.

Dajas-Bailador, F., I. Bantounas, E. V Jones, and A.J. Whitmarsh. 2014. “Regulation of Axon Growth by the JIP1-AKT Axis.” Journal of cell science. 127(November): 230–9.

Denley, A., S. Kang, U. Karst, and P.K. Vogt. 2008. “Oncogenic Signaling of Class I PI3K Isoforms.” Oncogene. 27: 2561–2574.

Diez, H., J.J. Garrido, and F. Wandosell. 2012. “Specific Roles of Akt Iso Forms in Apoptosis and Axon Growth Regulation in Neurons.” PLoS ONE. 7(4).

Di Donato, N., A. Rump, G.M. Mirzaa, D. Alcantara, A. Oliver, E. Schrock, W.B. Dobyns, and M. O’Driscoll. 2015. “Identification and Characterization of a Novel Constitutional PIK3CA Mutation in a Child Lacking the Typical Segmental Overgrowth of ‘PIK3CA-Related Overgrowth Spectrum.’” Human Mutation: 1–4.

Dudu, V., R.A. Able, V. Rotari, Q. Kong, and M. Vazquez. 2012. “Role of Epidermal Growth Factor-Triggered PI3K/Akt Signaling in the Migration of Medulloblastoma-Derived Cells.” Cellular and Molecular Bioengineering. 5(4): 403–413.

Easton, R., and H. Cho. 2005. “Role for Akt3/protein Kinase Bγ in Attainment of Normal Brain Size.” … and Cellular Biology. 25(5): 1869–1878.

Eickholt, B.J., A.I. Ahmed, M. Davies, E.A. Papakonstanti, W. Pearce, M.L. Starkey, A. Bilancio, A.C. Need, A.J.H. Smith, S.M. Hall, F.P. Hamers, K.P. Giese, E.J. Bradbury, and B. Vanhaesebroeck. 2007. “Control of Axonal Growth and Regeneration of Sensory Neurons by the p110d PI 3-Kinase.” PLoS ONE. 2(9): 1–9.

Endersby, R., X. Zhu, N. Hay, D.W. Ellison, and S.J. Baker. 2011. “Nonredundant Functions for Akt Isoforms in Astrocyte Growth and Gliomagenesis in an Orthotopic Transplantation Model.” Cancer Research. 71(12): 4106–4116.

Facchinetti, V., W. Ouyang, H. Wei, N. Soto, A. Lazorchak, C. Gould, C. Lowry, A.C. Newton, Y. Mao, R.Q. Miao, W.C. Sessa, J. Qin, P. Zhang, B. Su, and E. Jacinto. 2008. “The Mammalian Target of Rapamycin Complex 2 Controls Folding and Stability of Akt and Protein Kinase C.” The EMBO journal. 27(14): 1932–43.

Fairhurst, R.A., P. Imbach-weese, M. Gerspacher, G. Caravatti, P. Furet, T. Zoller, C. Fritsch, D. Haasen, J. Trappe, D.A. Guthy, D. Arz, and J. Wirth. 2009. “Bioorganic & Medicinal Chemistry Letters Identification and Optimisation of a 4 0 , 5-Bisthiazole Series of Selective Phosphatidylinositol-3 Kinase Alpha Inhibitors.” Bioorganic & Medicinal Chemistry Letters. 25(17): 3569–3574.

Fan, A.C., D. Deb-Basu, M.W. Orban, J.R. Gotlib, Y. Natkunam, R. O’Neill, R.-A. Padua, L. Xu, D. Taketa, A.E. Shirer, S. Beer, A.X. Yee, D.W. Voehringer, and D.W. Felsher. 2009. “Nanofluidic Proteomic Assay for Serial Analysis of Oncoprotein Activation in Clinical Specimens.” Nat. Med. 15(5): 566–71.

Folkes, A.J., K. Ahmadi, W.K. Alderton, S. Alix, S.J. Baker, G. Box, I.S. Chuckowree, P.A. Clarke, P. Depledge, S.A. Eccles, L.S. Friedman, A. Hayes, T.C. Hancox, A. Kugendradas, L. Lensun, P. Moore, A.G. Olivero, J. Pang, S. Patel, G.H. Pergl-wilson, F.I. Raynaud, A. Robson, N. Saghir, L. Salphati, S. Sohal, M.H. Ultsch, M. Valenti, H.J.A. Wallweber, N.C. Wan, C. Wiesmann, P. Workman, A. Zhyvoloup, M.J. Zvelebil, and S.J. Shuttleworth. 2008. “The Identification of 2- (1 H -Indazol-4-Yl) -6- (4-Methanesulfonyl-Piperazin-1-Ylmethyl) -4- Morpholin-4-Yl-Thieno [3 , 2- D] Pyrimidine

(GDC-0941) as a Potent , Selective , Orally Bioavailable Inhibitor of Class I PI3 Kinase for the Treatment of." J Med Chem. 51: 5522–5532.

Fritsch, R., I. De Krijger, K. Fritsch, R. George, B. Reason, M.S. Kumar, M. Diefenbacher, G. Stamp, and J. Downward. 2013. "XRAS and RHO Families of GTPases Directly Regulate Distinct Phosphoinositide 3-Kinase Isoforms." Cell. 153(5): 1050–1063.

Gao, T., F. Furnari, and A.C. Newton. 2005. "PHLPP: A Phosphatase That Directly Dephosphorylates Akt, Promotes Apoptosis, and Suppresses Tumor Growth." Molecular Cell. 18(1): 13–24.

Gross, C., and G.J. Bassell. 2014. "Neuron-Specific Regulation of Class I PI3K Catalytic Subunits and Their Dysfunction in Brain Disorders." Frontiers in molecular neuroscience. 7(February): 12.

Guo, H., M. Gao, Y. Lu, J. Liang, P.L. Lorenzi, S. Bai, D.H. Hawke, J. Li, T. Dogruluk, K.L. Scott, E. Jonasch, G.B. Mills, and Z. Ding. 2014. "Coordinate Phosphorylation of Multiple Residues on Single AKT1 and AKT2 Molecules." Oncogene. 33(26): 3463–3472.

Guo, S., A.T. Som, C. Waeber, and E.H. Lo. 2012. "Vascular Neuroprotection via TrkB- and Akt-Dependent Cell Survival Signaling." Journal of Neurochemistry. 123(SUPPL. 2): 58–64.

Guo, X., W.D. Snider, and B. Chen. 2016. "GSK3β Regulates AKT-Induced Central Nervous System Axon Regeneration via an eIF2Bε-Dependent, mTORC1-Independent Pathway." eLife. 5: 1–18.

Hart, J.R., and P.K. Vogt. 2011. "Phosphorylation of AKT: A Mutational Analysis." Oncotarget. 2(6): 467–76.

Hawkins, P.T., K.E. Anderson, K. Davidson, and L.R. Stephens. 2006. "Signalling through Class I PI3Ks in Mammalian Cells." Biochemical Society Transactions. 34(5): 647–662.

Hers, I., E.E. Vincent, and J.M. Tavar. 2011. "Akt Signalling in Health and Disease." Cellular Signalling. 23(10): 1515–1527.

Hopkins, B.D., B. Fine, N. Steinbach, M. Dendy, Z. Rapp, J. Shaw, K. Pappas, J.S. Yu, C. Hodakoski, S. Mense, J. Klein, S. Pegno, M.-L. Sulis, H. Goldstein, B. Amendolara, L. Lei, M. Maurer, J. Bruce, P. Canoll, H. Hibshoosh, and R. Parsons. 2013. "A Secreted PTEN Phosphatase That Enters Cells to Alter Signaling and Survival." Science. 341(6144): 399–402.

Huang, Y.Z., and J.O. McNamara. 2010. "Mutual Regulation of Src Family Kinases and the Neurotrophin Receptor TrkB." Journal of Biological Chemistry . 285 (11): 8207–8217.

Hussain, K., B. Challis, N. Rocha, F. Payne, M. Minic, A. Thompson, A. Daly, C. Scott, J. Harris, B.J.L. Smillie, D.B. Savage, U. Ramaswami, P. De Lonlay, S. O'Rahilly, I. Barroso, and R.K. Semple. 2011. "An Activating Mutation of AKT2 and Human Hypoglycemia." Science. 334(6055): 474.

Hwang, J.H., T. Jiang, S. Kulkarni, N. Faure, and B.S. Schaffhausen. 2013. "Protein Phosphatase 2A Isoforms Utilizing Aß Scaffolds Regulate Differentiation through Control of Akt Protein." Journal of Biological Chemistry. 288(44): 32064–32073.

Iacovides, D.C., A.B. Johnson, N. Wang, S. Boddapati, J. Korkola, and J.W. Gray. 2013. "Identification and Quantification of AKT Isoforms and Phosphoforms in Breast Cancer Using a Novel Nanofluidic Immunoassay." Molecular & cellular proteomics : MCP. 12(11): 3210–20.

Ikenoue, T., K. Inoki, Q. Yang, X. Zhou, and K.-L. Guan. 2008. “Essential Function of TORC2 in PKC and Akt Turn Motif Phosphorylation, Maturation and Signalling.” The EMBO journal. 27(14): 1919–31.

Islam, O., T.X. Loo, and K. Heese. 2009. “Brain-Derived Neurotrophic Factor (BDNF) Has Proliferative Effects on Neural Stem Cells through the Truncated TRK-B Receptor, MAP Kinase, AKT, and STAT-3 Signaling Pathways.” Current neurovascular research. 6(1): 42–53.

Jackson, S.P., S.M. Schoenwaelder, I. Goncalves, W.S. Nesbitt, C.L. Yap, C.E. Wright, V. Kenche, K.E. Anderson, S.M. Dopheide, Y. Yuan, S.A. Sturgeon, H. Prabaharan, P.E. Thompson, G.D. Smith, P.R. Shepherd, N. Daniele, S. Kulkarni, B. Abbott, D. Saylik, C. Jones, L. Lu, S. Giuliano, S.C. Hughan, J.A. Angus, A.D. Robertson, and H.H. Salem. 2005. “PI 3-Kinase p110 β : A New Target for Antithrombotic Therapy.” Nature medicine. 11(5): 507–514.

Jang, S.W., X. Liu, H. Fu, H. Rees, M. Yepes, A. Levey, and K. Ye. 2009. “Interaction of Akt-Phosphorylated SRPK2 with 14-3-3 Mediates Cell Cycle and Cell Death in Neurons.” Journal of Biological Chemistry. 284(36): 24512–24525.

Kreis, P., G. Leondaritis, I. Lieberam, and B.J. Eickholt. 2014. “Subcellular Targeting and Dynamic Regulation of PTEN: Implications for Neuronal Cells and Neurological Disorders.” Frontiers in molecular neuroscience. 7(April): 23.

Kwon, C.H., B.W. Luikart, C.M. Powell, J. Zhou, S.A. Matheny, W. Zhang, Y. Li, S.J. Baker, and L.F. Parada. 2006. “Pten Regulates Neuronal Arborization and Social Interaction in Mice.” Neuron. 50(3): 377–388.

Laketa, V., S. Zarbakhsh, A. Traynor-Kaplan, A. Macnamara, D. Subramanian, M. Putyrski, R. Mueller, A. Nadler, M. Mentel, J. Saez-Rodriguez, R. Pepperkok, and C. Schultz. 2014. “PIP3 Induces the Recycling of Receptor Tyrosine Kinases.” Science signaling. 7(308): ra5.

Law, A.J., Y. Wang, Y. Sei, P.O. Donnell, P. Piantadosi, F. Papaleo, R.E. Straub, W. Huang, C.J. Thomas, R. Vakkalanka, and A.D. Besterman. 2012. “Neuregulin 1-ErbB4-PI3K Signaling in Schizophrenia and Phosphoinositide 3-Kinase-p110 δ Inhibition as a Potential Therapeutic Strategy.” 4.

Leondaritis, G., L. Petrikkos, and D. Mangoura. 2009. “Regulation of the Ras-GTPase Activating Protein Neurofibromin by C-Tail Phosphorylation: Implications for Protein Kinase C/Ras/extracellular Signal-Regulated Kinase 1/2 Pathway Signaling and Neuronal Differentiation.” Journal of Neurochemistry. 109(2): 573–583.

Li, J., C. Yen, D. Liaw, K. Podsypanina, S. Bose, S.I. Wang, J. Puc, C. Miliaresis, L. Rodgers, R. McCombie, S.H. Bigner, B.C. Giovanella, M. Ittmann, B. Tycko, H. Hibshoosh, M.H. Wigler, and R. Parsons. 1997. “PTEN, a Putative Protein Tyrosine Phosphatase Gene Mutated in Human Brain, Breast, and Prostate Cancer.” Science. 275(5308): 1943–1947.

Lien, E.C., C.A. Lyssiotis, A. Juvekar, H. Hu, J.M. Asara, L.C. Cantley, and A. Toker. 2016. “Glutathione Biosynthesis Is a Metabolic Vulnerability in PI(3)K/Akt-Driven Breast Cancer.” Nature Cell Biology. 18(5).

Lin, C.H., S.Y. Liu, and E.H.Y. Lee. 2015. “SUMO Modification of Akt Regulates Global SUMOylation and Substrate SUMOylation Specificity through Akt Phosphorylation of Ubc9 and SUMO1.” Oncogene. (128): 1–13.

Lin, C.H., S.Y. Liu, and E.H.Y. Lee. 2016. “SUMO Modification of Akt Regulates Global

SUMOylation and Substrate SUMOylation Specificity through Akt Phosphorylation of Ubc9 and SUMO1." Oncogene. 35(5): 595–607.

Lindhurst, M.J., J.C. Sapp, J.K. Teer, J.J. Johnston, E.M. Finn, K. Peters, J. Turner, J.L. Cannons, D. Bick, L. Blakemore, C. Blumhorst, K. Brockmann, P. Calder, N. Cherman, M.A. Deardorff, D.B. Everman, G. Golas, R.M. Greenstein, B.M. Kato, K.M. Keppler-Noreuil, S.A. Kuznetsov, R.T. Miyamoto, K. Newman, D. Ng, K. O'Brien, S. Rothenberg, D.J. Schwartzentruber, V. Singhal, R. Tirabosco, J. Upton, S. Wientroub, E.H. Zackai, K. Hoag, T. Whitewood-Neal, P.G. Robey, P.L. Schwartzberg, T.N. Darling, L.L. Tosi, J.C. Mullikin, and L.G. Biesecker. 2011. "A Mosaic Activating Mutation in AKT1 Associated with the Proteus Syndrome." New England Journal of Medicine. 365(7): 611–619.

Liu, P., M. Begley, W. Michowski, H. Inuzuka, M. Ginzberg, D. Gao, P. Tsou, W. Gan, A. Papa, B.M. Kim, L. Wan, A. Singh, B. Zhai, M. Yuan, Z. Wang, S.P. Gygi, T.H. Lee, K.-P. Lu, A. Toker, P.P. Pandolfi, J.M. Asara, M.W. Kirschner, P. Sicinski, L. Cantley, and W. Wei. 2014. "Cell-Cycle-Regulated Activation of Akt Kinase by Phosphorylation at Its Carboxyl Terminus." Nature. 508(7497): 541–545.

Liu, Q., J. Qiu, M. Liang, J. Golinski, K. van Leyen, J.E. Jung, Z. You, E.H. Lo, a Degterev, and M.J. Whalen. 2014. "Akt and mTOR Mediate Programmed Necrosis in Neurons." Cell death & disease. 5: e1084.

Lois, C., E.J. Hong, S. Pease, E.J. Brown, and D. Baltimore. 2002. "Germline Transmission and Tissue-Specific Expression of Transgenes Delivered by Lentiviral Vectors." Science. 295(5556): 868–872.

Lugo, J.N., G.D. Smith, E.P. Arbuckle, J. White, A.J. Holley, C.M. Floruta, N. Ahmed, M.C. Gomez, and O. Okonkwo. 2014. Deletion of PTEN Produces Autism-like Behavioral Deficits and Alterations in Synaptic Proteins . Frontiers in Molecular Neuroscience .

Marques, L., and S. Thorsteinsdóttir. 2013. "Dynamics of Akt Activation during Mouse Embryo Development: Distinct Subcellular Patterns Distinguish Proliferating versus Differentiating Cells." Differentiation. 86(1)–(2): 48–56.

Matheny, R.W., and M.L. Adamo. 2009. "Current Perspectives on Akt Akt-Ivation and Akt-Ions." Experimental biology and medicine (Maywood, N.J.). 234(11): 1264–70.

Miao, L., L. Yang, H. Huang, F. Liang, C. Ling, and Y. Hu. 2016. "mTORC1 Is Necessary But mTORC2 And GSK3β Are Inhibitory For AKT3- Induced Axon Regeneration in the Central Nervous System." eLife. 1: 1–22.

Michels, D.A., A.W. Tu, W. McElroy, D. Voehringer, and O. Salas-Solano. 2012. "Charge Heterogeneity of Monoclonal Antibodies by Multiplexed Imaged Capillary Isoelectric Focusing Immunoassay with Chemiluminescence Detection." Analytical Chemistry. 84(12): 5380–5386.

Monaco, G., S. van Dam, J.L. Casal Novo Ribeiro, A. Larbi, and J.P. de Magalhães. 2015. "A Comparison of Human and Mouse Gene Co-Expression Networks Reveals Conservation and Divergence at the Tissue, Pathway and Disease Levels." BMC evolutionary biology. 15(1): 259.

Mora, A., D. Komander, D.M.F. van Aalten, and D.R. Alessi. 2004. "PDK1, the Master Regulator of AGC Kinase Signal Transduction." Seminars in Cell & Developmental Biology. 15(2): 161–170.

Myers, M.P., J.P. Stolarov, C. Eng, J. Li, S.I. Wang, M.H. Wigler, R. Parsons, and N.K. Tonks. 1997. "P-TEN, the Tumor Suppressor from Human Chromosome 10q23, Is a

Dual-Specificity Phosphatase." Proceedings of the National Academy of Sciences of the United States of America. 94(17): 9052–7.

Najafov, A., N. Shpiro, and D.R. Alessi. 2012. "Akt Is Efficiently Activated by PIF-Pocket- and PtdIns(3,4,5)P3-Dependent Mechanisms Leading to Resistance to PDK1 Inhibitors." Biochemical Journal. 448(2): 285–295.

Ni, J., Q. Liu, S. Xie, C. Carlson, T. Von, K. Vogel, S. Riddle, C. Benes, M. Eck, T. Roberts, N. Gray, and J. Zhao. 2012. "Functional Characterization of an Isoform-Selective Inhibitor of PI3K-p110ß as a Potential Anticancer Agent." Cancer Discovery. 2(5): 425–433.

O'Donnell, M., R.K. Chance, and G.J. Bashaw. 2009. "Axon Growth and Guidance: Receptor Regulation and Signal Transduction." Annual review of neuroscience. 32: 383–412.

O'Neill, R.A., A. Bhamidipati, X. Bi, D. Deb-Basu, L. Cahill, J. Ferrante, E. Gentalen, M. Glazer, J. Gossett, K. Hacker, C. Kirby, J. Knittle, R. Loder, C. Mastroieni, M. Maclaren, T. Mills, U. Nguyen, N. Parker, A. Rice, D. Roach, D. Suich, D. Voehringer, K. Voss, J. Yang, T. Yang, and P.B. Vander Horn. 2006. "Isoelectric Focusing Technology Quantifies Protein Signaling in 25 Cells." Proceedings of the National Academy of Sciences of the United States of America. 103(44): 16153–8.

Ojeda, L., J. Gao, K.G. Hooten, E. Wang, J.R. Thonhoff, T.J. Dunn, T. Gao, and P. Wu. 2011. "Critical Role of PI3k/Akt/GSK3ß in Motoneuron Specification from Human Neural Stem Cells in Response to FGF2 and EGF." PLoS ONE. 6(8).

Okano, J., I. Gaslightwala, M.J. Birnbaum, A.K. Rustgi, and H. Nakagawa. 2000. "Akt/protein Kinase B Isoforms Are Differentially Regulated by Epidermal Growth Factor Stimulation." J Biol Chem. 275(40): 30934–30942.

Park, K.K., K. Liu, Y. Hu, J.L. Kanter, and Z. He. 2010. "PTEN/mTOR and Axon Regeneration." Experimental Neurology. 223(1): 45–50.

Paul-Samojedny, M., A. Pudelko, M. Kowalczyk, A. Fila-Danilow, R. Suchanek-Raif, P. Borkowska, and J. Kowalski. 2015. "Knockdown of AKT3 and PI3KCA by RNA Interference Changes the Expression of the Genes That Are Related to Apoptosis and Autophagy in T98G Glioblastoma Multiforme Cells." Pharmacological Reports. 67(6): 1115–1123.

Posor, Y., M. Eichhorn-Gruenig, D. Puchkov, J. Schoneberg, A. Ullrich, A. Lampe, R. Muller, S. Zarbakhsh, F. Gulluni, E. Hirsch, M. Krauss, C. Schultz, J. Schmoranzer, F. Noe, and V. Haucke. 2013. "Spatiotemporal Control of Endocytosis by Phosphatidylinositol-3,4-Bisphosphate." Nature. 499(7457): 233–237.

Puehringer, D., N. Orel, P. Lüningschrör, N. Subramanian, T. Herrmann, M. V Chao, and M. Sendtner. 2013. "EGF Transactivation of Trk Receptors Regulates the Migration of Newborn Cortical Neurons." Nature neuroscience. 16(4): 407–15.

Pulido, R., S.J. Baker, J.T. Barata, A. Carracedo, V.J. Cid, I.D. Chin-Sang, V. Davé, J. den Hertog, P. Devreotes, B.J. Eickholt, C. Eng, F.B. Furnari, M.-M. Georgescu, A. Gericke, B. Hopkins, X. Jiang, S.-R. Lee, M. Lösche, P. Malaney, X. Matias-Guiu, M. Molina, P.P. Pandolfi, R. Parsons, P. Pinton, C. Rivas, R.M. Rocha, M.S. Rodríguez, A.H. Ross, M. Serrano, V. Stambolic, B. Stiles, A. Suzuki, S.-S. Tan, N.K. Tonks, L.C. Trotman, N. Wolff, R. Woscholski, H. Wu, and N.R. Leslie. 2014. "A Unified Nomenclature and Amino Acid Numbering for Human PTEN." Science Signaling. 7(332): pe15–pe15.

Righetti, P.G., R. Sebastiano, and A. Citterio. 2013. "Capillary Electrophoresis and Isoelectric Focusing in Peptide and Protein Analysis." Proteomics. 13(2): 325–340.

Rivière, J.-B., G.M. Mirzaa, B.J. O'Roak, M. Beddaoui, D. Alcantara, R.L. Conway, J. St-Onge, J.A. Schwartzentruber, K.W. Gripp, S.M. Nikkel, T. Worthylake, C.T. Sullivan, T.R. Ward, H.E. Butler, N.A. Kramer, B. Albrecht, C.M. Armour, L. Armstrong, O. Caluseriu, C. Cytrynbaum, B.A. Drolet, A.M. Innes, J.L. Lauzon, A.E. Lin, G.M.S. Mancini, W.S. Meschino, J.D. Reggin, A.K. Saggar, T. Lerman-Sagie, G. Uyanik, R. Weksberg, B. Zirn, C.L. Beaulieu, J. Majewski, D.E. Bulman, M. O'Driscoll, J. Shendure, J.M. Graham, K.M. Boycott, and W.B. Dobyns. 2012. "De Novo Germline and Postzygotic Mutations in AKT3, PIK3R2 and PIK3CA Cause a Spectrum of Related Megalencephaly Syndromes." Nature genetics. 44(8): 934–40.

Roskoski, R. 2014. "The ErbB/HER Family of Protein-Tyrosine Kinases and Cancer." Pharmacological Research. 79: 34–74.

Sabnis, H., H.L. Bradley, S.T. Bunting, T.M. Cooper, and K.D. Bunting. 2014. "Capillary Nano-Immunoassay for Akt 1/2/3 and 4EBP1 Phosphorylation in Acute Myeloid Leukemia." Journal of translational medicine. 12(1): 166.

Sadhu, C., B. Masinovsky, K. Dick, and C. Gregory. 2003. "Essential Role of Phosphoinositide 3-Kinase δ in Neutrophil Directional Movement." J Immunol. 170: 2647–2654.

Santi, S. a, and H. Lee. 2010. "The Akt Isoforms Are Present at Distinct Subcellular Locations." American journal of physiology. Cell physiology. 298(3): C580–C591.

Sarbassov, D.D., D. a Guertin, S.M. Ali, and D.M. Sabatini. 2005. "Phosphorylation and Regulation of Akt/PKB by the Rictor-mTOR Complex." Science (New York, N.Y.). 307(5712): 1098–1101.

Schlessinger, J. 2004. "Common and Distinct Elements in Cellular Signaling via EGF and FGF Receptors." Science. 306(5701): 1506–7.

Schmit, F., T. Utermark, S. Zhang, Q. Wang, T. Von, T.M. Roberts, and J.J. Zhao. 2014. "PI3K Isoform Dependence of PTEN-Deficient Tumors Can Be Altered by the Genetic Context." Proceedings of the National Academy of Sciences of the United States of America. 111(17): 6395–6400.

Schwartz, S., J. Wongvipat, C.B. Trigwell, U. Hancox, B.S. Carver, V. Rodrik-outmezguine, M. Will, P. Yellen, E. De Stanchina, H.I. Scher, S.T. Barry, and C.L. Sawyers. 2015. "Feedback Suppression of PI3Ka Signaling in PTEN Mutated Tumors Is Relieved by Selective Inhibition of PI3K β." 27(1): 109–122.

Settembre, C., R. Zoncu, D.L. Medina, F. Vetrini, S. Erdin, S. Erdin, T. Huynh, M. Ferron, G. Karsenty, M.C. Vellard, V. Facchinetti, D.M. Sabatini, and A. Ballabio. 2012. "A Lysosome-to-Nucleus Signalling Mechanism Senses and Regulates the Lysosome via mTOR and TFEB." The EMBO journal. 31(5): 1095–108.

She, Q.-B., S. Chandarlapaty, Q. Ye, J. Lobo, K.M. Haskell, K.R. Leander, D. Defeo-jones, H.E. Huber, and N. Rosen. 2008. "Breast Tumor Cells with PI3K Mutation or HER2 Amplification Are Selectively Addicted to Akt Signaling." PLoS ONE. 3(8): e3065.

Sibilia, M., J.P. Steinbach, L. Stingl, A. Aguzzi, and E.F. Wagner. 1998. "A Strain-Independent Postnatal Neurodegeneration in Mice Lacking the EGF Receptor." EMBO Journal. 17(3): 719–731.

Song, M.S., L. Salmena, and P.P. Pandolfi. 2012. "The Functions and Regulation of the PTEN Tumour Suppressor." Nat Rev Mol Cell Biol. 13(5): 283–296.

Sosa, L., S. Dupraz, L. Laurino, F. Bollati, M. Bisbal, A. Cáceres, K.H. Pfenninger, and S. Quiroga. 2006. "IGF-1 Receptor Is Essential for the Establishment of Hippocampal

Neuronal Polarity.” Nature neuroscience. 9(8): 993–995.

Speed, N.K., H.J.G. Matthies, J.P. Kennedy, R.A. Vaughan, J.A. Javitch, S.J. Russo, C.W. Lindsley, K. Niswender, and A. Galli. 2010. “Akt-Dependent and Isoform-Specific Regulation of Dopamine Transporter Cell Surface Expression.” ACS Chemical Neuroscience. 1(7): 476–481.

St-Denis, N., and A.-C. Gingras. 2012. Mass Spectrometric Tools for Systematic Analysis of Protein Phosphorylation. Progress in molecular biology and translational science. 1st ed. . Vol. 106. Elsevier Inc.

Stiles, J., and T.L. Jernigan. 2010. “The Basics of Brain Development.” Neuropsychology Review. 20(4): 327–348.

Sundaresan, N.R., V.B. Pillai, D. Wolfgeher, S. Samant, P. Vasudevan, V. Parekh, H. Raghuraman, J.M. Cunningham, M. Gupta, and M.P. Gupta. 2011. “The Deacetylase SIRT1 Promotes Membrane Localization and Activation of Akt and PDK1 During Tumorigenesis and Cardiac Hypertrophy.” Science Signaling. 4(182): ra46–ra46.

Tang, Y., M. Ye, Y. Du, X. Qiu, X. Lv, W. Yang, and J. Luo. 2015. “EGFR Signaling Upregulates Surface Expression of the GluN2B-Containing NMDA Receptor and Contributes to Long-Term Potentiation in the Hippocampus.” Neuroscience. 304: 109–121.

Testa, J.R., and A. Bellacosa. 2001. “AKT Plays a Central Role in Tumorigenesis.” Proceedings of the National Academy of Sciences . 98 (20): 10983–10985.

Tschopp, O., Z.-Z. Yang, D. Brodbeck, B.A. Dummler, M. Hemmings-Mieszczak, T. Watanabe, T. Michaelis, J. Frahm, and B.A. Hemmings. 2005. “Essential Role of Protein Kinase B{gamma} (PKB{gamma}/Akt3) in Postnatal Brain Development but Not in Glucose Homeostasis.” Development. 132(13): 2943–2954.

Turner, K.M., Y. Sun, P. Ji, K.J. Granberg, B. Bernard, L. Hu, D.E. Cogdell, X. Zhou, O. Yli-Harja, M. Nykter, I. Shmulevich, W.K.A. Yung, G.N. Fuller, and W. Zhang. 2015. “Genomically Amplified Akt3 Activates DNA Repair Pathway and Promotes Glioma Progression.” Proceedings of the National Academy of Sciences of the United States of America. 112(11): 3421–6.

Vazquez, F., and P. Devreotes. 2006. “Regulation of PTEN Function as a PIP3 Gatekeeper Through Membrane Interaction.” Cell Cycle. 5(14): 1523–1527.

Vivanco, I., Z.C. Chen, B. Tanos, B. Oldrini, W.-Y. Hsieh, N. Yannuzzi, C. Campos, and I.K. Mellinghoff. 2014. “A Kinase-Independent Function of AKT Promotes Cancer Cell Survival.” eLife. 3: 1–13.

Waite, K., and B.J. Eickholt. 2011. “The Neurodevelopmental Implications of PI3K Signaling.” In , edited by C. Rommel, B. Vanhaesebroeck, and K.P. Vogt. , pp.245–265. Berlin, Heidelberg: Springer Berlin Heidelberg.

Wang, L., S. Cheng, Z. Yin, C. Xu, S. Lu, J. Hou, T. Yu, X. Zhu, X. Zou, Y. Peng, Y. Xu, Z. Yang, and G. Chen. 2015. “Conditional Inactivation of Akt Three Isoforms Causes Tau Hyperphosphorylation in the Brain.” Molecular Neurodegeneration. 10(1): 33.

Wang, S., X. Huang, D. Sun, X. Xin, Q. Pan, S. Peng, Z. Liang, C. Luo, Y. Yang, H. Jiang, M. Huang, W. Chai, J. Ding, and M. Geng. 2012. “Extensive Crosstalk between O-GlcNAcylation and Phosphorylation Regulates Akt Signaling.” PLoS ONE. 7(5): e37427.

Wockner, L.F., E.P. Noble, B.R. Lawford, R.M. Young, C.P. Morris, V.L.J. Whitehall, and J. Voisey. 2014. “Genome-Wide DNA Methylation Analysis of Human Brain Tissue from

Schizophrenia Patients." Translational Psychiatry. 4(1): e339.

Xiang, Q., J. Zhang, C.Y. Li, Y. Wang, M.J. Zeng, Z.X. Cai, R.B. Tian, W. Jia, and X.H. Li. 2015. "Insulin Resistance-Induced Hyperglycemia Decreased the Activation of Akt/CREB in Hippocampus Neurons: Molecular Evidence for Mechanism of Diabetes-Induced Cognitive Dysfunction." Neuropeptides. 54: 9–15.

Xue, M., Y.Q. Lin, H. Pan, K. Reim, H. Deng, H.J. Bellen, and C. Rosenmund. 2009. "Tilting the Balance between Facilitatory and Inhibitory Functions of Mammalian and Drosophila Complexins Orchestrates Synaptic Vesicle Exocytosis." Neuron. 64(3): 367–380.

Yang, J., J. Ru, W. Ma, Y. Gao, Z. Liang, J. Liu, J. Guo, and L. Li. 2016. "BDNF Promotes the Growth of Human Neurons through Crosstalk with the Wnt/ß-Catenin Signaling Pathway via GSK-3ß." Neuropeptides. 54: 35–46.

Yang, W.-L., J. Wang, C.-H. Chan, S.-W. Lee, A.D. Campos, B. Lamothe, L. Hur, B.C. Grabiner, X. Lin, B.G. Darnay, and H.-K. Lin. 2009. "The E3 Ligase TRAF6 Regulates Akt Ubiquitination and Activation." Science. 325(5944): 1134–1138.

Yang, Z., O. Tschopp, N. Di-poı, E. Bruder, A. Baudry, B. Du, W. Wahli, and B.A. Hemmings. 2005. "Dosage-Dependent Effects of Akt1 / Protein Kinase B Alpha (PKB a) and Akt3 / PKB Gamma on Thymus , Skin , and Cardiovascular and Nervous System Development in Mice." Molecular and cellular biology. 25(23): 10407–10418.

Zhou, J., and L.F. Parada. 2012. "PTEN Signaling in Autism Spectrum Disorders." Current Opinion in Neurobiology. 22(5): 873–879.

Zschätzsch, M., C. Oliva, M. Langen, N. De Geest, M.N. Özel, W.R. Williamson, W.C. Lemon, A. Soldano, S. Munck, P.R. Hiesinger, N. Sanchez-Soriano, and B.A. Hassan. 2014. "Regulation of Branching Dynamics by Axon-Intrinsic Asymmetries in Tyrosine Kinase Receptor Signaling." eLife. 2014(3): 1–24.

Zurashvili, T., L. Cordón-Barris, G. Ruiz-Babot, X. Zhou, J.M. Lizcano, N. Gómez, L. Giménez-Llort, and J.R. Bayascas. 2013. "Interaction of PDK1 with Phosphoinositides Is Essential for Neuronal Differentiation but Dispensable for Neuronal Survival." Molecular and cellular biology. 33(5): 1027–40.

6. Supplementary Information

6.1. Publication list

- **Sandra Schrötter**, George Leondaritis, Britta J Eickholt. (2016). *Capillary isoelectric focusing of Akt isoforms identifies highly dynamic phosphorylation in neuronal cells and brain tissue*. J Biol Chem. 291(19): 10239–10251

- Hao Hu, Michelle L Matter, Lina Issa-Jahns, Mayumi Jijiwa, Nadine Kraemer, Luciana Musante, Michelle de la Vega, Olaf Ninnemann, Detlev Schindler, Natalia Damatova, Katharina Eirich, Marco Sifringer, **Sandra Schrötter**, Britta J Eickholt, Lambert van den Heuvel, Chanel Casamina, Gisela Stoltenburg-Didinger, Hans-Hilger Ropers, Thomas F Wienker, Christoph Hübner, and Angela M Kaindl. (2014). *Mutations in PTRH2 cause novel infantile-onset multisystem disease with intellectual disability, microcephaly, progressive ataxia, and muscle weakness.* Ann Clin Transl Neurol. 1(12): 1024–1035

6.2. Awards

For the poster “Capillary isoelectric focusing of Akt isoforms identifies highly dynamic phosphorylation in neuronal cells and brain tissue” I was awarded with the poster prize at the SFB958 retreat in Kloster Lehnin, Germany.

6.3. Posters and talks

- **Spatial (EMBO) 2013, Dead Sea, Israel**. “Quantitative analysis of Akt isoform-specific phosphorylation using isoelectric focusing” (poster presentation)
- **SFB958 and GRK1459 retreat 2013, Wismar, Germany**. “Quantitative analysis of Akt isoform-specific phosphorylation using isoelectric focusing” (oral presentation)
- **Horizons 2013, Göttingen, Germany**. “Quantitative analysis of Akt isoform-specific phosphorylation using isoelectric focusing” (poster presentation)
- **Membranes and Modules 2014, Berlin, Germany**. “Characterization of the PI3K/PTEN pathway through tunable and targeted PTEN stabilization in ES-cell derived motoneurons” (poster presentation)
- **FENS 2014, Milan, Italy**. “Analysis of PI3K/PTEN - Akt signaling in cortical neurons through capillary-based isoelectric focusing (cIEF)” (poster presentation)
- **FEBS 2015, Berlin, Germany**. “Identification of a novel interaction partner of protein/lipid phosphatase PTEN” (poster presentation)
- **Biochemistry/ Biophysics Institute Seminar, 2016**. “Identification of dynamic Akt phosphorylation using capillary isoelectric focusing (cIEF)” (oral presentation)
- **SFB958 retreat 2016, Kloster Lehnin, Germany**. “Capillary isoelectric focusing of Akt isoforms identifies highly dynamic phosphorylation in neuronal cells and brain tissue” (poster presentation)

- **NeuroCure Lunchtime Seminar, 2016** "Identification of dynamic Akt phosphorylation using capillary isoelectric focusing (cIEF)" (oral presentation)
- **PI3K-mTOR-PTEN Network in Health & Disease (CSHL) 2016, New York, USA**. "Capillary isoelectric focusing of Akt isoforms identifies highly dynamic phosphorylation in neuronal cells and brain tissue" (poster presentation)

6.4. Teaching experience

- Practical course for medical students Module 1 "Einführung in die Labordiagnostik" (SS2013 - SS2016)

- Practical course for medical students Module 2 "Genetischer Fingerabdruck" (SS2013 - WS2013/14)

- Supervision of 6th semester medical student Tahnita Kulow for her lab project in the course of Module 23

7. Acknowledgments

First and foremost I would like to thank my supervisor Britta Eickholt, without whom this work would not have been possible. Her constant, unwavering support and scientific mentoring guided me through many challenges of this project, scientific and other. I greatly appreciated that she allowed me to work very independently, but even more that her door was always open when I needed advice, inspiration or encouragement. I am much obliged to Prof. Peter-Michael Kloetzel for accepting my official supervision at the Humboldt University.

Special thanks to George Leondaritis, who not only contributed in a major way to my scientific education, but without whose frequent support and practical jokes many long days would have been much less entertaining. I am thankful for the many discussions we had (with or without Margaritas) that were often an inspiration. I kept count, and in the last 4 years there was only one single lab-related question you could not answer!

I could not have wished for better colleagues to spend the last four years with. Apart from outstanding scientific input ("there should be something on youtube") and your altruistic help in the daily lab routine (music, Mensa, planking), sharing life in our spacious but cozy office during summer (with occasional afternoons by the fountain) and winter times with you was real fun. From the Eickholt lab, I particularly want to thank Annika for keeping my head straight by making me as fit as ever (who would have thought that I could run 21km?), and for being a wonderful friend. Furthermore, thank you Willem for your contagious enthusiasm and constant supply of cookies and, together with Patricia, countless dinner nights.

Finally, I am deeply grateful to my parents and my brother for always believing in me, and for giving me the freedom to pursue my not always easy to communicate interests, and your support to travel the world and do as I like, although I'm sure it was often more terrifying for you than for me. Thank you for making me the person I am today! A special thank you to Dean, Bonnie and Brigitta for taking me in as a crazy, foreign family member and opening your home to me. I also want to thank Natalie and Ina, even though we all went our own ways after the Masters I know I can always count on you for encouragement, to drink a good bottle of Malbec and fun vacations. I guess it is true, that you meet some of the best friends in university! Last but not least, it is an honor to thank the people who have known me the longest, Mixi, Fabi, Mike, Kati and Holdi, for countless nights in Hafenbar, Volksbar, Birgit&Bier, your apartments etc. as an excellent means of recreation.

8. Selbstständigkeitserklärung

Hiermit erkläre ich, dass ich die vorliegende Arbeit selbständig und nur unter Verwendung der angegebenen Hilfsmittel angefertigt habe.

Berlin, den

Sandra Schrötter